The Institute of OPTICS

HAJIM SCHOOL OF ENGINEERING & APPLIED SCIENCES
UNIVERSITY of ROCHESTER

Fienup Group:
Image-Based Wavefront Sensing and Interferometric Imaging

James R. Fienup

University of Rochester, Institute of Optics

fienup@optics.rochester.edu

Presented to the Astrophysics Science Division
NASA Goddard Space Flight Center
January 15, 2016

Jim Fienup — Vita

- B.A., Holy Cross College, Physics and Mathematics
- M.S. and Ph.D., Stanford University, Applied Physics (under Joseph Goodman)
- ERIM (formerly Willow Run Laboratories of the U. of Michigan)
  - ERIM International, Veridian Systems, (General Dynamics; now: MacDonald Dettwiler & Assoc.)
    - Contract research, Lead over 40 programs
- U.Rochester, Institute of Optics since 2002: Robert E. Hopkins Professor of Optics & Professor, Center for Visual Science and of ECE; Senior Scientist, LLE

- Major Honors:
  - NSF Graduate Fellow
  - Rudolph Kingslake Medal and Prize (SPIE)
  - International Prize in Optics (International Commission for Optics)
  - Fellow of OSA, SPIE; OSA's Emmett Leith Medal
  - Member, National Academy of Engineering

- Other Major Activities:
  - Past Chair, Publications Council of the O.S.A.
  - Past Editor-in-Chief of the *Journal of the Optical Society of America A*
  - Past Editor, *Applied Optics - Information Processing; Optics Letters*

Outline

- Image-based wavefront sensing for optical telescopes
  - Hubble Space Telescope
  - JWST
    - NIRCam/ISIM testing
    - On orbit
  - Other Future Systems

+ Efficient optical propagations for PIAA coronography simulation

- Other Wavefront Sensing
  - Freeform Optics
  - High-energy laser beams
  - Hermite-Gaussian and Laguerre-Gaussian beams

- Interferometric Imaging
  - Of geosynchronous satellites from the ground
  - NASA space-based spatio-spectral interferometric imaging

Efficient Propagation of Highly Aspheric Wavefronts

Prof. James R. Fienup

Institute of Optics

University of Rochester

15 October 2009

Portions of this work were funded by Jet Propulsion Laboratories

Presented at Frontiers in Optics 2009, San Jose, CA, paper FThX5

Outline

- Motivation
- Propagation approaches
- Computational problem with highly aspheric wavefronts
- Divide and conquer approach

Motivation

Need efficient diffraction modeling computation when have large aspheric wavefronts/surfaces, particularly for desktop/laptop, e.g., for

- Computational imaging systems
  - Large amounts of (cubic) phase error for extended depth of field[1,2]
- Systems with extremely wide FOV[3]
- **Phase-induced amplitude apodization (PIAA)[4]**
- Phase retrieval for highly aspheric surfaces[5]

1. E.R. Dowski, Jr. and W.T. Cathey, "Extended depth of field through wave-front coding," Appl. Opt. 34, 1859-1866 (1995).
2. W. Chi and N. George, "Computational imaging with the logarithmic asphere: theory," J. Opt. Soc. Am. A 20, 2260-2273 (2003).
3. A.B. Meinel and M.P. Meinel, "Spherical Primary Telescope with Aspheric Correction at a Small Internal Pupil," Appl. Opt. 39, 5093-5100 (2000).
4. R.J. Vanderbei, “Diffraction Analysis of Two-Dimensional Pupil Mapping for High-Contrast Imaging,” Ap.J. 636,528-543 (2006 January 1).
5. G.R. Brady and J.R. Fienup, “Measurement Range of Phase Retrieval in Optical Surface and Wavefront Metrology,” Appl. Opt. 48, 442-449 (2009).

Propagation Calculation by Angular Spectrum or Fresnel Transform

Compute field in plane (x, y, z) from field in plane (x, y, z = 0)

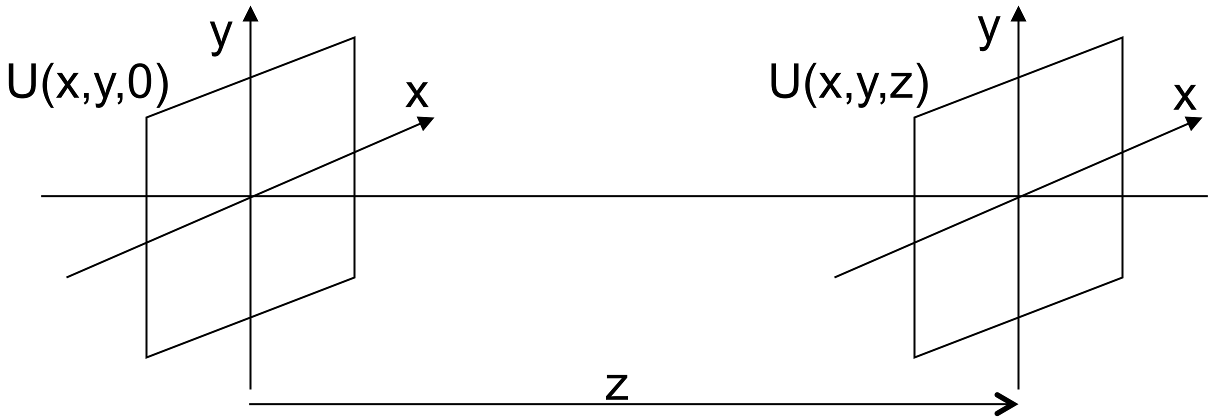

- Angular spectrum (uses 2 Fourier transforms):

$$U(x,y,z)=\int\int_{-\infty}^{\infty} A\left(f_x,f_y;0\right)\exp\left[i2\pi\sqrt{(k/2\pi)^2-f_x^2-f_y^2}\;z\right]\exp\left[i2\pi\left(f_x x+f_y y\right)\right]df_x\,df_y$$

$$\boxed{A\left(f_x,f_y;0\right)=\mathcal{F}\left[U(x,y,0)\right]}$$

- Fresnel propagation (uses 1 Fourier transform):

$$U(x,y)=\frac{e^{ikz}}{i\lambda z}\exp\left[\frac{i\pi\left(x^2+y^2\right)}{\lambda z}\right]\int\int_{-\infty}^{\infty}U(\xi,\eta)\exp\left[\frac{i\pi\left(\xi^2+\eta^2\right)}{\lambda z}\right]\exp\left[\frac{-i2\pi(x\xi+y\eta)}{\lambda z}\right]d\xi d\eta$$

Single-FFT Fresnel Transform

$$\boxed{U_z(pd_x, qd_y) \propto e^{ikz} \exp\left\{\frac{i\pi}{\lambda z}\left[(pd_x)^2 + (qd_y)^2\right]\right\} DFT\left[U_{m,n} \exp\left\{\frac{i\pi}{\lambda z}\left[(md_\xi)^2 + (nd_\eta)^2\right]\right\}\right]}$$

- DFT computed with FFT; then stuck with sample spacing

$$d_x = \frac{\lambda z}{M d_\xi} \qquad M = \frac{\lambda z}{d_\xi d_x}$$

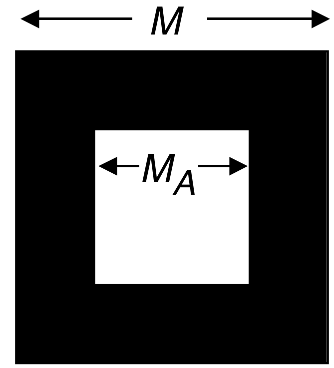

Input sample spacing d_ξ
Aperture width $D = M_A d_\xi$

- To avoid phase jumps $> \pi$, in quadratic phase term, to avoid aliasing, must also satisfy

$$M_A > \frac{D^2}{\lambda z} = 4\ N_F \qquad \text{Fresnel Number: } N_F = \frac{(M_A d_\xi)^2}{4\lambda z}$$

- Small-z Fresnel transform by single-FFT often impractical on desktop computer
  - e.g., for $\lambda = 0.5$ µm, $D = M_A d_\xi = 1$ cm , z = 1 cm
    - Have $N_F = 5{,}000$, need $M_A > 20{,}000$ pixels (need 6.4 GB for one array)
- To get finer sampling of PSF, want $Q = M/M_A > 2$, making $M > 2\ M_A$
- Single-FFT Fresnel best for larger z (smaller N_F) or pupil ==> focus

Double-FFT Angular Spectrum

$$U_z(md_x, nd_y) \propto e^{ikz} IDFT\left\{ DFT\left[U(m_1 d_x, n_1 d_y)\right] \exp\left[i2\pi \frac{z}{\lambda} \sqrt{1 - \left(\frac{p\lambda}{Md_x}\right)^2 - \left(\frac{q\lambda}{Nd_y}\right)^2} \right] \right\}$$

- Well behaved for small z and for relatively planar wavefronts
- $d_x = d_\xi$ (output sample spacing = input sample spacing)
- Inefficient for aperture plane to focal plane calculations
  - (Large aperture)/(Small d_x) may be too large
  - E.g., 10 cm pupil to focal plane with 5 µm d_x ==> $M > 20{,}000$
  - Focusing term in U requires large first FFT

Example 1: Small Galilean Telescope

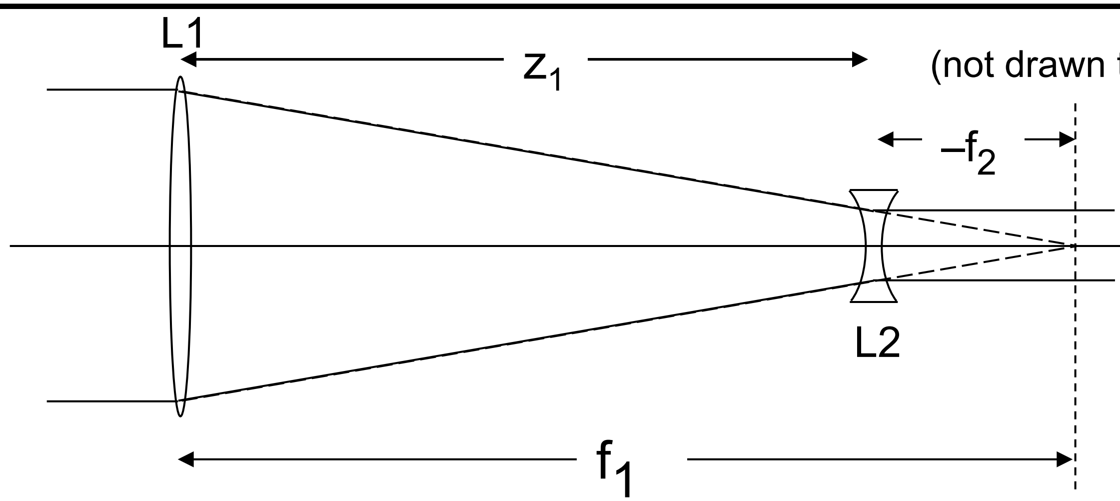

$D = 25$ mm,
$z_1 = 15D = 375$ mm
$\text{Mag} = 3 = -f_1/f_2$
$f_1 = \text{Mag}\ z_1 / (\text{Mag}-1)$
$= 1.5\ z_1 = 562.5$ mm

Direct Fresnel transform from <u>before</u> L1 to <u>before</u> L2:

Fresnel kernel — Lens term

$$U_2(x,y) = \frac{e^{ikL_o}}{i\lambda z_1}\exp\left[\frac{i\pi}{\lambda z_1}\left(x^2+y^2\right)\right]\int\int_{-\infty}^{\infty}\left\{U_1(\xi,\eta)\exp\left[\frac{i\pi\left(1-\frac{z_1}{f_1}\right)}{\lambda z_1}\left(\xi^2+\eta^2\right)\right]\right\}\exp\left[\frac{-i2\pi}{\lambda z_1}(\xi x+\eta y)\right]d\xi d\eta$$

- To avoid aliasing:

  Fresnel needs $M_A > 878$, angular spectrum needs $M_A > 1{,}756$

Small Galilean Telescope
Single Fresnel Transform L1 to L2

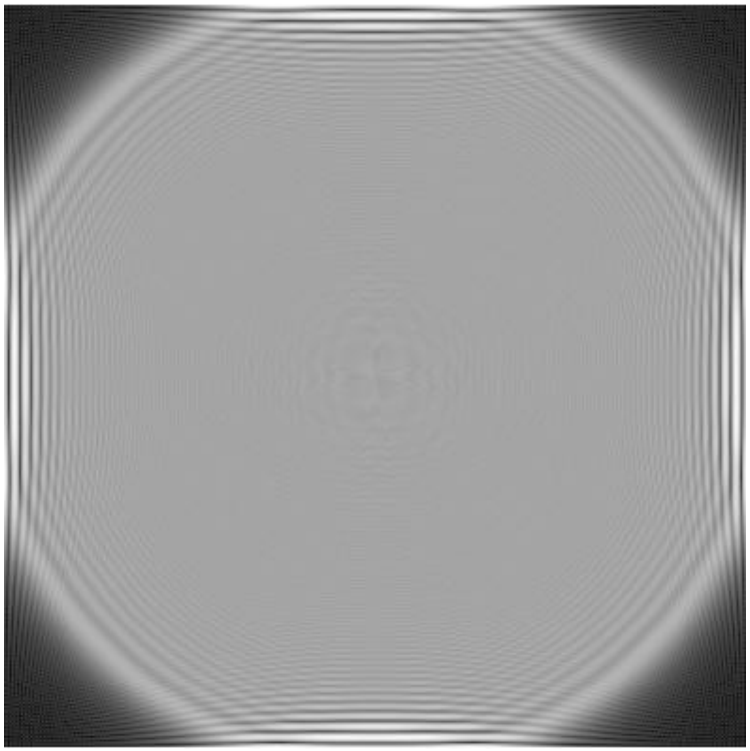

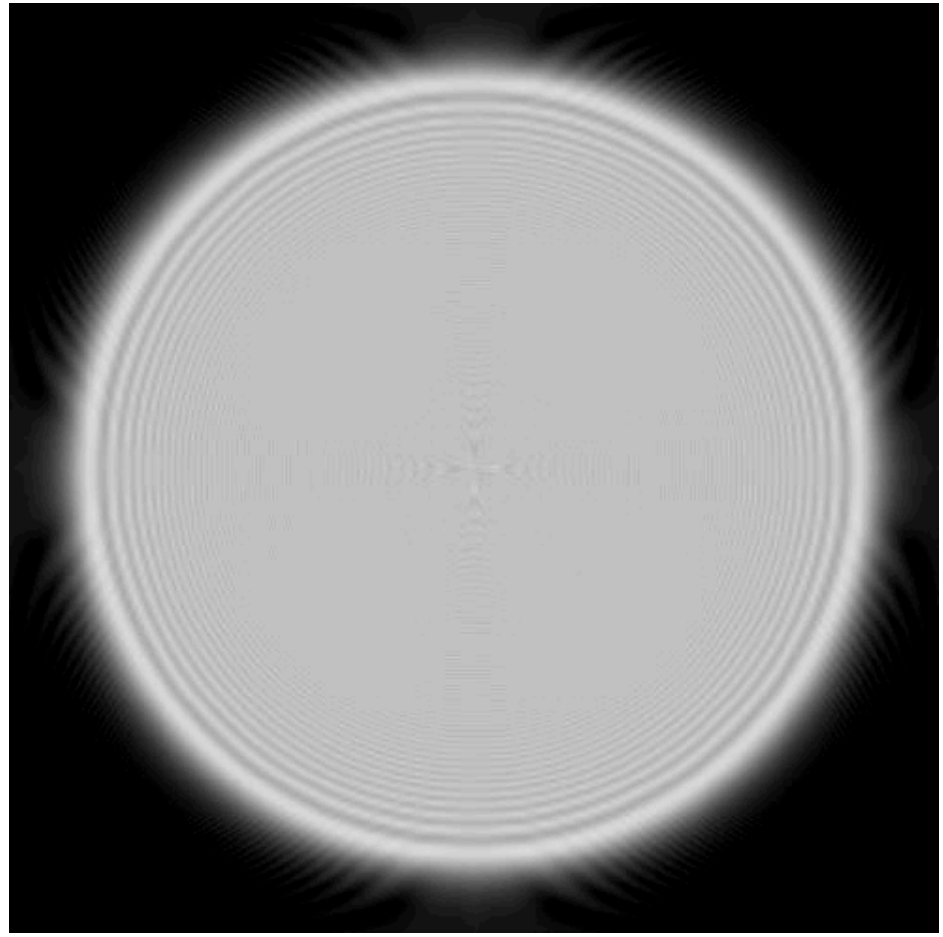

$M = M_A = 800$ Both shown (Intensity)$^{1/4}$ $M = M_A = 1000$

To minimize aliasing, want FFT length, M, larger (more embedding)
Also gives desirable finer PSF sampling PSF. Typically want $Q = M/M_A > 2$

Much Better: Intermediate Propagation to (Virtual) Focus

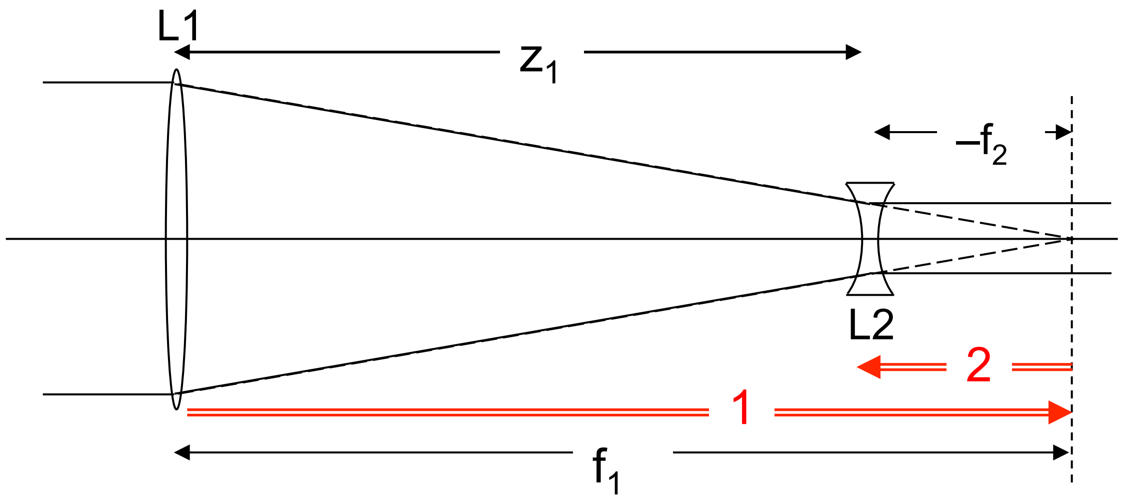

- Propagate first to virtual focus, f_1 from L1 with 1-FFT Fresnel
  — Quadratic phase terms in integral cancel
- Then back propagate by f_2 to front of L2 with 1-FFT Fresnel
  — Both propagations well behaved
- Then continue the propagation through L2 ...

Previous example can be performed with $M_A < 50$!

J.R. Fienup, J.C. Marron, T.J. Schulz and J.H. Seldin, "Hubble Space Telescope Characterized by Using Phase Retrieval Algorithms," Appl. Opt. 32 1747-1768 (1993).
equivalent to
E.A. Sziklas and A.E. Siegman, "Mode Calculations in Unstable Resonators with Flowing Saturable Gain. 2: Fast Fourier Transform Method," Appl. Opt. 14, 1874-1889 (1975).

Example 2: Large Galilean Telescope with Large Spherical Aberration

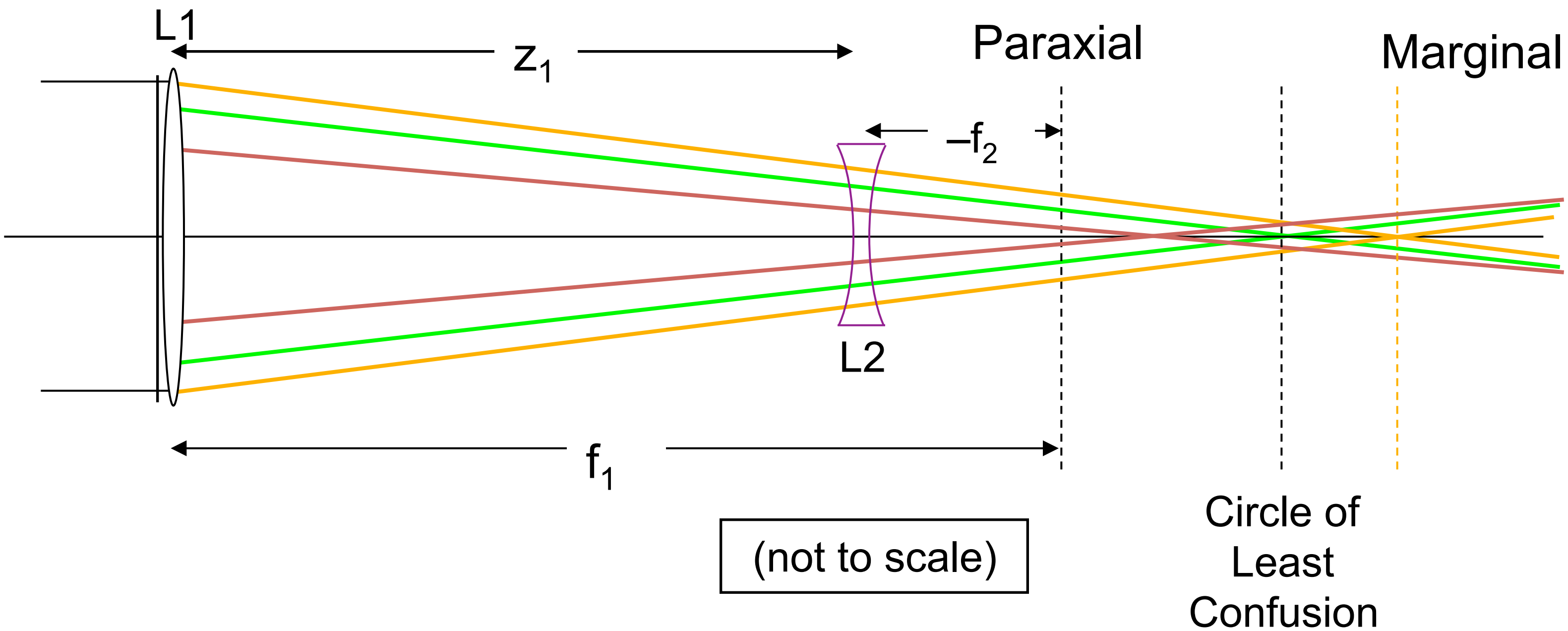

(Case shown: overcorrected spherical aberration)

- For smallest possible M_A,
  propagate first to circle of least confusion
- M_A may still be too large
  —If beam is too wide throughout focal volume

D = 1 m,
f_1 = 20 m
Mag = 20 = $-f_1/f_2$
$-f_2$ = 1 m
z_1 = 19 m
spherical aberration (r^4) :
130 waves (W_{040})
l = 0.6328 mm

Approach: Divide and Conquer

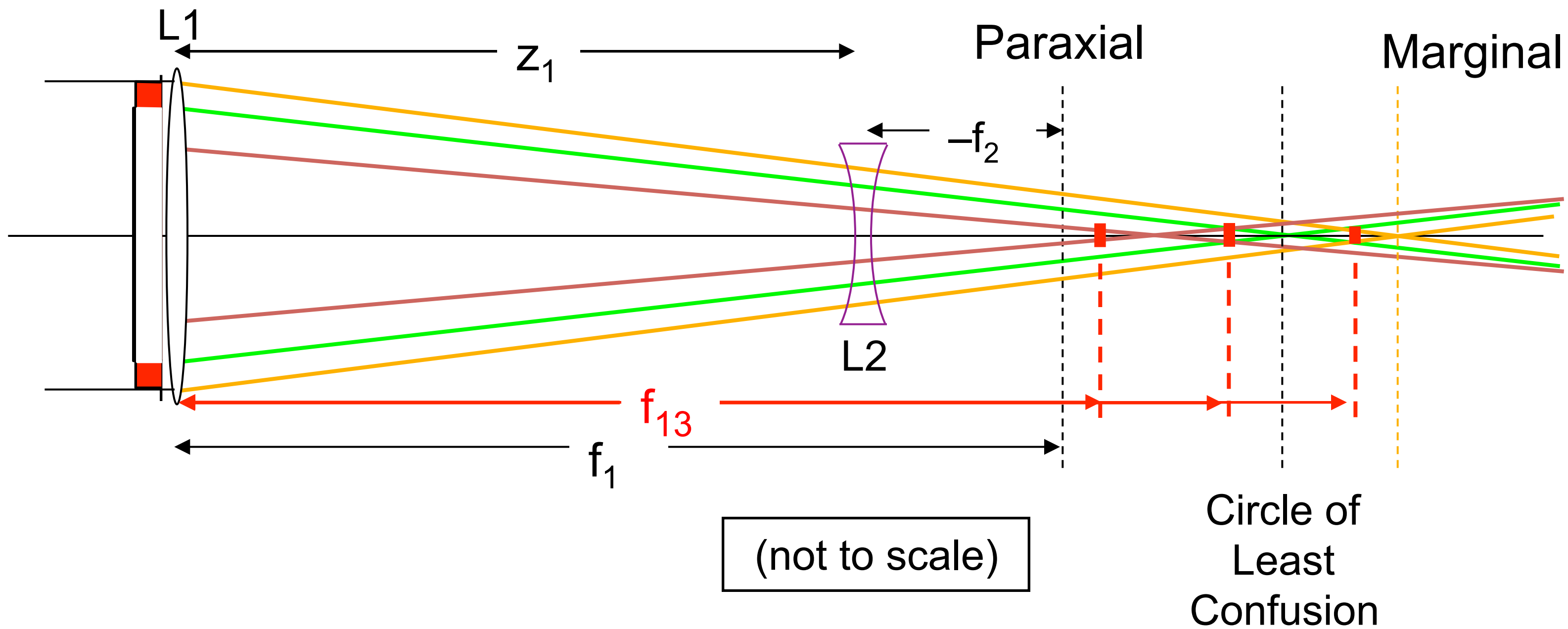

Divide L1 into annuli, propagate each annulus separately, sum

— Use two-Fresnel transform method, to nominal focus, and back to L2

— Need computational apodizations to minimize edge ringing & aliasing

- Have overlap, with sum of apodizations = 1

— Variations in foci f_{1k} cause variable sample spacing at L2

- Need interpolation to common sample spacing (use embedding)

Equalizing Sample Spacing at L2

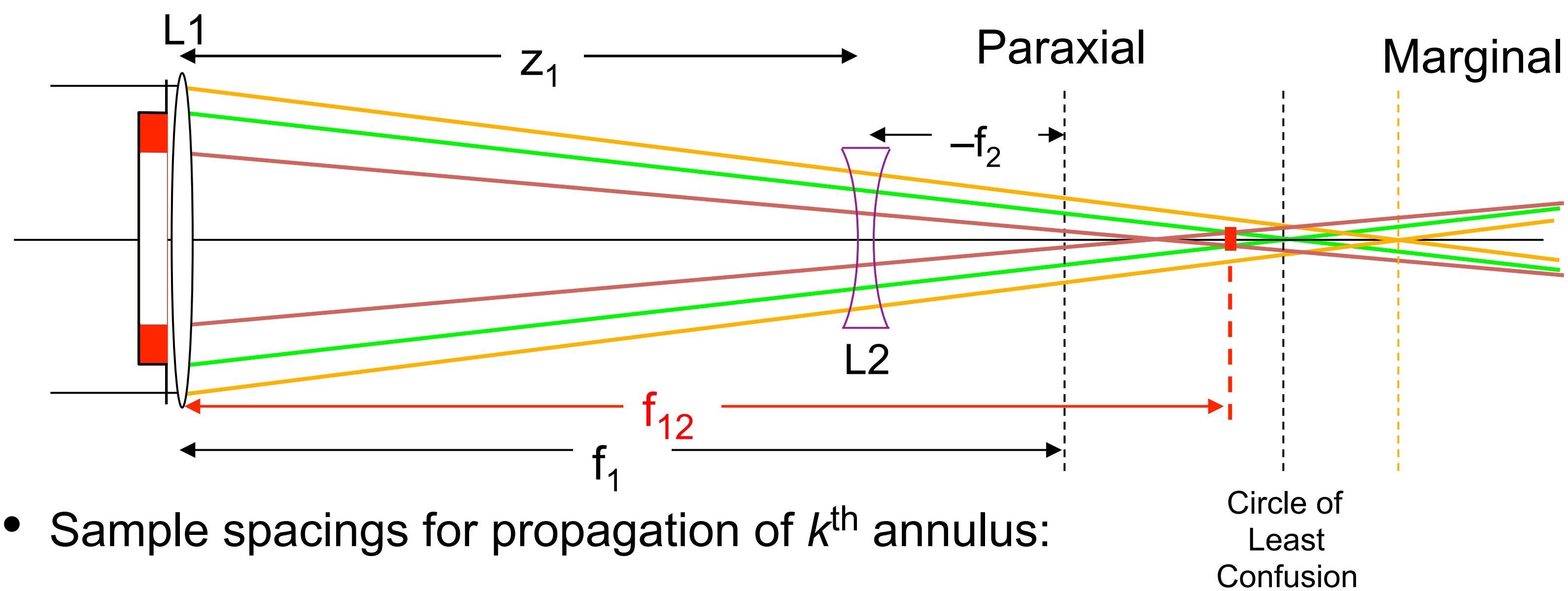

- Sample spacings for propagation of k^{th} annulus:

at k^{th} nominal focus (P1): $d_{x1k} = \dfrac{\lambda f_{1k}}{M_{1k} d_\xi}$, where M_{1k} = first FFT length

at L2: $$d_{x2k} = \frac{\lambda (f_{1k} - z_1)}{M_{2k} d_{x1k}} = \boxed{\frac{(f_{1k} - z_1)}{f_{1k}} \frac{M_{1k}}{M_{2k}} d_\xi}$$

- Using more or less zero padding at L1 (adjust M_{1k}) & truncation/zero-padding at nominal focus plane (adjust M_{2k}), compensate for $(f_{1k} - z_1)/f_{1k}$ factor to make d_{x2k} same for all k

The Institute of OPTICS

Determine Nominal Focus from Ray Intercept

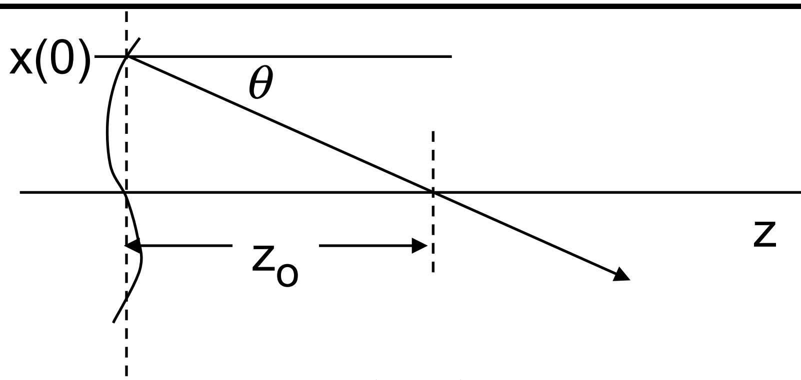

α = sin(θ) in x-z plane

$$\alpha = \frac{\partial w(x,y)}{\partial x}\ ,\quad \phi(x,y) = \frac{2\pi}{\lambda} w(x,y)$$

x direction cosine

phase

optical path length

Ray height vs z

$$x(z) = x(0) + z\tan\theta$$

$$x(z_o) = 0 = x(0) + z_o\tan\theta$$

$$z_o = \frac{-x(0)}{\tan\theta} \approx \frac{-x(0)}{\theta} \approx \frac{-x(0)}{\alpha}$$

Ray crosses axis at z_o

For spherical aberration + focus:

$$w(r) = W_{040}\lambda(2r/D)^4 - \frac{r^2}{2f_1}$$

Determines best intermediate focus to which to propagate for that region of the wave front

Intensities of Fields (130 λ W_{040} spherical) Propagated from L1 to L2 with $Q = 2$

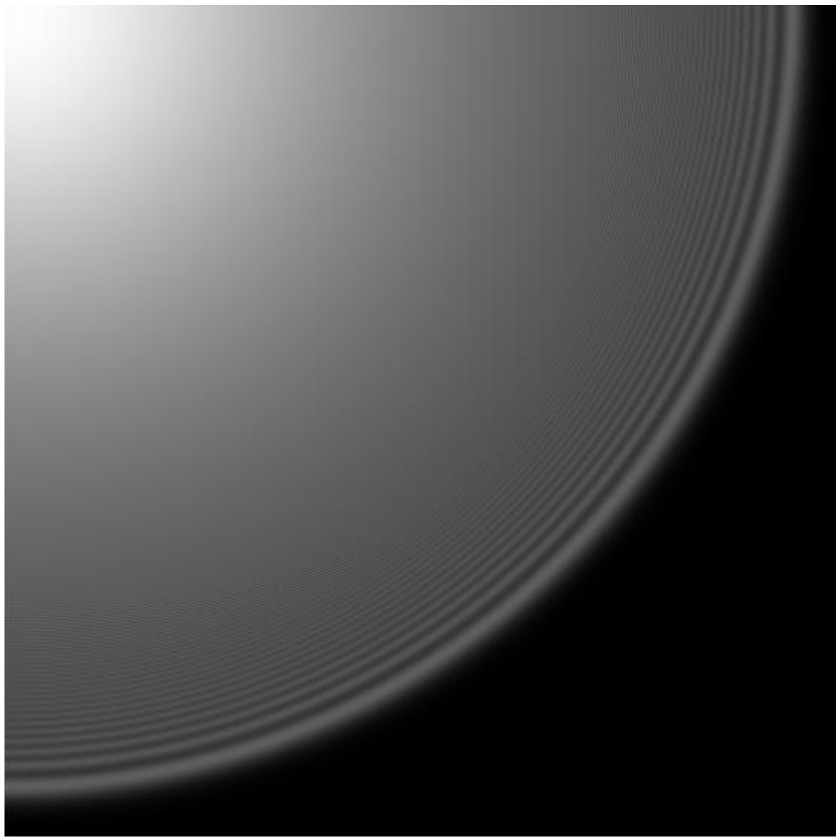

2,000 x 2,000 FFT of circle
2-step Fresnel
via circle of least confusion

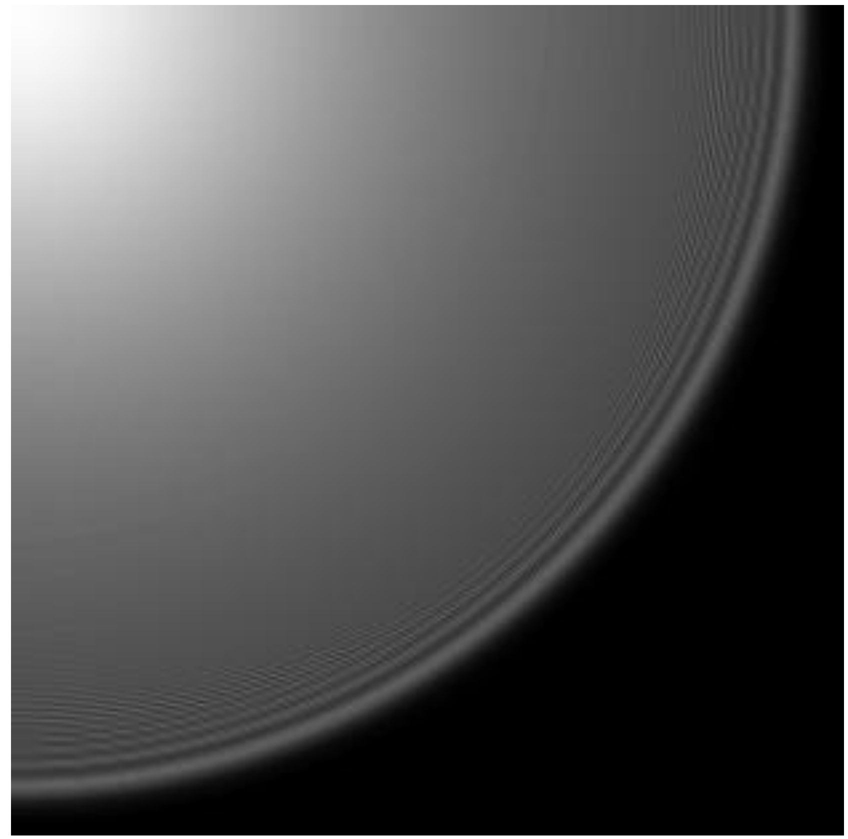

1,000 x 1,000 FFT
Sum of 2 terms
2-step Fresnel via f_{11}, f_{12}

Limit to the Approach

- If the aspheric term is too large, then the annuli become too narrow
  - — Apodization less effective
  - — Diffraction from thin annuli suffer more aliasing
  - — May need finer sampling near edge
    where third derivative of OPD is large

Summary

For performing propagations of wavefronts having large asphericity with ordinary desktop computers (few GB RAM):

- Fresnel propagation to intermediate focus plane greatly helps
  - Cancels large quadratic phase terms
- With large asphericity, **divide** aperture into subapertures **and conquer**
  - For r^n (spherical) aberrations, divide into annuli
  - Propagate each separately, then sum
    - Each propagated to a different intermediate focus, then to desired plane
    - Use different FFT lengths to arrive at same sample spacing for all
    - Use complementary digital apodization to minimize aliasing

Outline

- Image-based wavefront sensing for optical telescopes
  - Hubble Space Telescope
  - JWST
    - NIRCam/ISIM testing
    - On orbit
  - Other Future Systems

- Other Wavefront Sensing
  - Freeform Optics
  - High-energy laser beams
  - Hermite-Gaussian and Laguerre-Gaussian beams

- Interferometric Imaging
  - Of geosynchronous satellites from the ground
  - NASA space-based spatio-spectral interferometric imaging

First HST Point-Spread Function, 1990

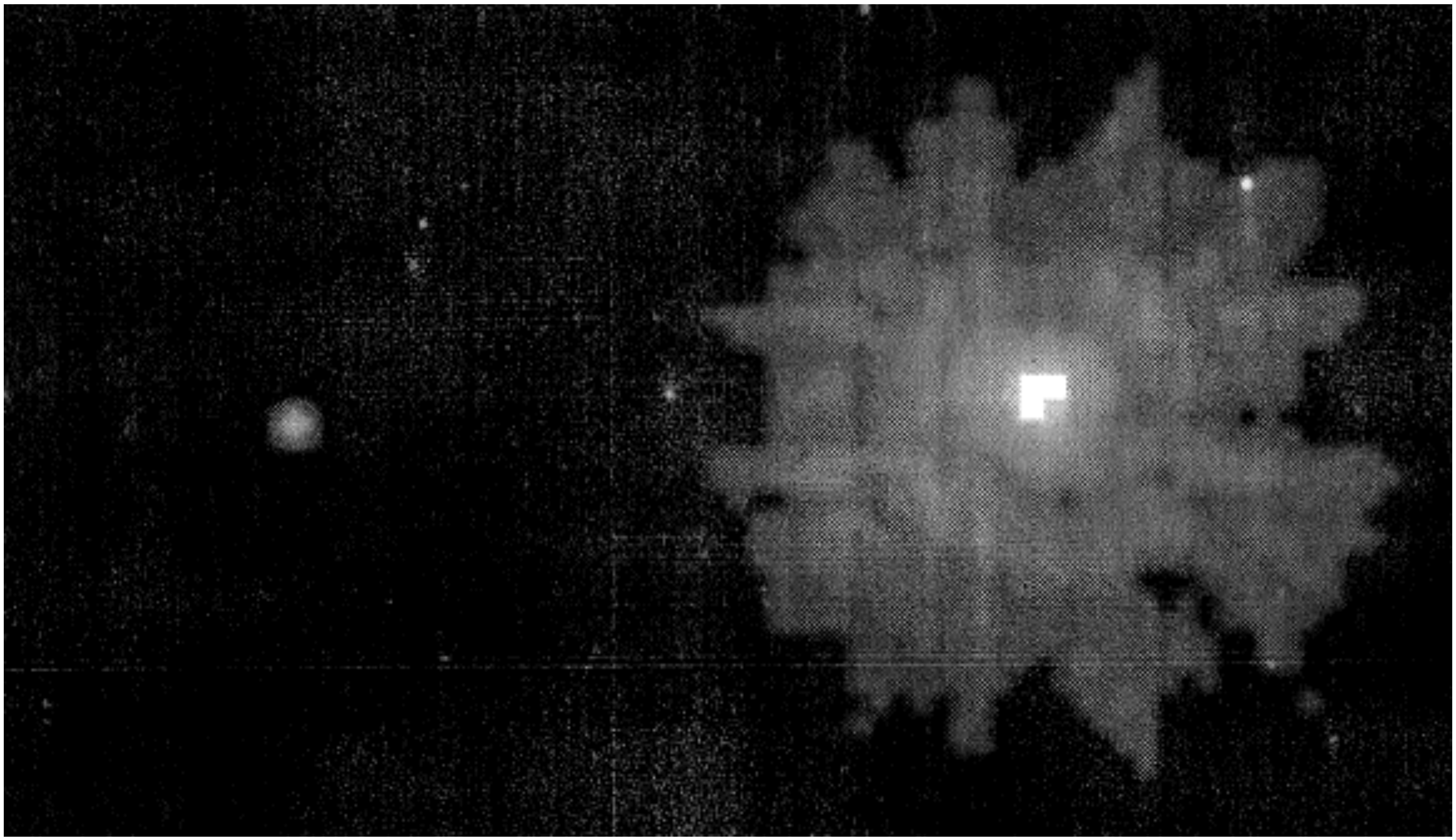

Expected Actual

Can Correct Primary Mirror Error on Secondary of WF/PC2 Relay Telescope

K. LESCHLY

CORRECTION APPROACH

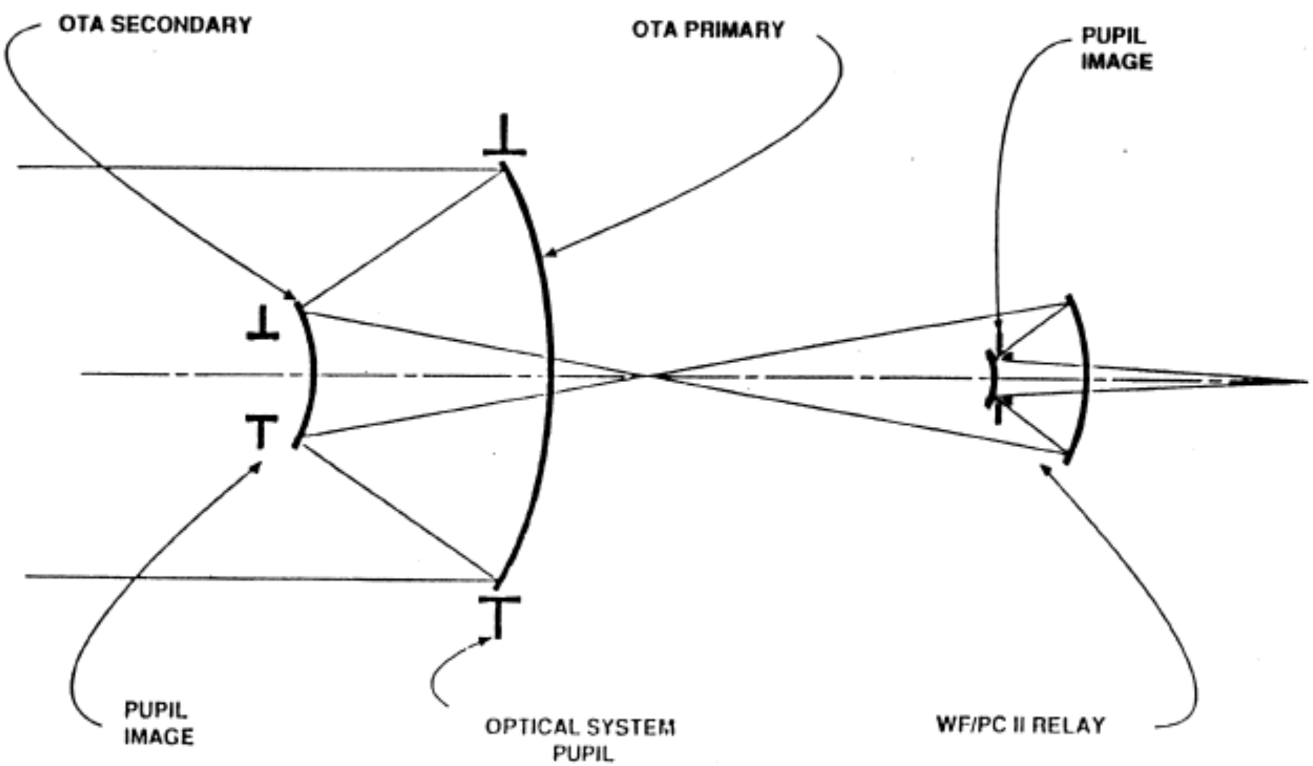

(Not to scale)

Determine HST Aberrations from PSF

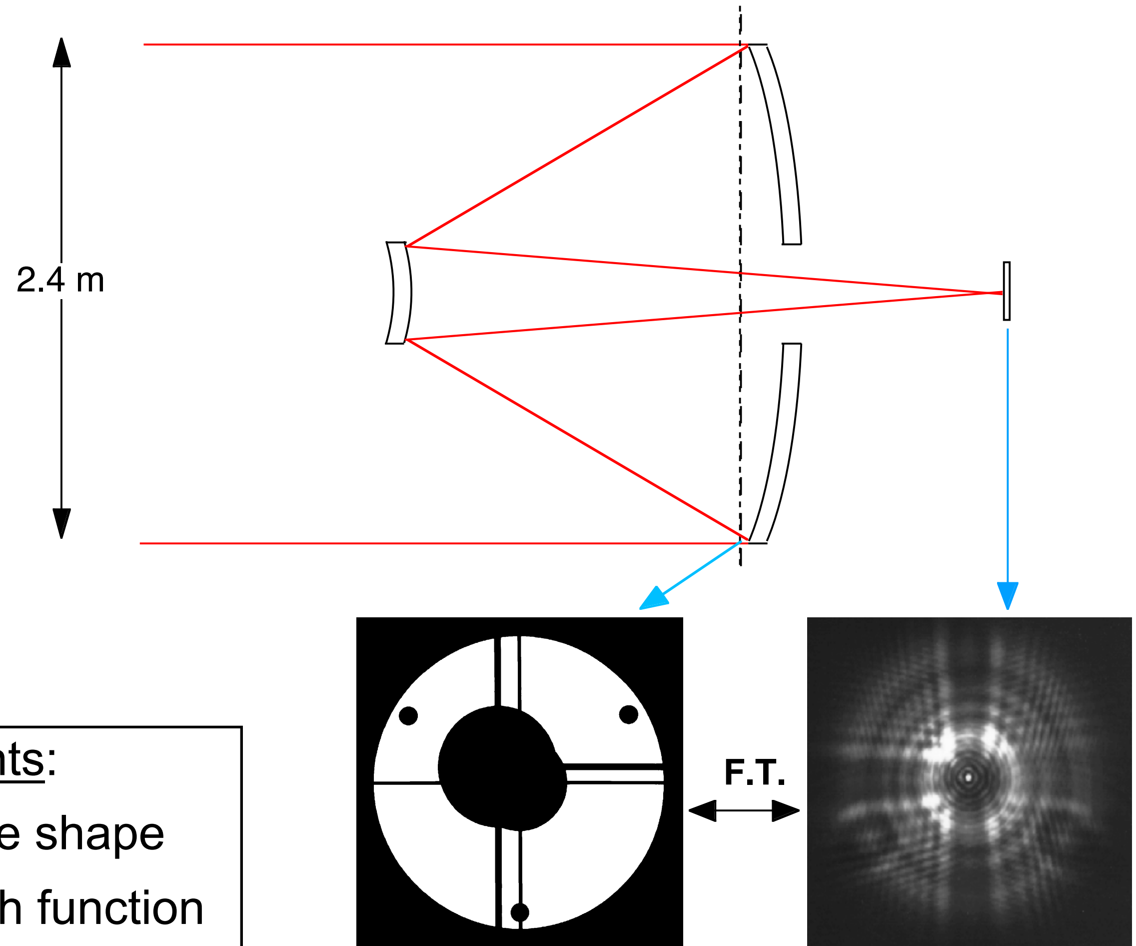

(Hubble Space Telescope)

<u>Measurements & Constraints</u>:

Pupil plane: known aperture shape

phase error fairly smooth function

Focal plane: measured PSF intensity

Wavefronts in pupil plane and focal plane are related by a Fourier Transform

Benefits of Phase Retrieval

Knowing aberrations precisely allows for:

- Design correction optics to fix the HST
  - WF/PC II
  - COSTAR
- Optimize alignment of secondary mirror of HST OTA
- Monitor telescope shrinkage (desorption) and focus
- Compute analytic point-spread functions for image deconvolution
  - Noise-free
  - Depends on λ, $\Delta\lambda$, camera, field position
  - Is highly space-variant for WF/PC
  - Eliminates requirement to measure numerous PSF's

In addition, reconstruction of pupil function allows determination of alignment between OTA and WF/PC

Phase Retrieval Basics

Focal plane field   Pupil plane field

Fourier transform: $F(u,v) = \iint_{-\infty}^{\infty} f(x,y) e^{-i2\pi(ux+vy)} dx\,dy$

$= |F(u,v)| e^{i\psi(u,v)} = \mathcal{F}[f(x,y)]$

Focal plane field magnitude
= sqrt(intensity)

Focal plane field phase

Inverse transform: $f(x,y) = \iint_{-\infty}^{\infty} F(u,v) e^{i2\pi(ux+vy)} du\,dv = \mathcal{F}^{-1}[F(u,v)]$

Phase retrieval problem:

Given $|F(u,v)|$ and some constraints on $f(x,y)$,
Reconstruct $f(x,y)$, or equivalently retrieve $\psi(u,v)$

— its phase is the phase of $f(x,y)$ in the pupil which we wish to correct

HST Phase Retrieval Techniques

Minimize error metric by

- Cut & try [Jon Holtzman (Lowell Observatory)]
- Iterative transform algorithm (Gerchberg-Saxton/Misell/Fienup)
- Gradient search (steepest descent, conjugate gradient, . . .)
- Damped least squares (Newton-Raphson)
- Neural network [Todd Barrett & David Sandler (Thermo Electron)]
- Linear programming
- Prescription retrieval [David Redding (Draper Lab)]
- Phase diversity
- etc. (intensity transport, tracking zero sheets, simulated annealing, ...)

- Other groups doing phase retrieval
  - Rick Lyon *et al.* Hughes Danbury Optical Systems
  - Chris Burrows (Space Telescope Science Institute)
  - Mike Shao, Marty Levine *et. al.* (JPL)
  - Francois Roddier (U. Hawaii), . . .

Iterative Transform Algorithm

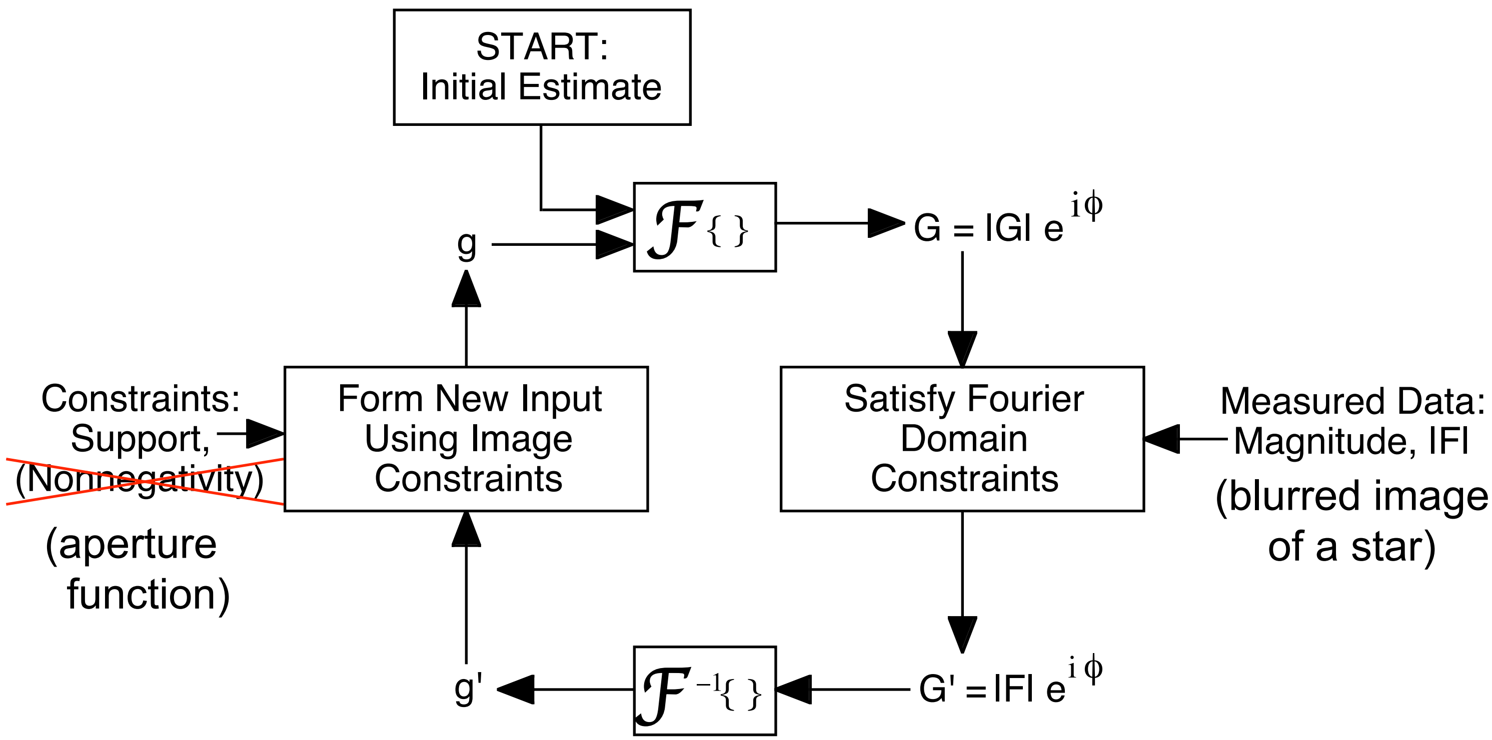

Enforcing magnitude constraints in both domains
is the "Gerchberg-Saxton" algorithm

Phase Retrieval by Nonlinear Optimization

- Model optical system
  - Known parameters (constraints)
  - Unknown parameters (to retrieve)
- Compute model of data
- Compare model of data with actual measured data
  - Compute error metric
- Minimize error metric over space of unknown parameters
  - Using nonlinear optimization algorithms

Nonlinear Optimization Algorithms Employing Gradients

pupil model: $g(x) = |g(x)| e^{i\phi(x)}$, $G(u) = \mathcal{F}[g(x)]$

Minimize Error Metric, e.g.: $E = \sum_u W(u)\left[|G(u)| - |F(u)|\right]^2$

Contour Plot of Error Metric

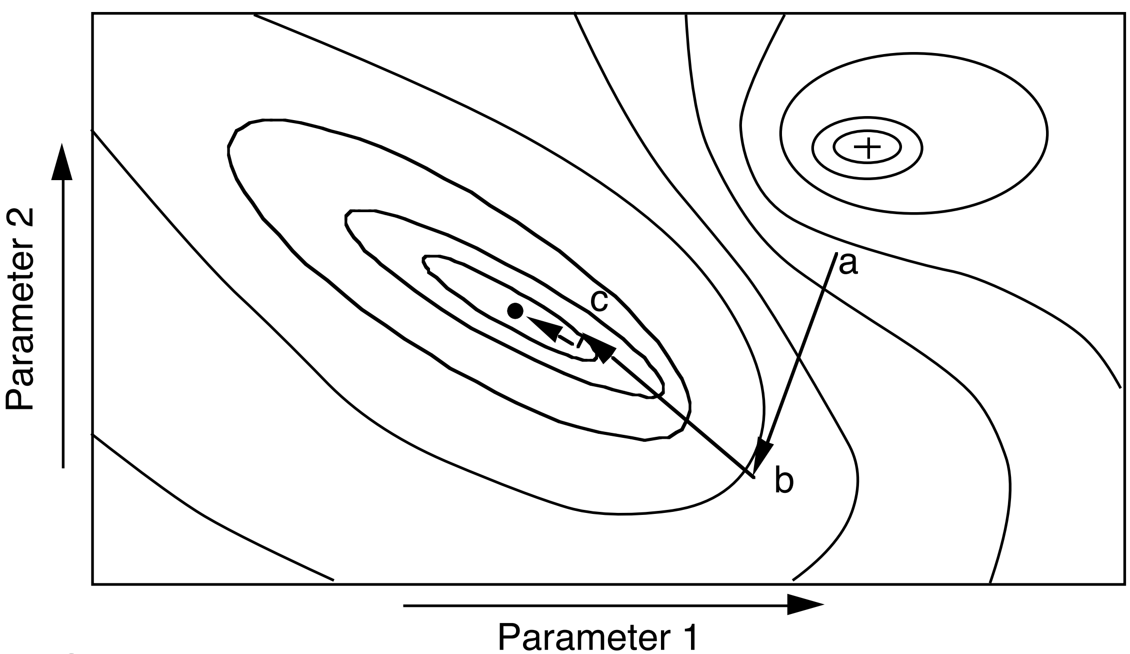

Gradient methods:

(Steepest Descent)
Conjugate Gradient
BFGS/Quasi-Newton
…

Repeat three steps:

1. Compute gradient: $\frac{\partial E}{\partial p_1}, \frac{\partial E}{\partial p_2}, \ldots$
2. Compute direction of search
3. Perform line search

Analytic Gradients of $E = \sum_u W(u)\left[|G(u)| - |F(u)|\right]^2$

Pupil:

$$g(x) = m_o(x) e^{i\theta(x)} \longrightarrow$$

Detector plane:

$$G(u) = P\left[g(x)\right]$$

$$\downarrow$$

$$g^W(x) = P^\dagger\left[G^W(u)\right] \longleftarrow G^W(u) = W(u)\left[|F(u)|\frac{G(u)}{|G(u)|} - G(u)\right]$$

Derivative w.r.t. general parameter: $\frac{\partial E}{\partial p} = -2\,\mathrm{Re}\left[\sum_x \frac{\partial g(x)}{\partial p} g^{W*}(x)\right]$

For point-by-point phase map, $\theta(x)$, $\frac{\partial E}{\partial \theta(x)} = 2\ \mathrm{Im}\left\{g(x)\ g^{W*}(x)\right\}$

For Zernike polynomial coefficients, $\frac{\partial E}{\partial a_j} = 2\ \mathrm{Im}\left\{\sum_x g(x)\ g^{W*}(x)\ Z_j(x)\right\}$

where $\theta(x) = \sum_{j=1}^{J} a_j Z_j(x)$

Propagator P[•] can be single FFT or multiple-plane Fresnel transforms with phase factors and obscurations

Analytic gradients very fast compared with finite differences

J.R. Fienup, "Phase-Retrieval Algorithms for a Complicated Optical System," Appl. Opt. 32, 1737-1746 (1993).

A.S. Jurling and J.R. Fienup, "Applications of Algorithmic Differentiation to Phase Retrieval Algorithms," J. Opt. Soc. Am. A 31, 1348-1359 (2014).

The Institute of OPTICS

More System Modeling Considerations

- Multi-plane propagation including vignetting or multiple aberration planes
- Jitter in telescope pointing during exposure time
- Exclude bad pixels from error metric (dust/saturation/cosmic rays)
- Finite spectral bandwidth
- Shifted WF/PC obscurations vs. field position
- Correct plate scale (depends on field position)
- CCD pixel integration, sampling (undersampling/aliasing)
- Include model of noise (photon, readout)
- Higher-order Zernike's and micro-roughness
- Effect of aberrations in OTA secondary, in WF/PC cameras
- Design aberrations versus field position
- Possibility of non-point-like star

Hubble Telescope Retrieval Approach

- Pupil (support constraint) was known imperfectly
- Phase was relatively smooth and dominated by low-order Zernike's
  - — Use boot-strapping approach

1. With initial guess for pupil, fit Zernike polynomial coefficients
2. With initial guess for Zernike polynomials, estimate pupil by ITA

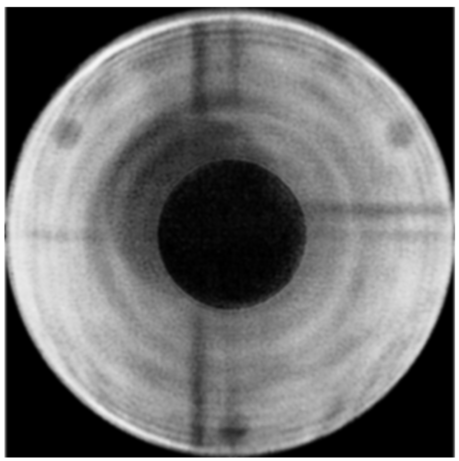

Pupil Reconstructed by ITA

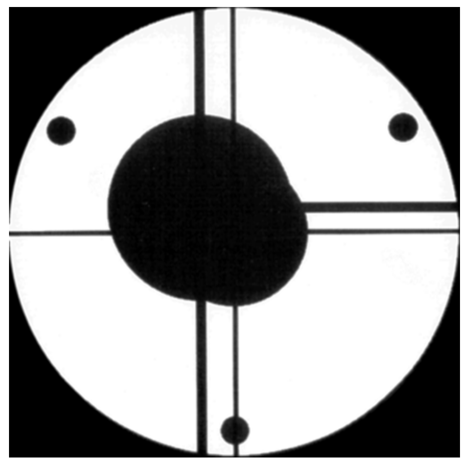

Inferred Model of Pupil

3. Redo steps 1 and 2 until convergence (2 iterations)

Comparison of Actual and Simulated HST Image of a Point Star

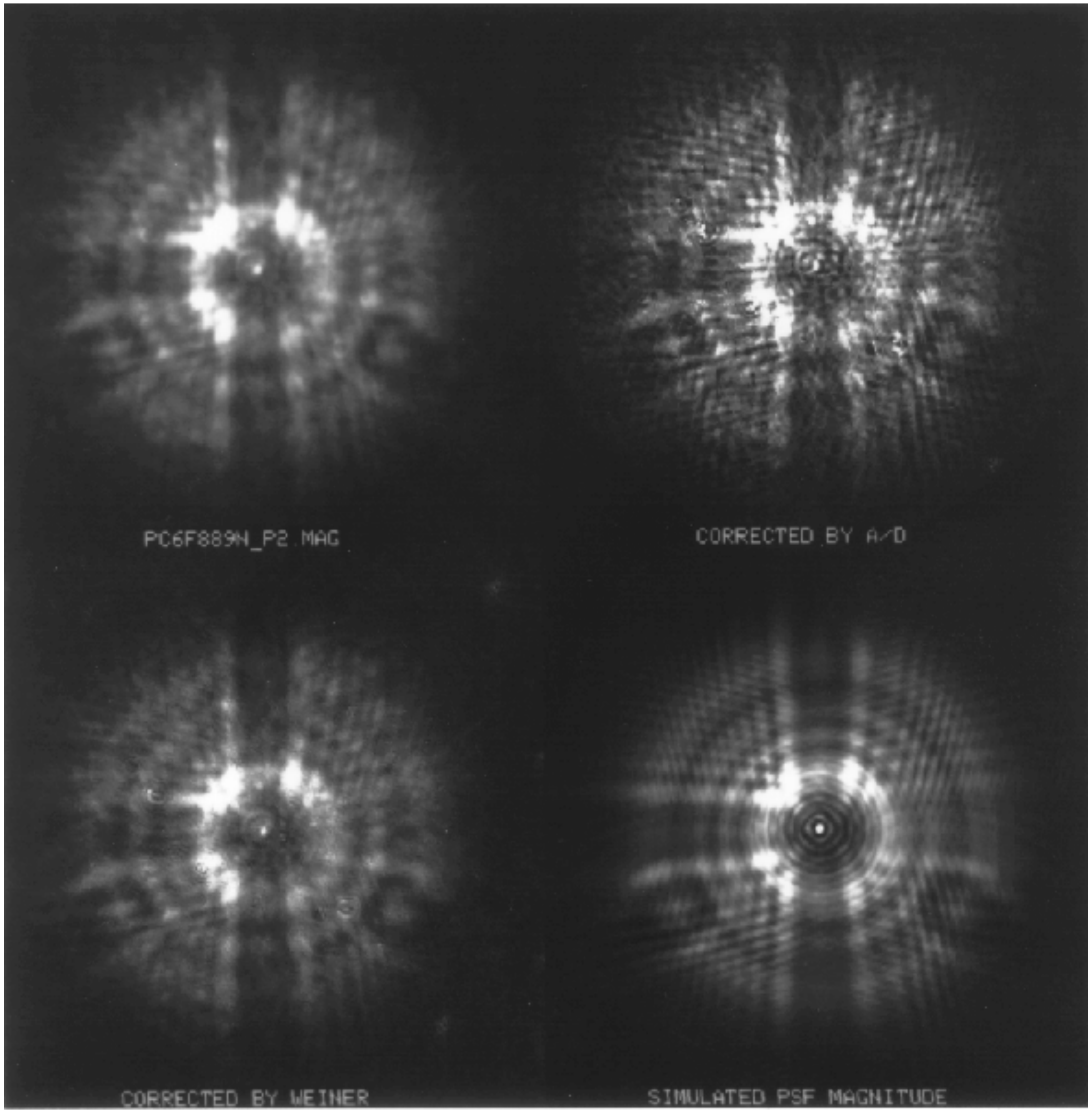

The Institute of OPTICS

Hubble Fixed

James Webb Space Telescope
(Next Generation Space Telescope)

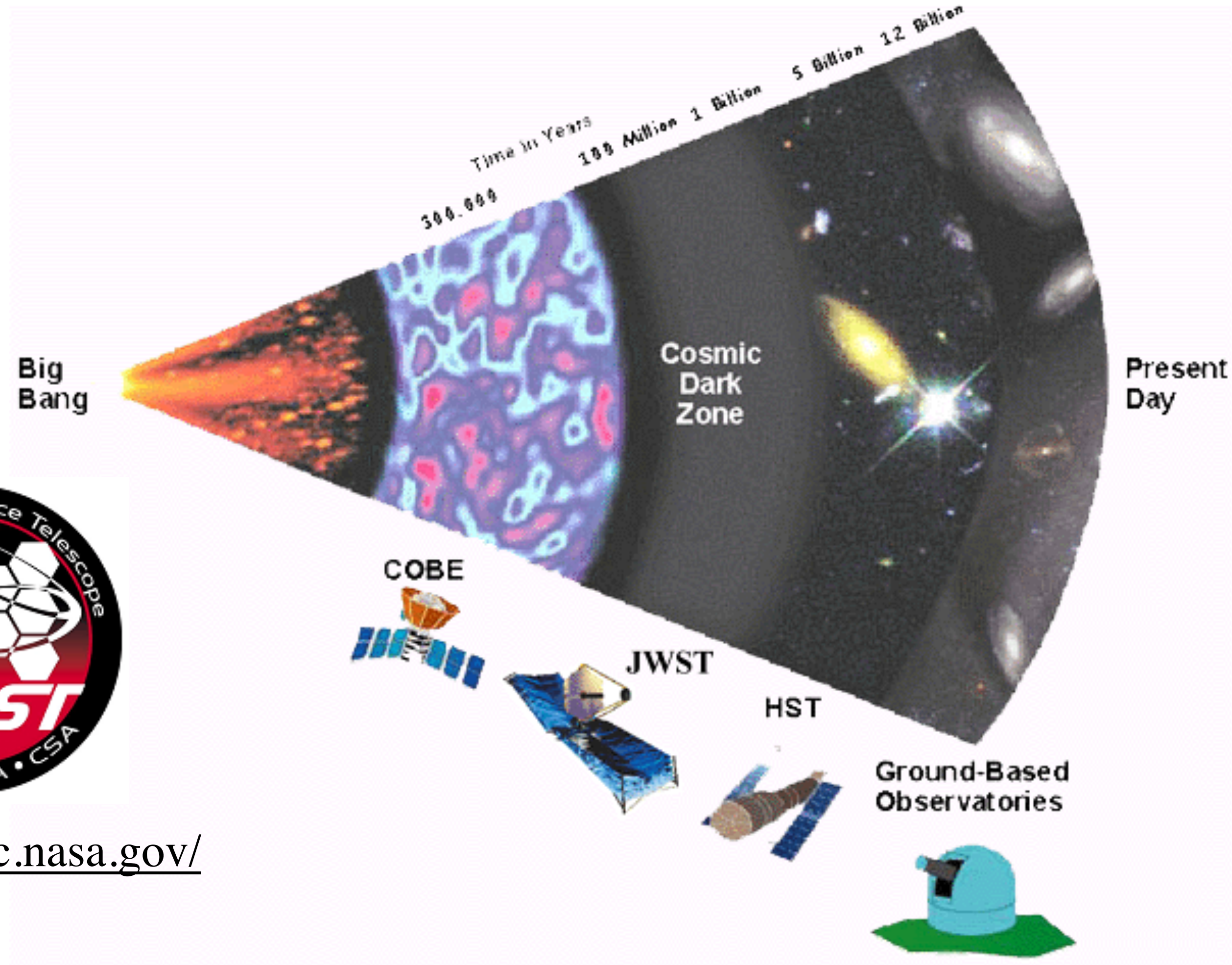

http://ngst.gsfc.nasa.gov/

See farther back towards the beginnings of the universe
Light is red-shifted into infrared

James Webb Space Telescope (JWST)

- See red-shifted light from early universe
  - 0.6 µm to 28 µm
  - L2 orbit for passive cooling, avoiding light from sun and earth
  - 6.5 m diameter primary mirror
    - Deployable, segmented optics
    - Phase retrieval to align segments

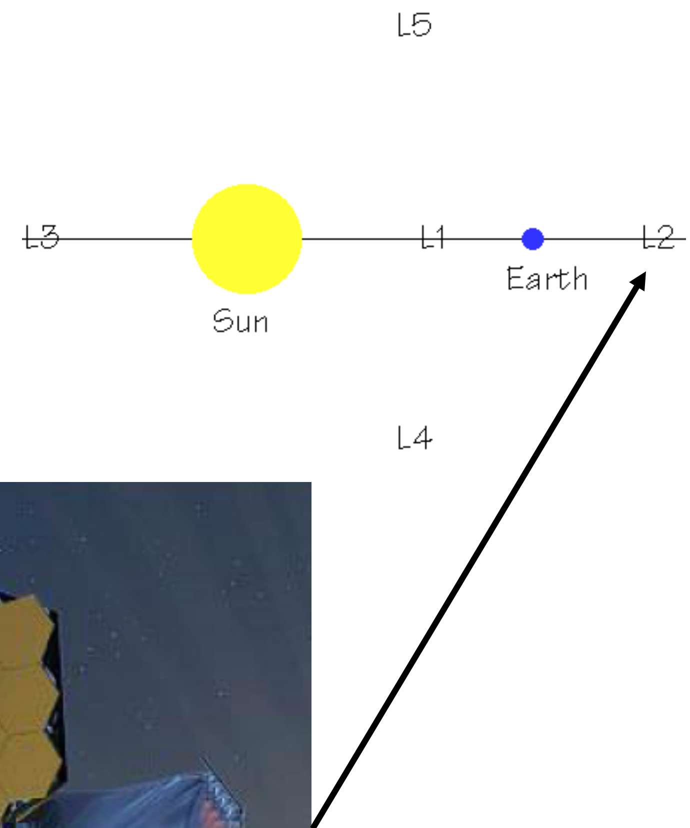

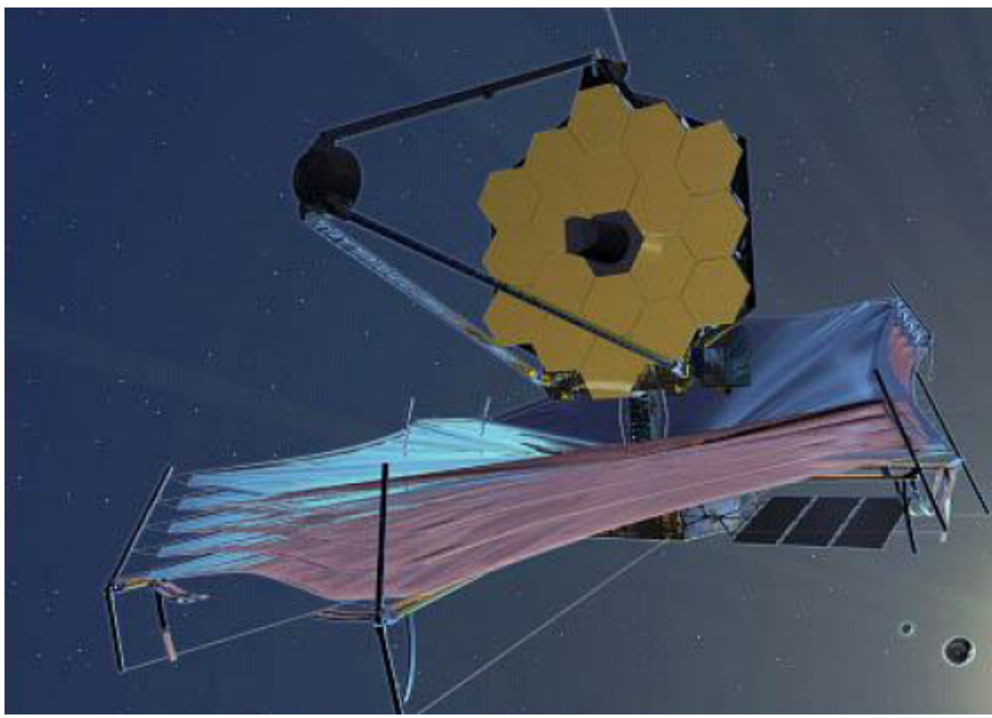

Phase Retrieval for JWST

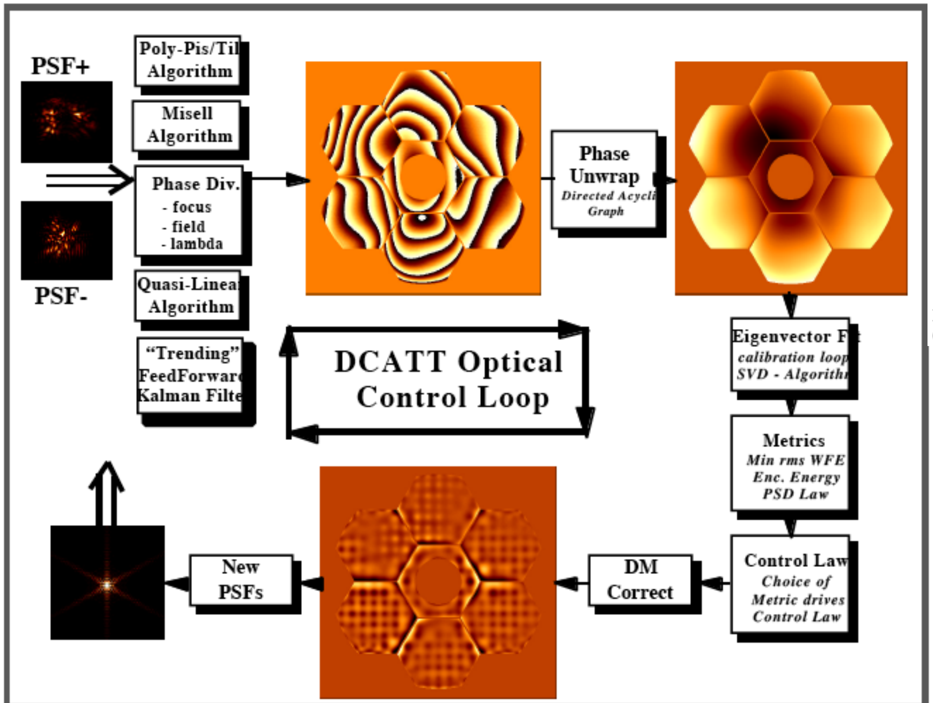

R. Lyon et *al.*, (GSFC)

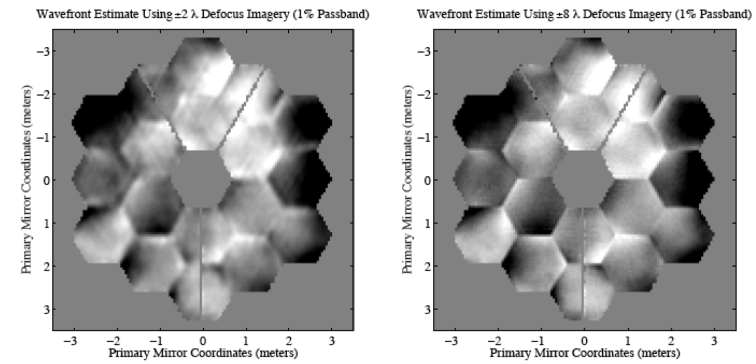

Figure 3: Estimates of the JWST OPD from the ±2 wave defocus PSF pair (left) and the ±8 wave pair (right). As in Figure 1, the OPDs are shown with a linear intensity scale stretched over ±200nm.

J. Green (JPL), B. Dean (GSFC) *et al.*, Proc. SPIE (Glasgow 2004)

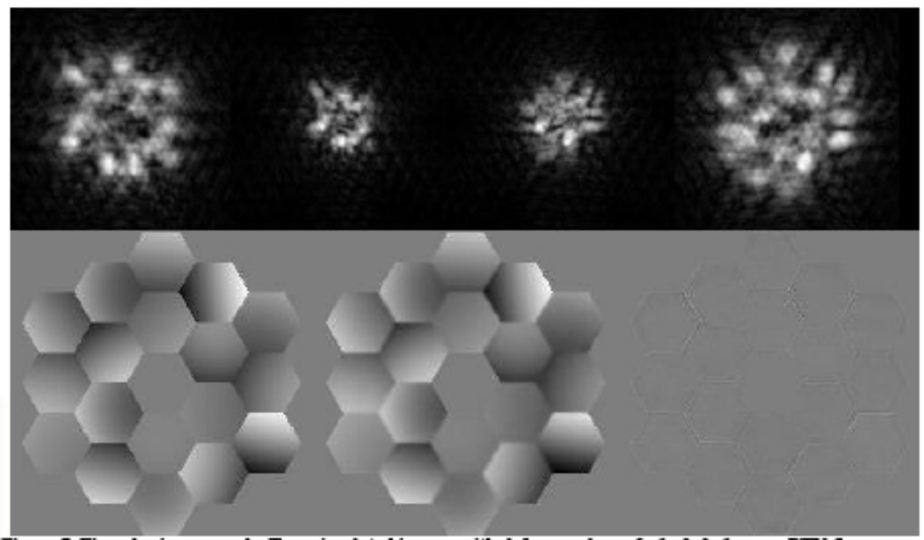

Figure 7. Fine phasing example. Top: simulated images with defocus values of –6, -3, 3, 6 waves PTV (log display). Lower left: the actual phase map (~250 nm rms). Lower center: estimated phase. Lower right: difference (~10 nm rms).

D.S Acton et *al.*(Ball Aerospace), Proc. SPIE (Glasgow 2004)

NASA has chosen phase retrieval as the fine phasing approach for JWST.

JWST at UofR
Robust WaveFront Sensing

- Develop improved WFS (phase retrieval) algorithms
  - Faster, converge more reliably, less sensitive to noise, 2π jumps
  - Work with larger aberrations, broadband illumination, jitter
    - Refining iterative transform, gradient search algorithms
    - Increase robustness and accuracy
  - Extended objects
  - Phase retrieval performance

- Laboratory experiments at UR
  - A-O MEMS DM (hexagonal segments)
  - Interferometer measure wavefront independently
  - Put in misalignment, reconstruct wavefronts, compare with interferometer “truth”
  - Point source or extended scene

- Assisting NASA with ground testing

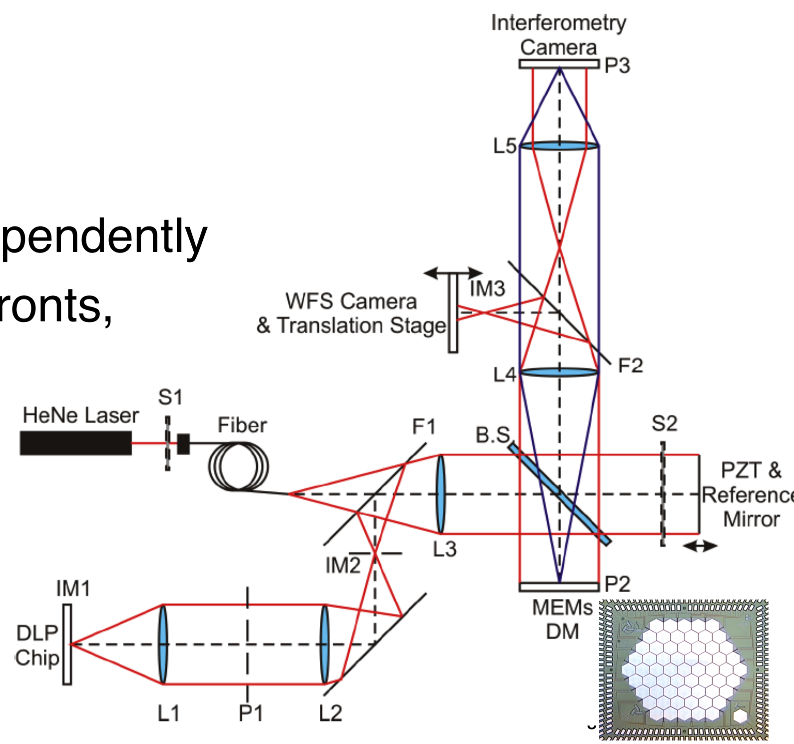

Fine Phasing of JWST with Focus-Diverse Phase Retrieval

Problem : Want to find JWST system wavefront

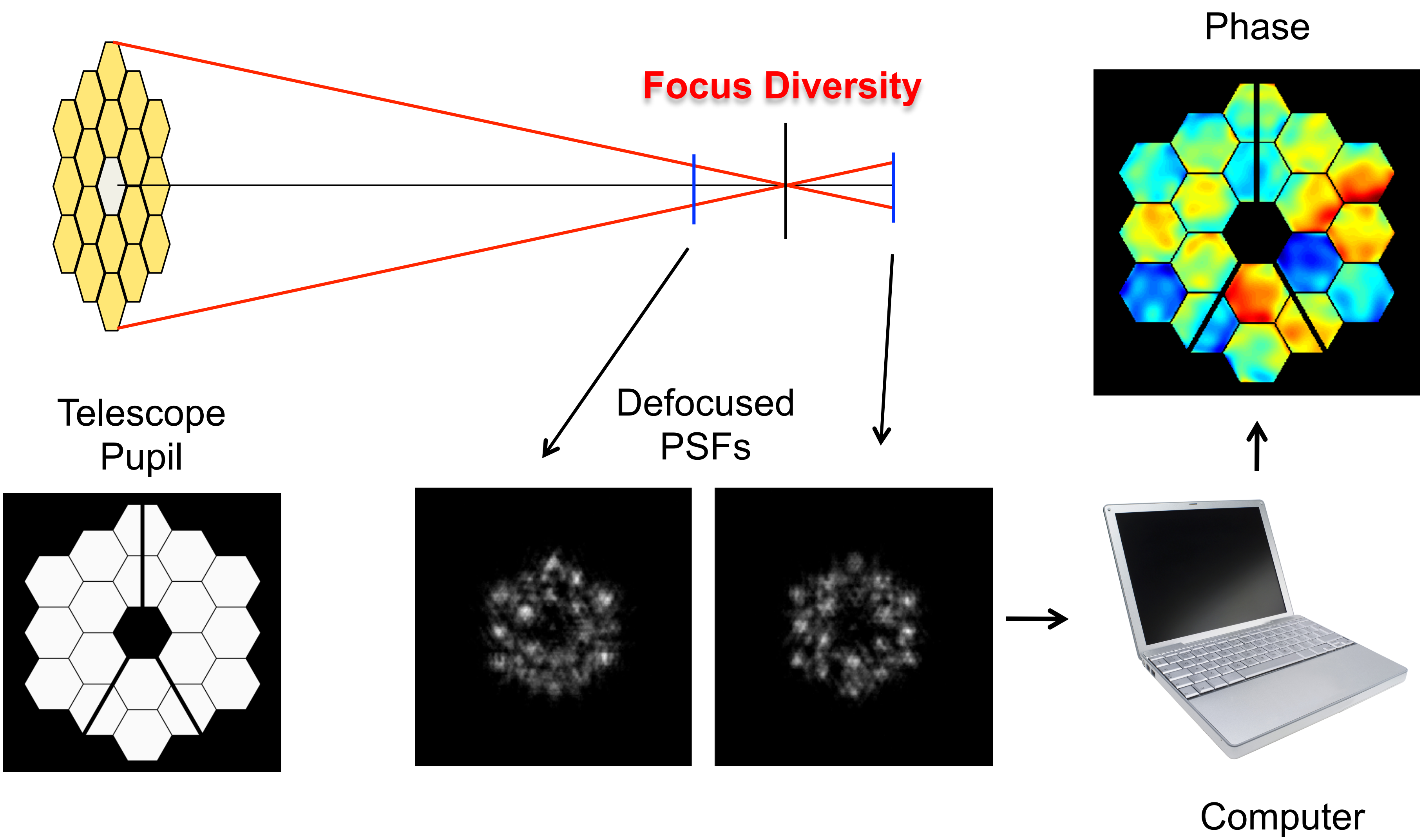

Dustin Moore

Unknown Transverse-Translation Diversity for *in-situ* Optical Metrology of NIRCam

Optical Test Technologies for JWST

- Phase retrieval involved with
  - Instrument testing
  - All-instrument (ISIM) testing
  - Observatory level testing
  - On-orbit commissioning
  - On-orbit figure maintenance

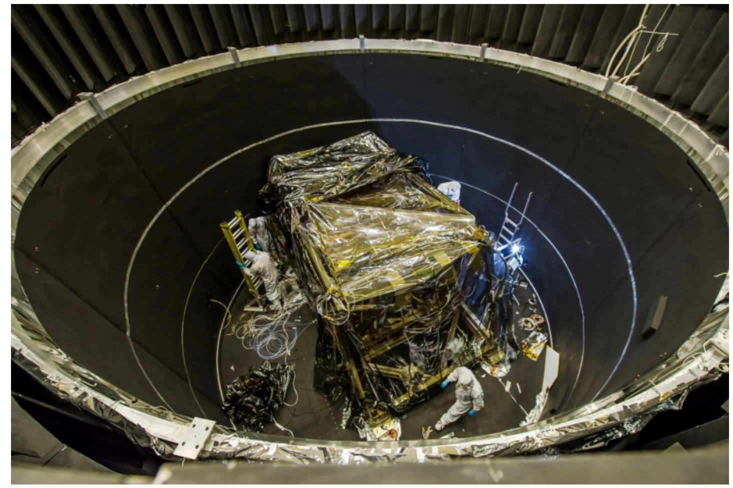

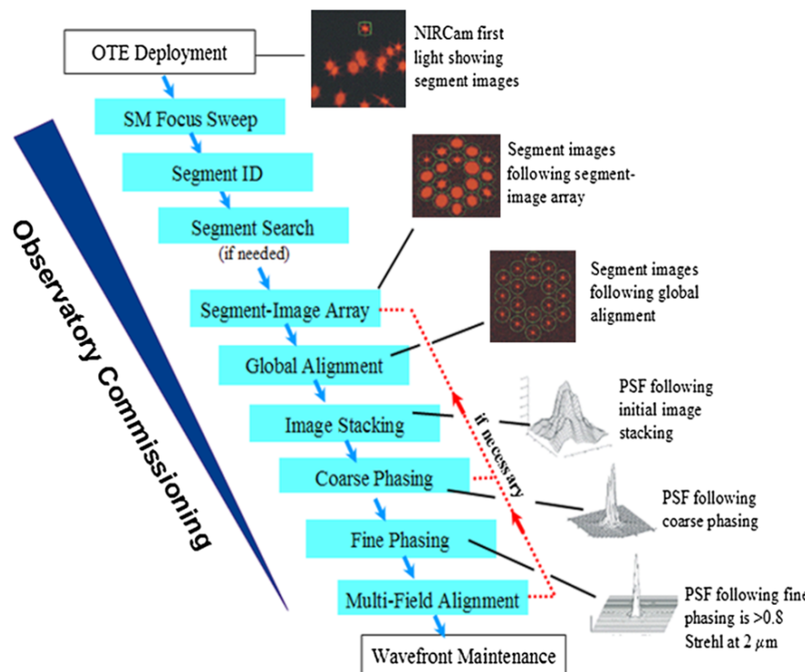

- Assisting NASA: NIRCam optical stability during ground testing and on-orbit

Graphics: https://www.flickr.com/photos/nasawebbtelescope/9549725296/in/set-72157649329984611
http://opticalengineering.spiedigitallibrary.org/article.aspx?articleid=1183208

Metrology of NIRCam by Unknown Translation-Diversity Phase Retrieval

- Need light path traversing only NIRCam
  - Can view point sources with prism + Lyot stop selected in pupil wheel:
  - Lyot stop part of coronograph
- Wheel rotation yields diversity of PSFs

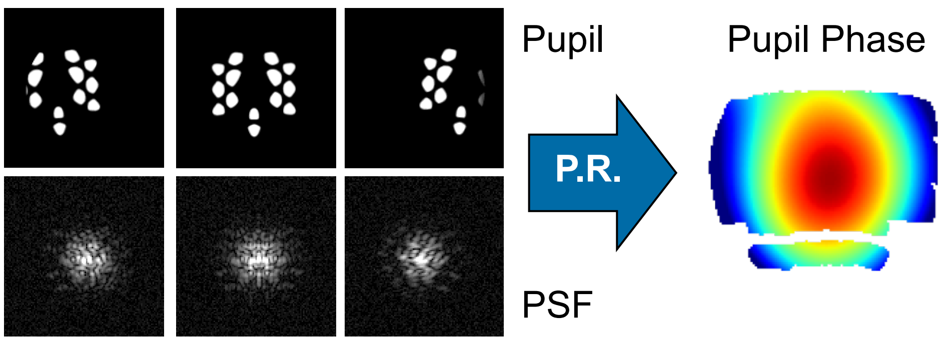

- Challenges to classic trans. diversity:
  - Translation & rotation of Lyot stop imprecisely known in exit pupil
  - Unknown pupil illumination
  - Unknown linear pupil phase varies with PSF (moving prism/target jitter)
  - Unknown plate scale

NIRCam Module A

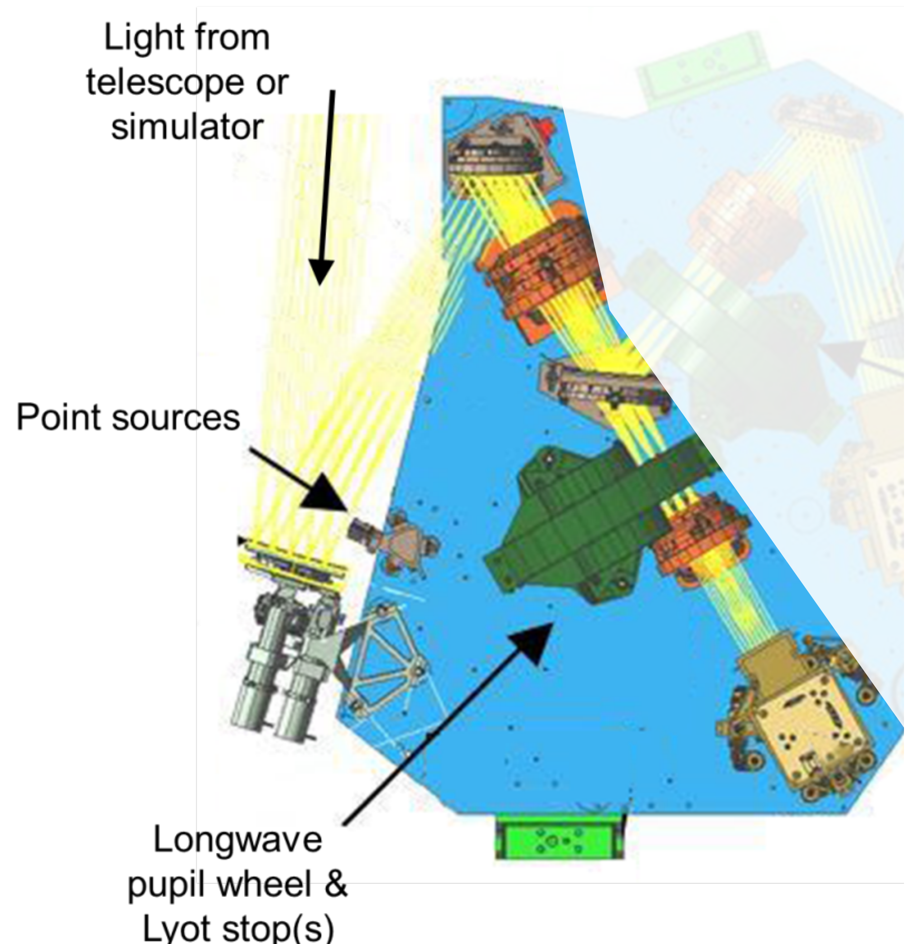

http://www.stsci.edu/jwst/instruments/nircam/instrumentdesign

The Institute of OPTICS

Metrology of NIRCam by Unknown Translation-Diversity Phase Retrieval

- Unknown linear phase per PSF impedes translation estimation from PSFs

- We devised a new TTD algorithm that tends to recover all unknowns
  - Needs no explicit direction or distance of translation information
  - Assumes subaperture translations were sequentially contiguous
  - Bootstrapping process that restricts the number of unknowns that must be confronted in early stages [1]:

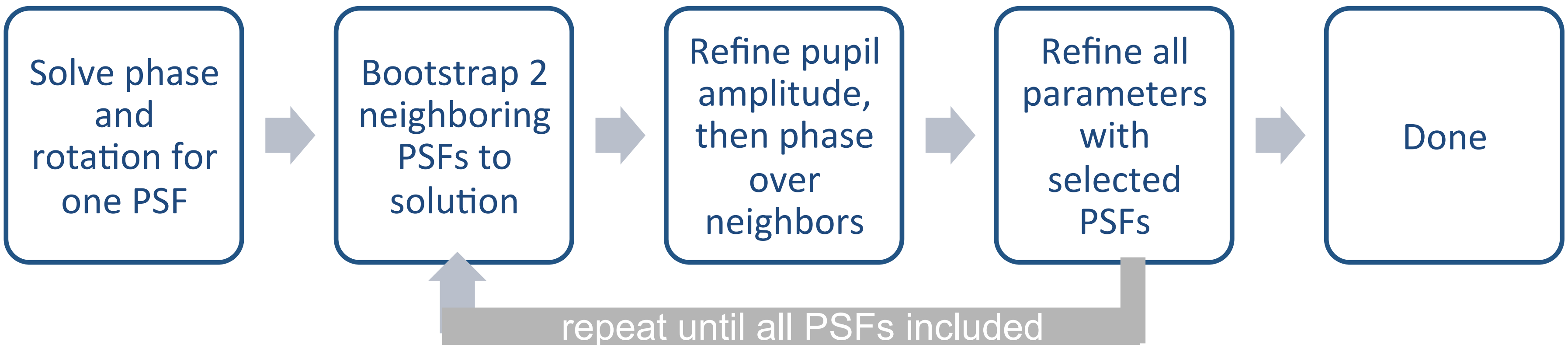

- **Considerably relaxes requirements on hardware for flexible metrology**
  - Wave a known transmission function through pupil in an unknown fashion while collecting a time-series of PSFs and apply algorithm

[1] D. B. Moore and J. R. Fienup, "Transverse Translation Diversity Wavefront Sensing with Limited Position and Pupil Illumination Knowledge," Proc. SPIE **9143**, 91434F (2014).

Laboratory TTD Experiment

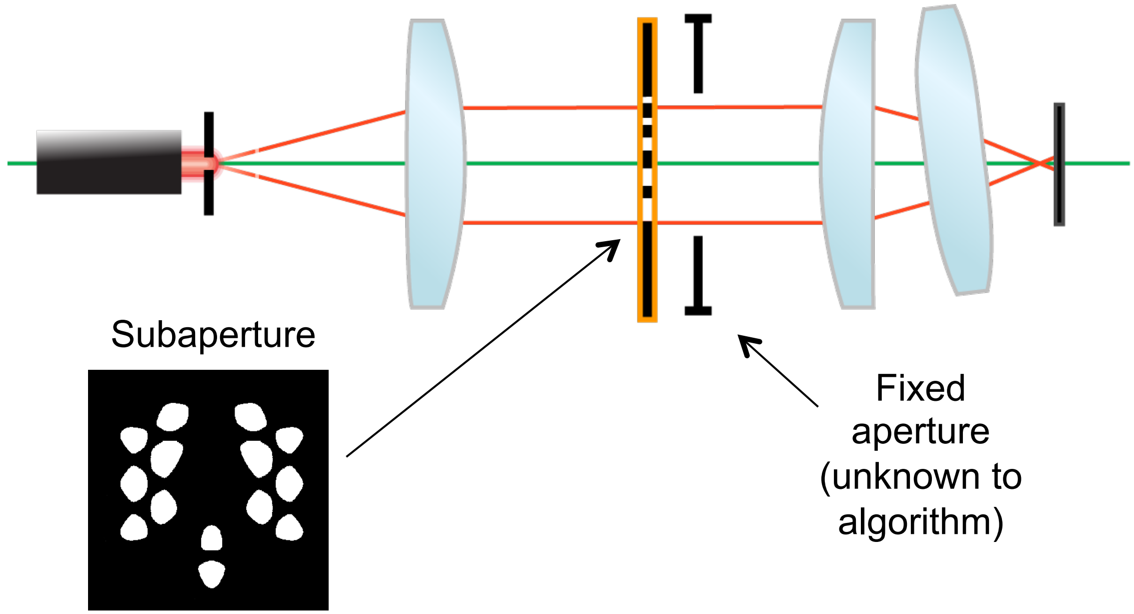

- 4-*f* system with aberrations induced by a misaligned third-element
- Subaperture raster-scanned in two-dimensional grid
  —Small subaperture translations between each PSF / contiguous motion

Solving one PSF

1. Select one PSF, define its subaperture position as the middle of the pupil
2. Operator guesses approximate defocus, sub-aperture rotation, plate scale
3. Minimize metric to fit linear phase
4. Minimize to fit higher-order pupil phase terms
5. Add subaperture rotation and plate scale to estimable unknowns, minimize

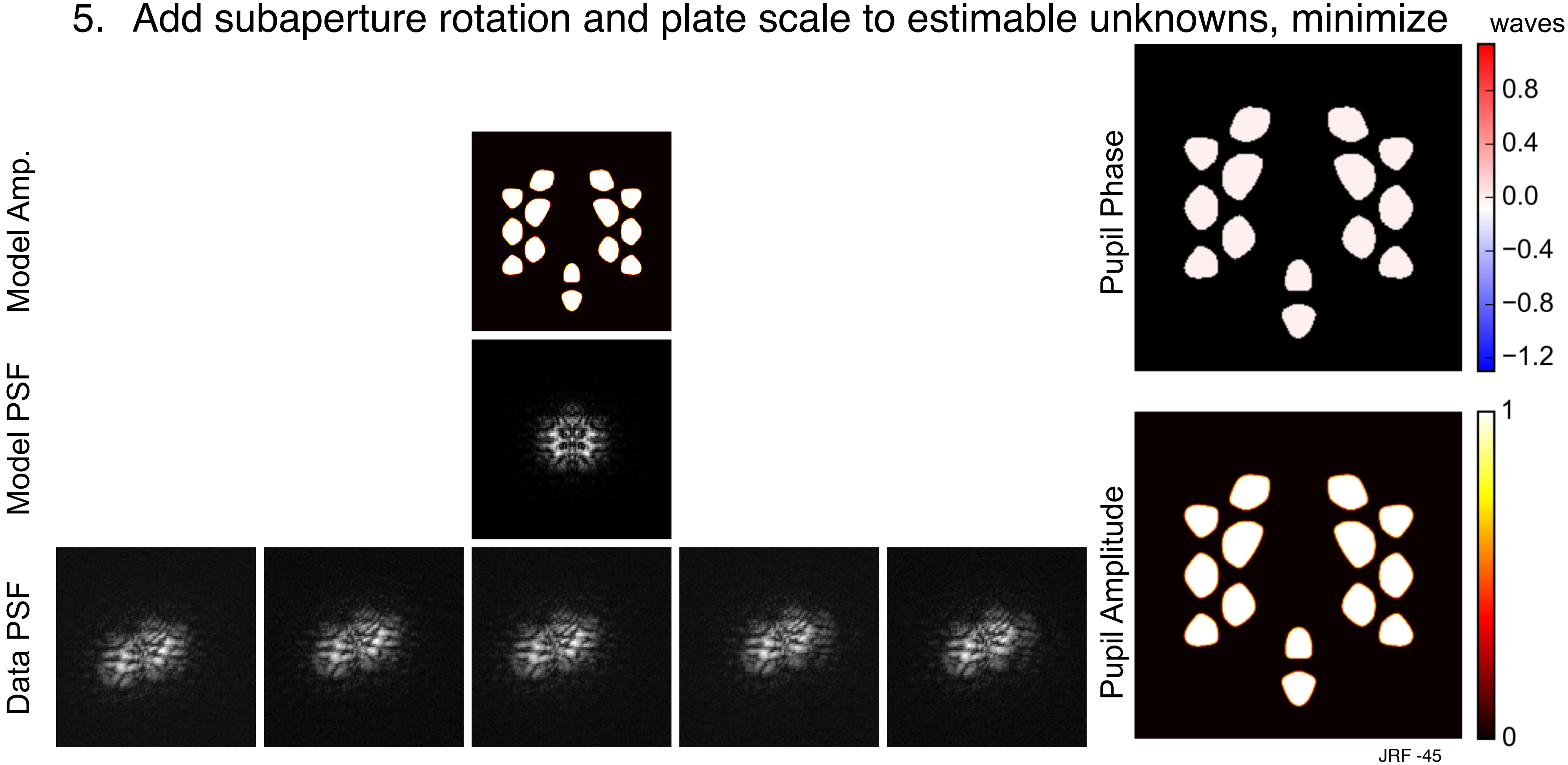

Solving one PSF

1. Select one PSF, define its subaperture position as the middle of the pupil
2. Operator guesses approximate defocus, sub-aperture rotation, plate scale
3. Minimize metric to fit linear phase
4. Minimize to fit higher-order pupil phase terms
5. Add subaperture rotation and plate scale to estimable unknowns, minimize

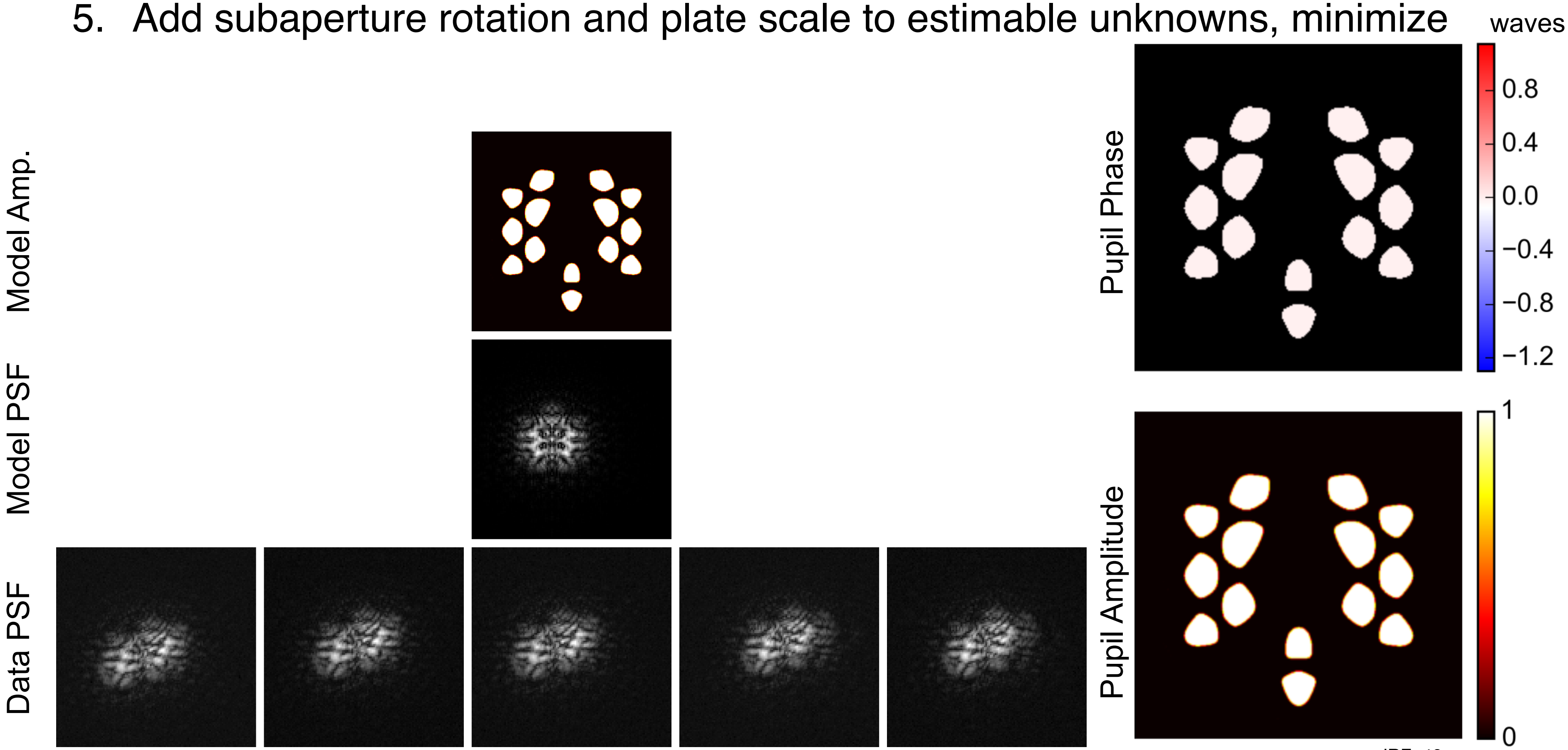

Solving one PSF

1. Select one PSF, define its subaperture position as the middle of the pupil
2. Operator guesses approximate defocus, sub-aperture rotation, plate scale
3. Minimize metric to fit linear phase
4. Minimize to fit higher-order pupil phase terms
5. Add subaperture rotation and plate scale to estimable unknowns, minimize

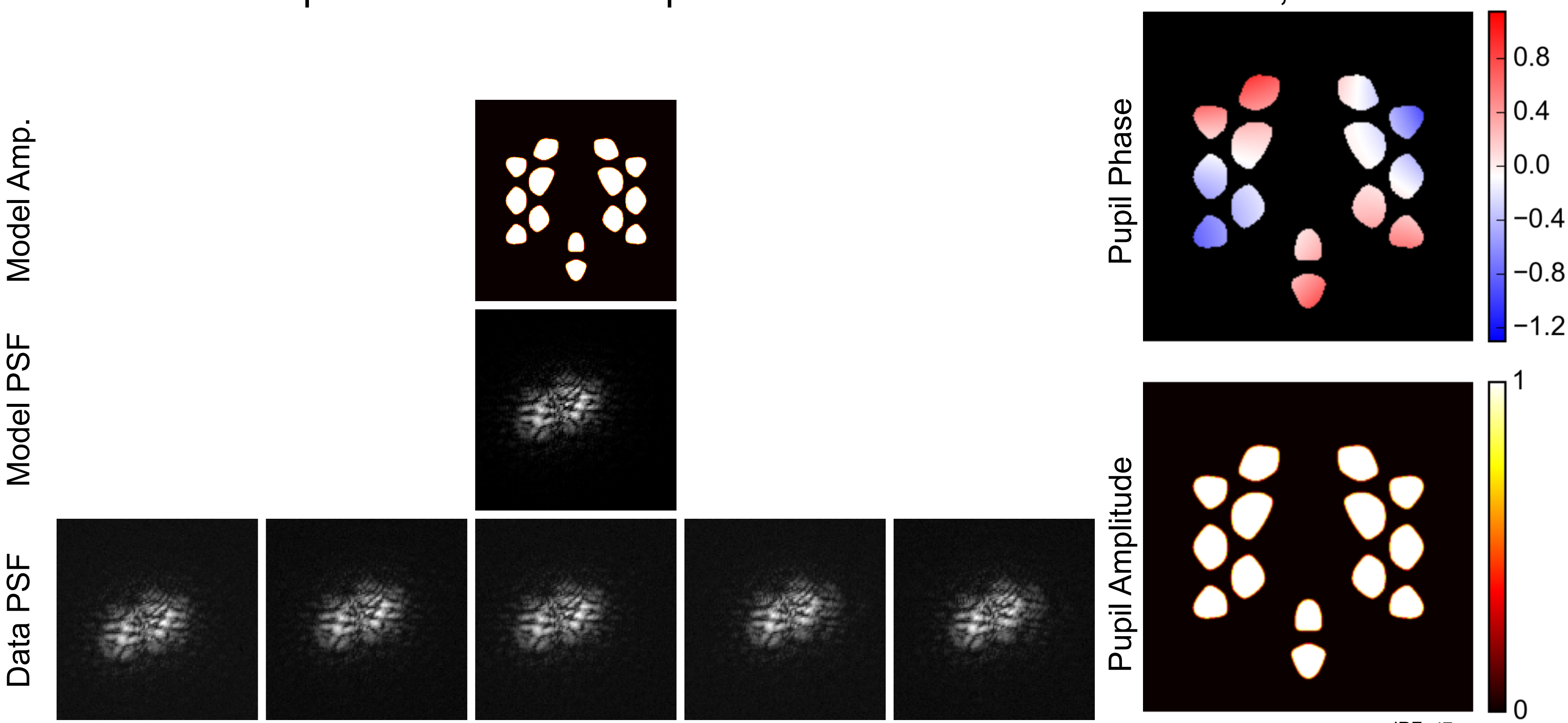

Solving one PSF

1. Select one PSF, define its subaperture position as the middle of the pupil
2. Operator guesses approximate defocus, sub-aperture rotation, plate scale
3. Minimize metric to fit linear phase
4. Minimize to fit higher-order pupil phase terms
5. Add subaperture rotation and plate scale to estimable unknowns, minimize

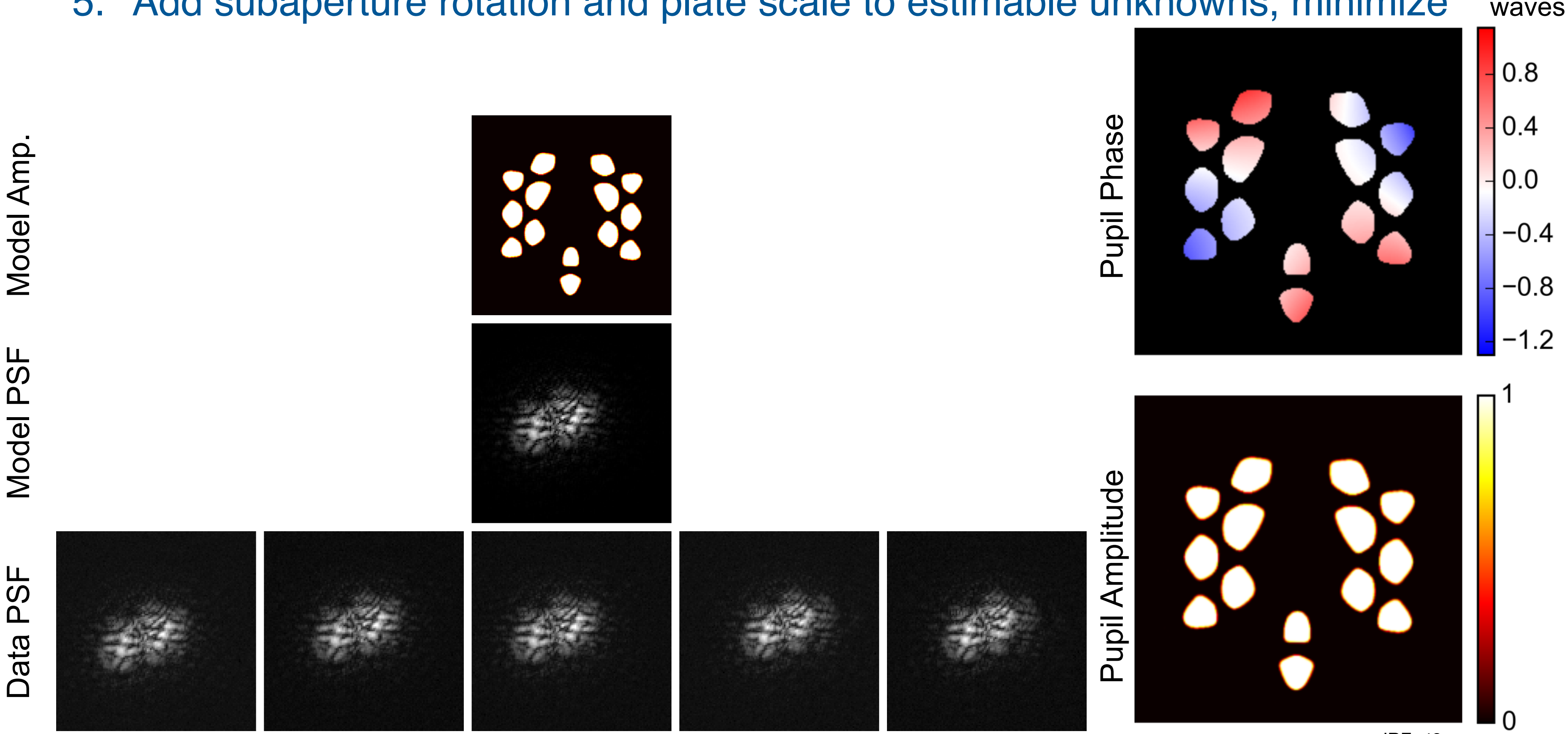

Boostrap Neighboring PSFs

1. Select two neighboring PSF, assume the sub-aperture orientation of first
2. Minimize metric to fit linear phase of neighbors
3. Minimize metric to fit subaperture trans. and linear phase of neighbors
4. Add subaperture rotation of neighbors to estimable unknowns, minimize

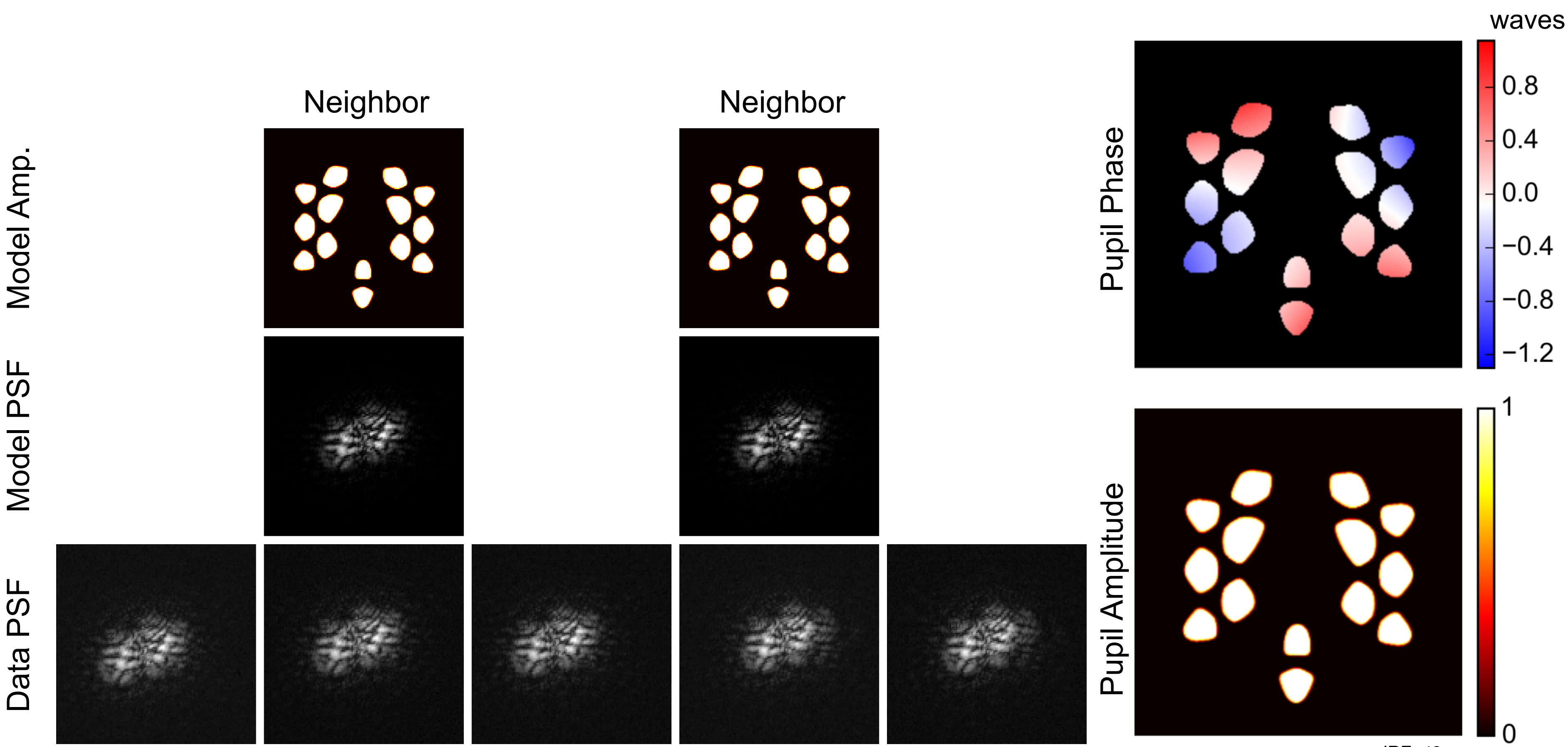

Boostrap Neighboring PSFs

1. Select two neighboring PSF, assume the sub-aperture orientation of first
2. Minimize metric to fit linear phase of neighbors
3. Minimize metric to fit subaperture trans. and linear phase of neighbors
4. Add subaperture rotation of neighbors to estimable unknowns, minimize

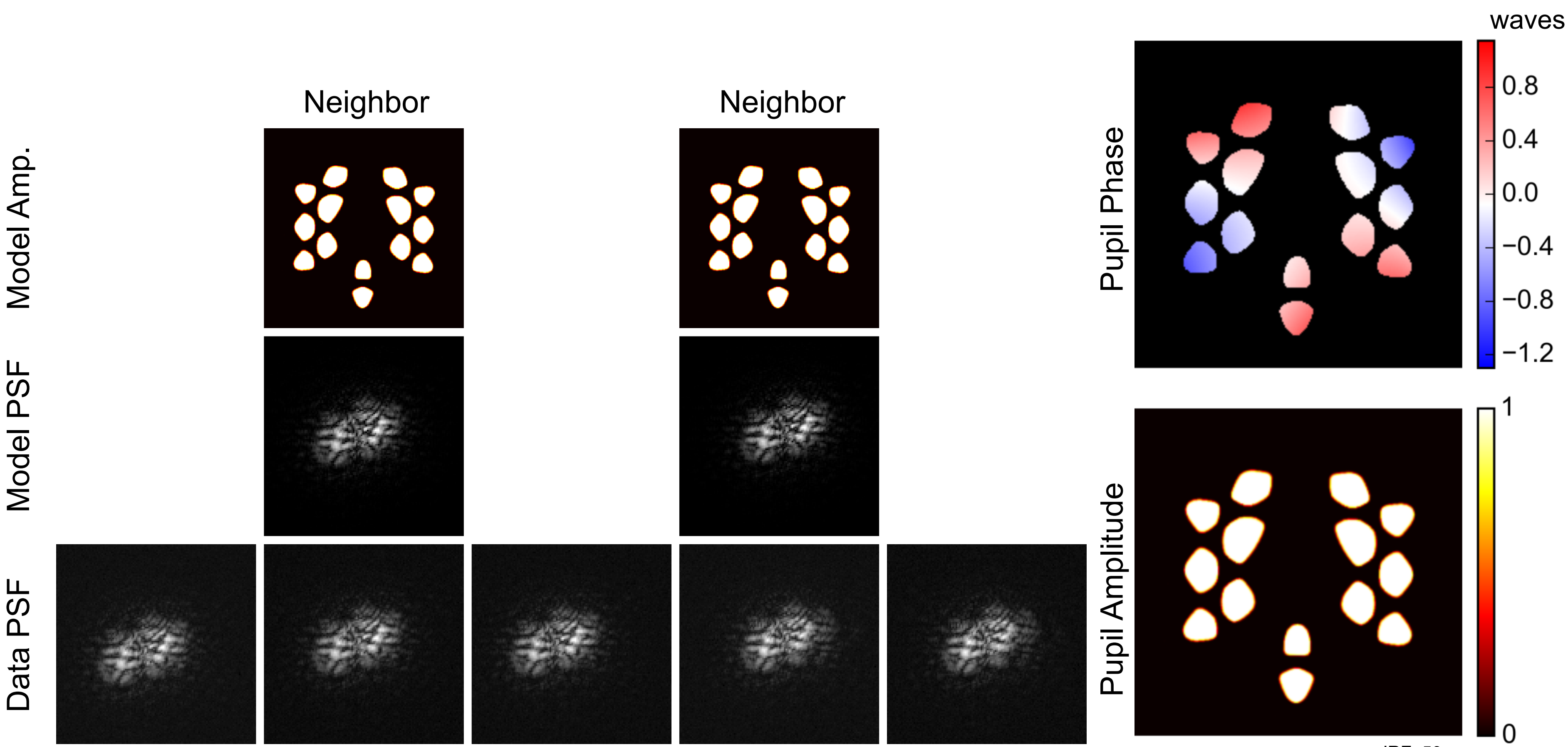

Boostrap Neighboring PSFs

1. Select two neighboring PSF, assume the sub-aperture orientation of first
2. Minimize metric to fit linear phase of neighbors
3. Minimize metric to fit subaperture trans. and linear phase of neighbors
4. Add subaperture rotation of neighbors to estimable unknowns, minimize

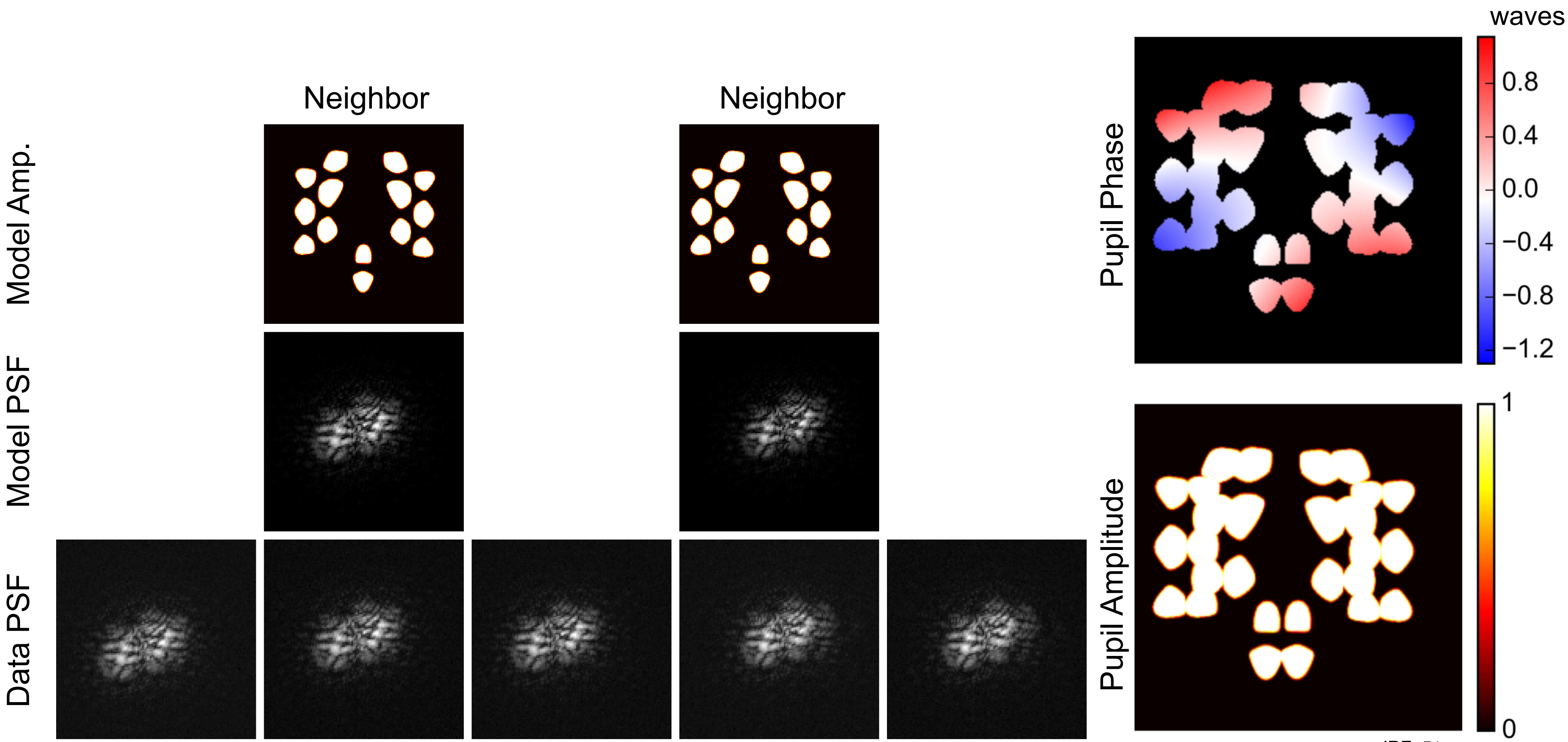

Boostrap Neighboring PSFs

1. Select two neighboring PSF, assume the sub-aperture orientation of first
2. Minimize metric to fit linear phase of neighbors
3. Minimize metric to fit subaperture trans. and linear phase of neighbors
4. Add subaperture rotation of neighbors to estimable unknowns, minimize

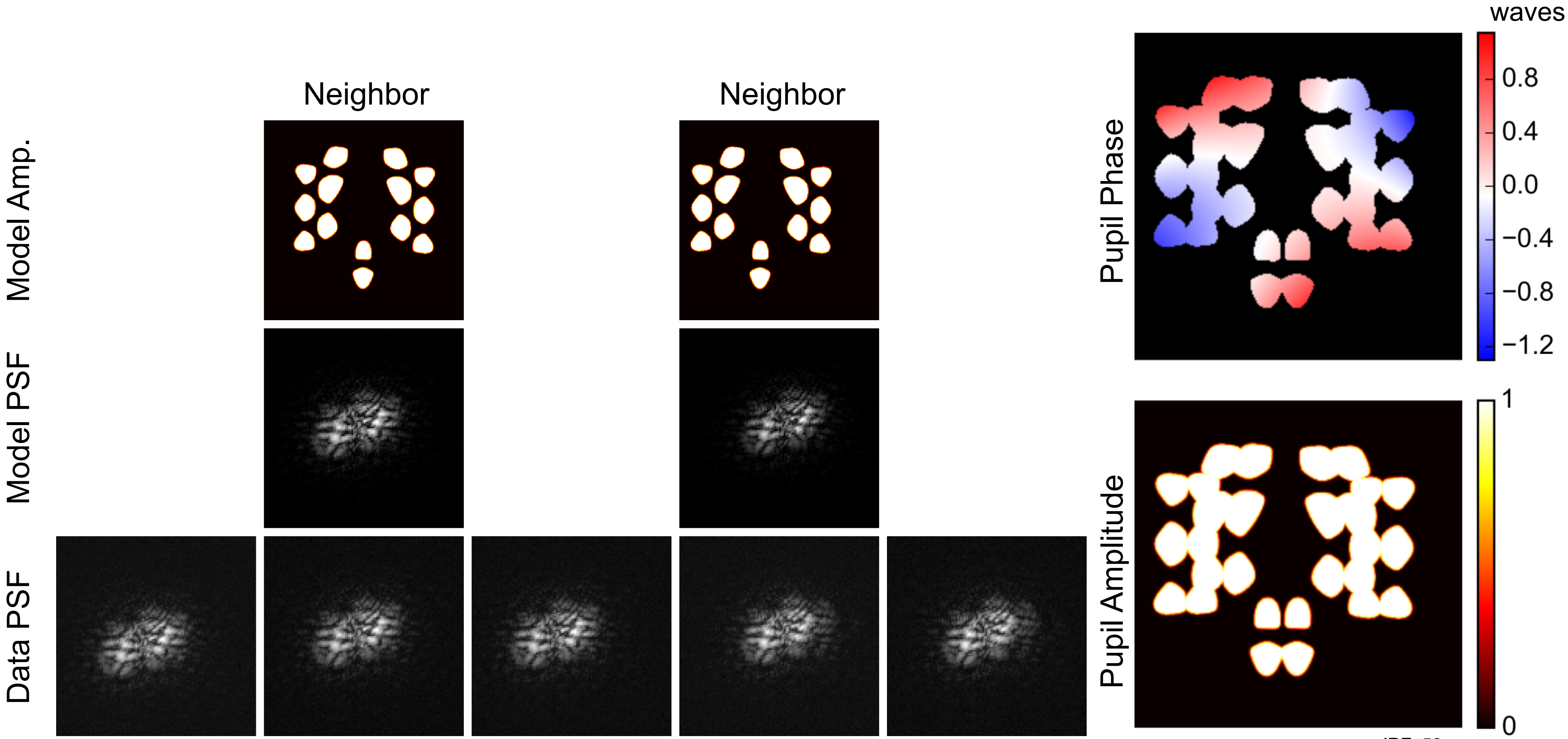

Refine Overall Solution

1. Bring back earlier PSF solution(s)
2. Minimize metric to fit pupil amplitude, neighbor linear phase, neighbor subaperture translations and rotations
3. Add overall pupil phase to list of unknowns, minimize
4. Add translations/rotations of earlier PSFs to estimable unknowns, minimize

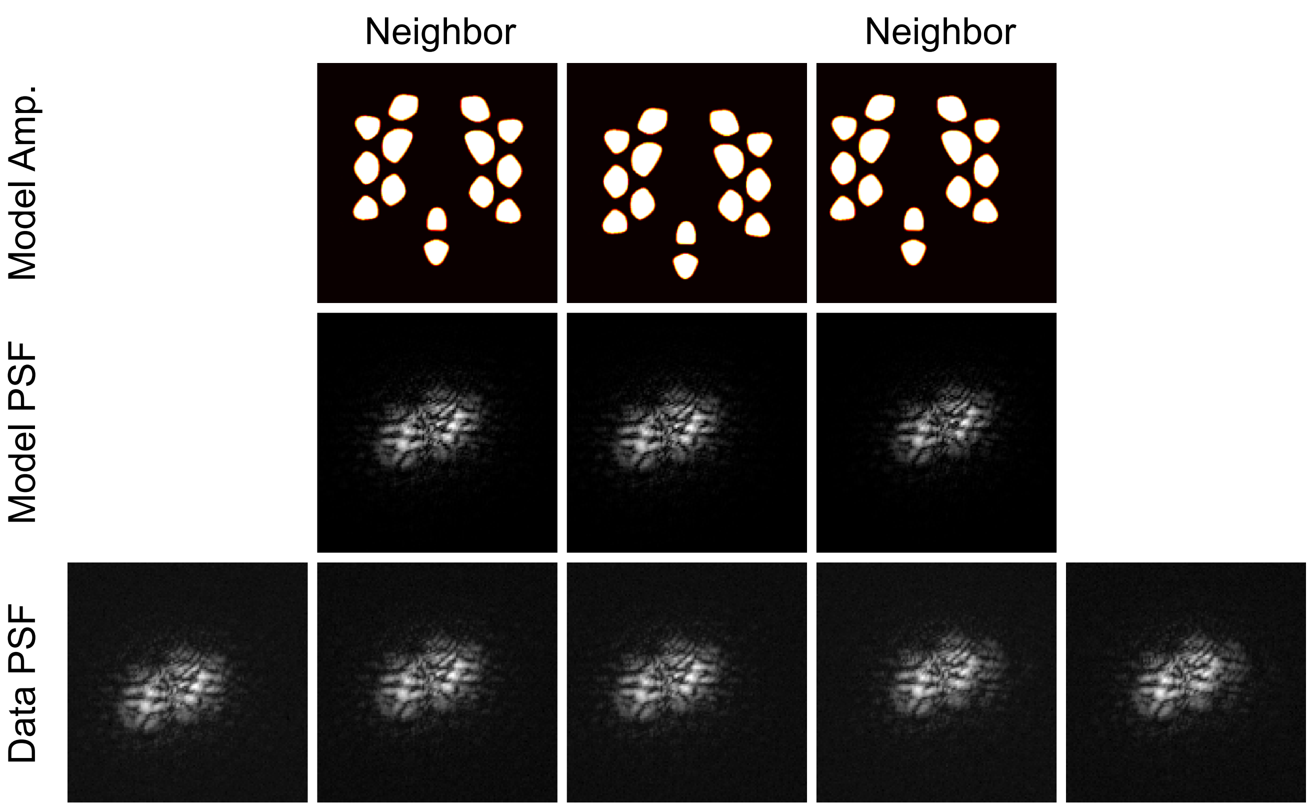

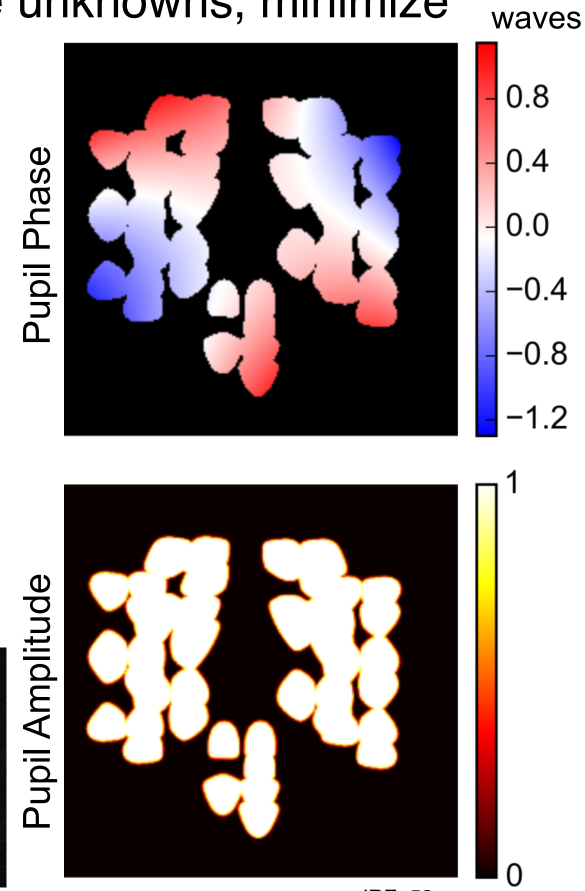

Refine Overall Solution

1. Bring back earlier PSF solution(s)
2. Minimize metric to fit pupil amplitude, neighbor linear phase, neighbor subaperture translations and rotations
3. Add overall pupil phase to list of unknowns, minimize
4. Add translations/rotations of earlier PSFs to estimable unknowns, minimize

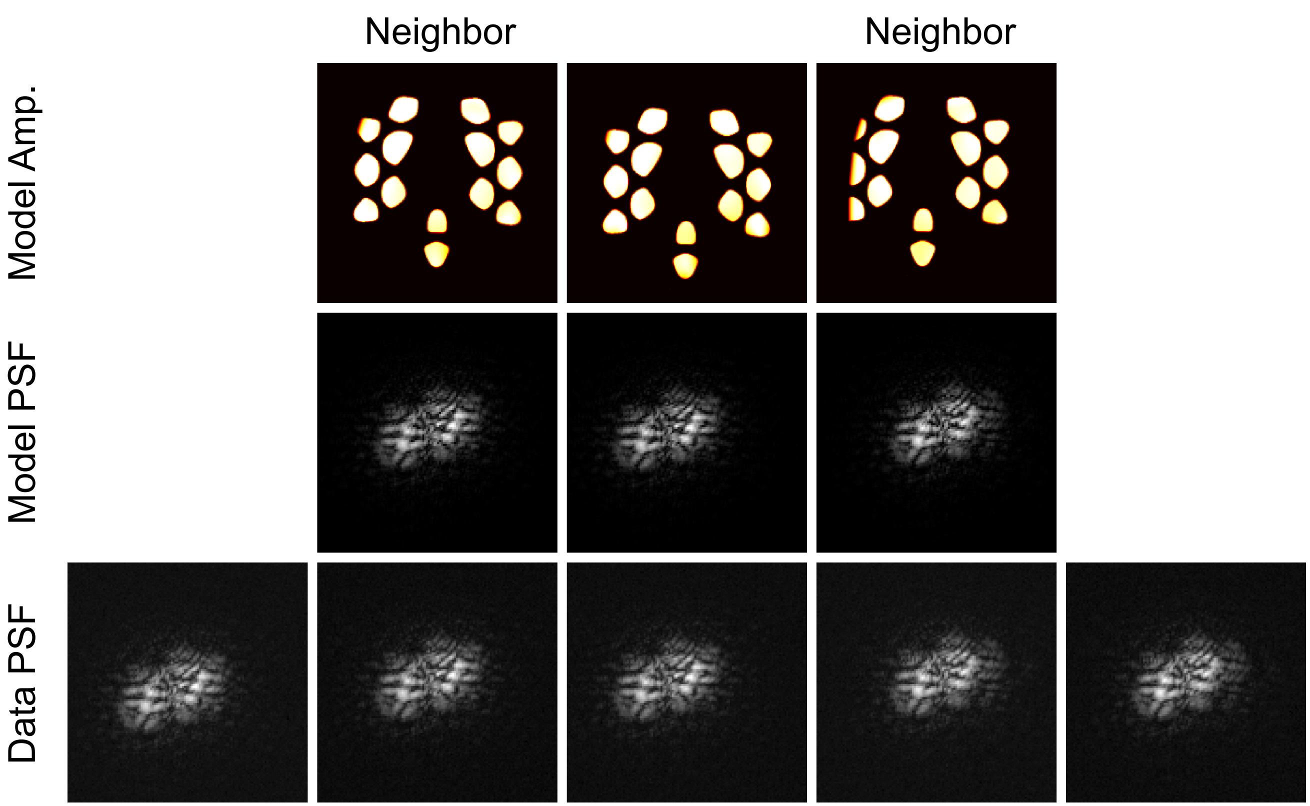

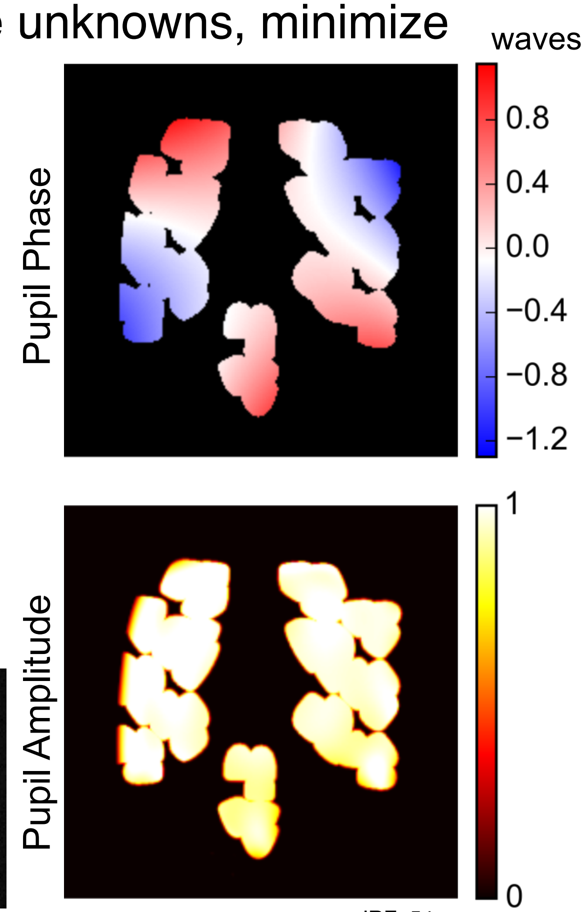

Refine Overall Solution

1. Bring back earlier PSF solution(s)
2. Minimize metric to fit pupil amplitude, neighbor linear phase, neighbor subaperture translations and rotations
3. Add overall pupil phase to list of unknowns, minimize
4. Add translations/rotations of earlier PSFs to estimable unknowns, minimize

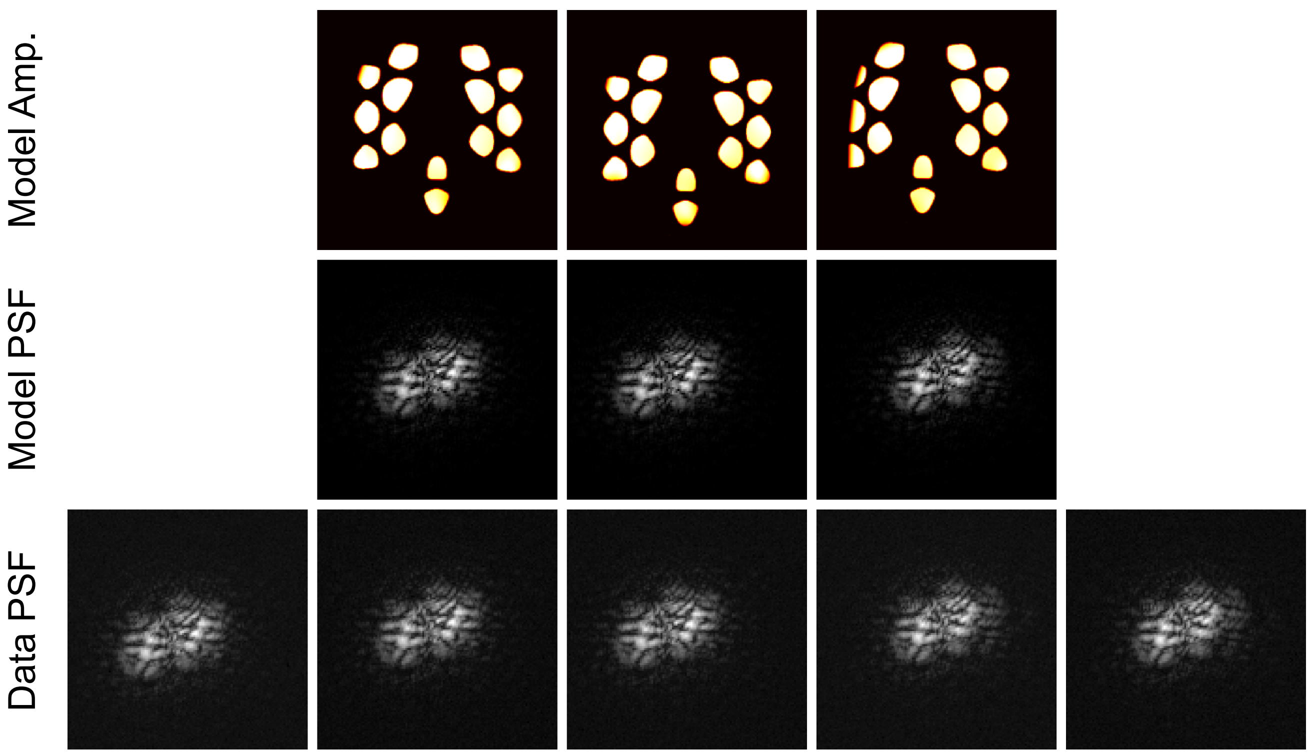

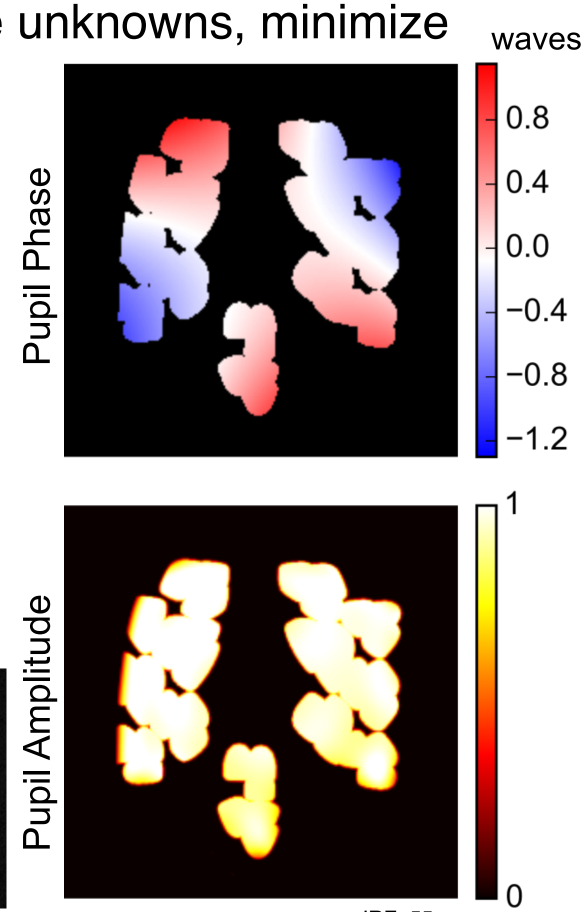

Refine Overall Solution

1. Bring back earlier PSF solution(s)
2. Minimize metric to fit pupil amplitude, neighbor linear phase, neighbor subaperture translations and rotations
3. Add overall pupil phase to list of unknowns, minimize
4. Add translations/rotations of earlier PSFs to estimable unknowns, minimize

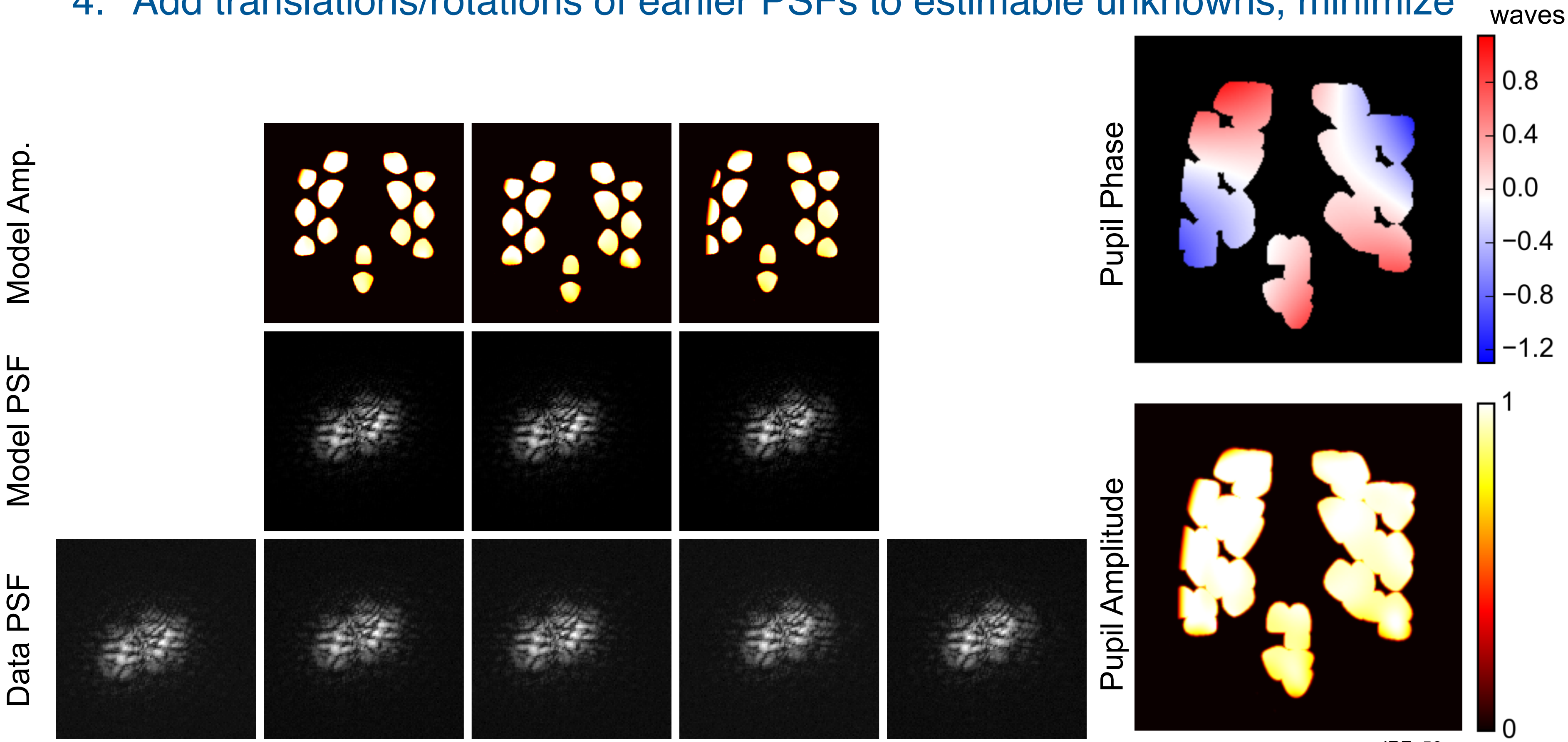

Repeat

- Repeat bootstraping and refinement procedures with neighbors until all PSFs are included in solution

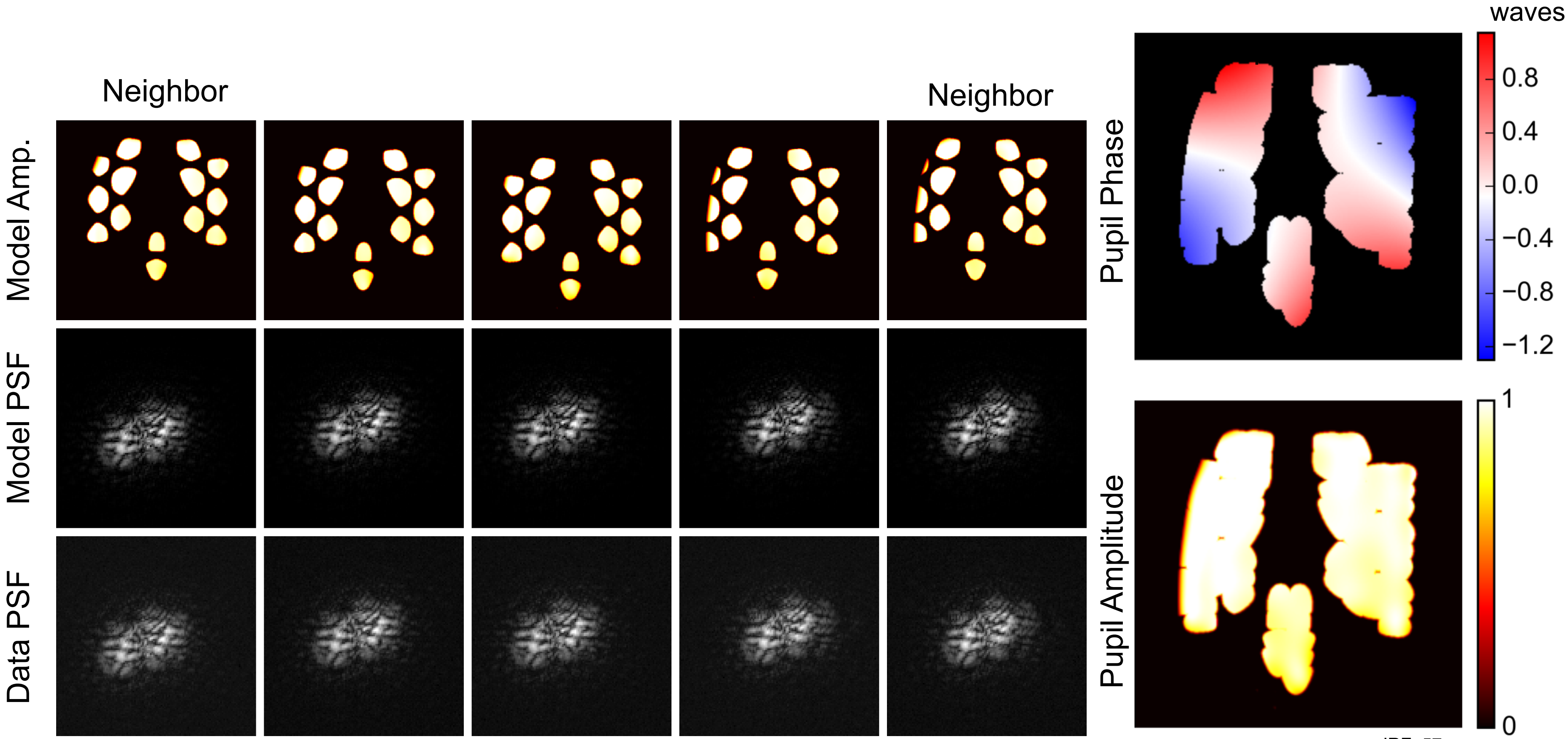

…And Repeat

- Including 25 PSFs in the solution:

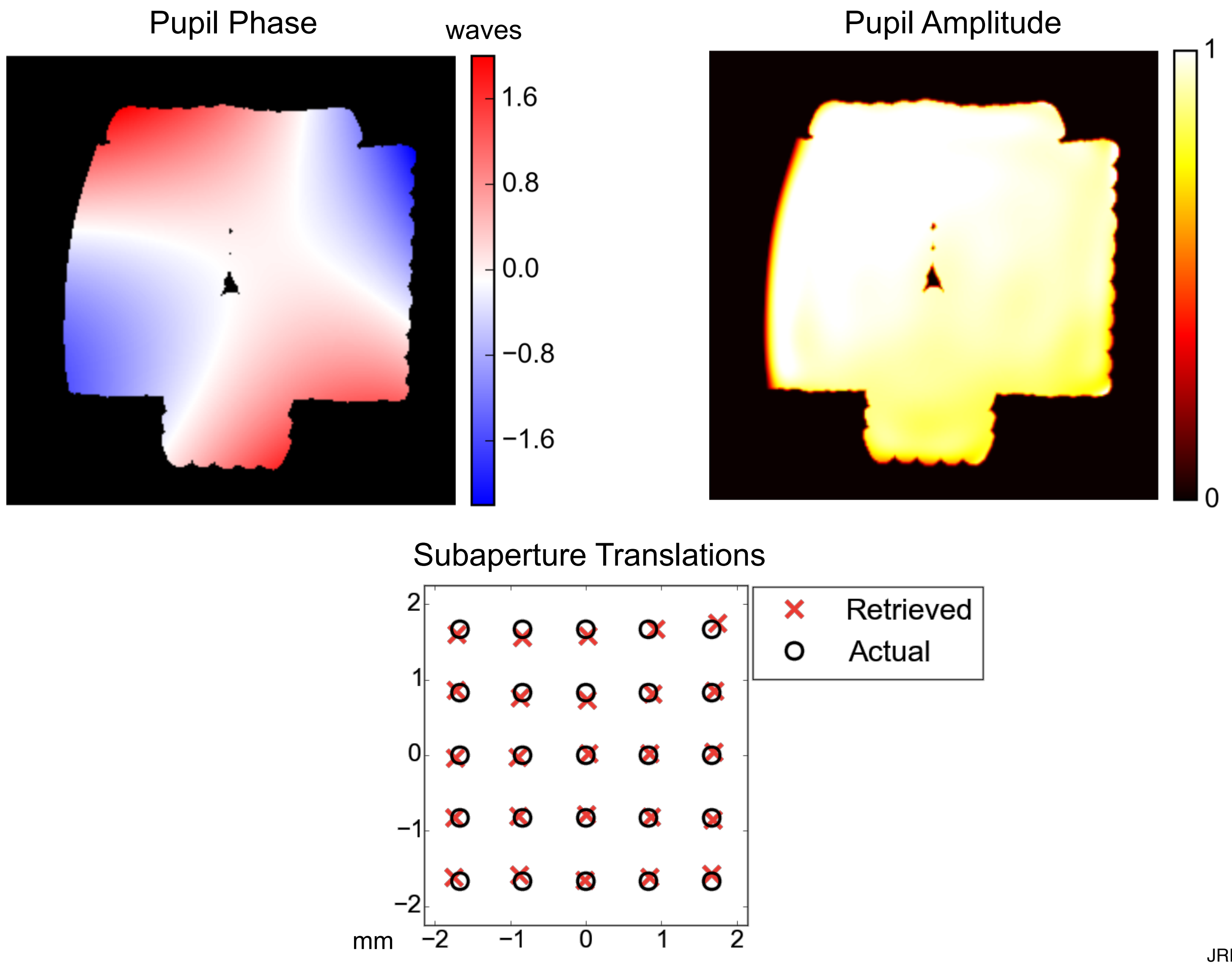

Unknown TTD Conclusion

- Extremely flexible wavefront measurement technique
  - Knowledge of sub-aperture transmission function
  - “Small” unknown translations of the subaperture between PSFs
  - Requires significant higher order aberrations like coma, trefoil, spherical
- Successfully demonstrated in a lab experiment
- Successfully applied to NIRCam data during ISIM CV2 August 2014
- Algorithm transferred to Goddard for ISIM CV3 testing
  -
- For more information: Two conference papers [1-2] and two upcoming journal papers on translation diversity

[1] D. B. Moore and J. R. Fienup, "Transverse Translation Diversity Wavefront Sensing with Limited Position and Pupil Illumination Knowledge," Proc. SPIE **9143**, 91434F (2014).
[2] D. B. Moore and J. R. Fienup, "Sub-Aperture Position Estimation in Transverse-Translation Diversity Wavefront Sensing," in *Imaging and Applied Optics*, OSA Technical Digest (Optical Society of America, 2015), paper AOM3F.4.

Joint Coherence and Phase Retrieval for Metrology

Spatial Coherence and Phase Retrieval

- If target (pinhole) is resolved and the illumination not coherent, PSF could be partially-coherent

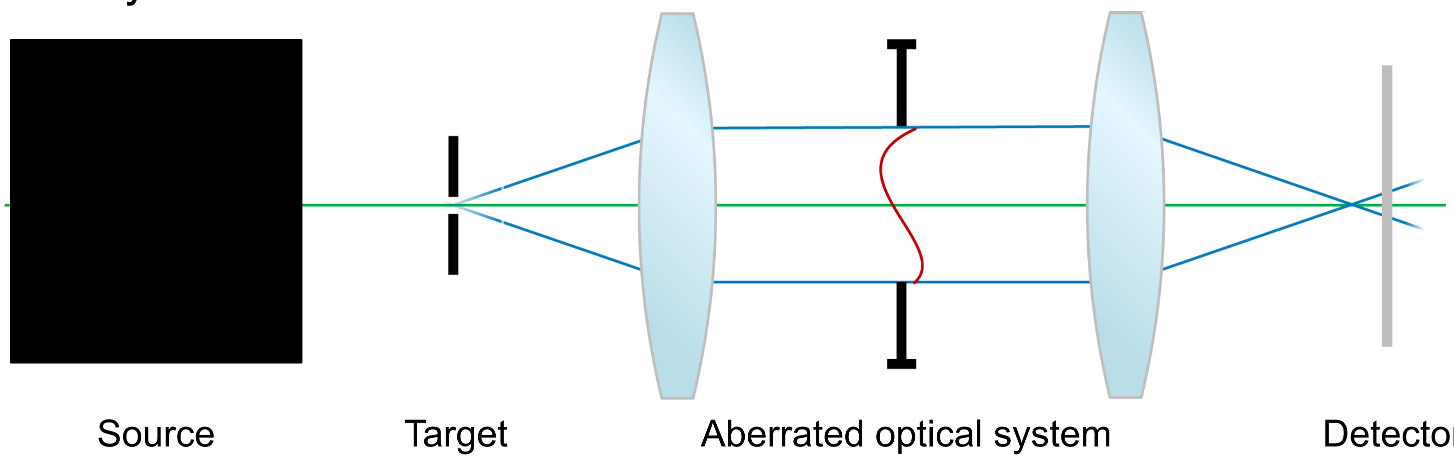

- What if we do not know the spatial coherence on target and must infer it from the PSFs?

- Requirements for a useful phase and coherence retrieval algorithm:
  - Should not need to know spatial coherence of the light prior
  - Should avoid doing the full 4D partial coherence intensity integral due to computational time

Spatial Coherence and Phase Retrieval

- Our work: Model the unknown coherence as a notional Köhler imaging source making PSF intensity linear in a point-wise approximation [1]

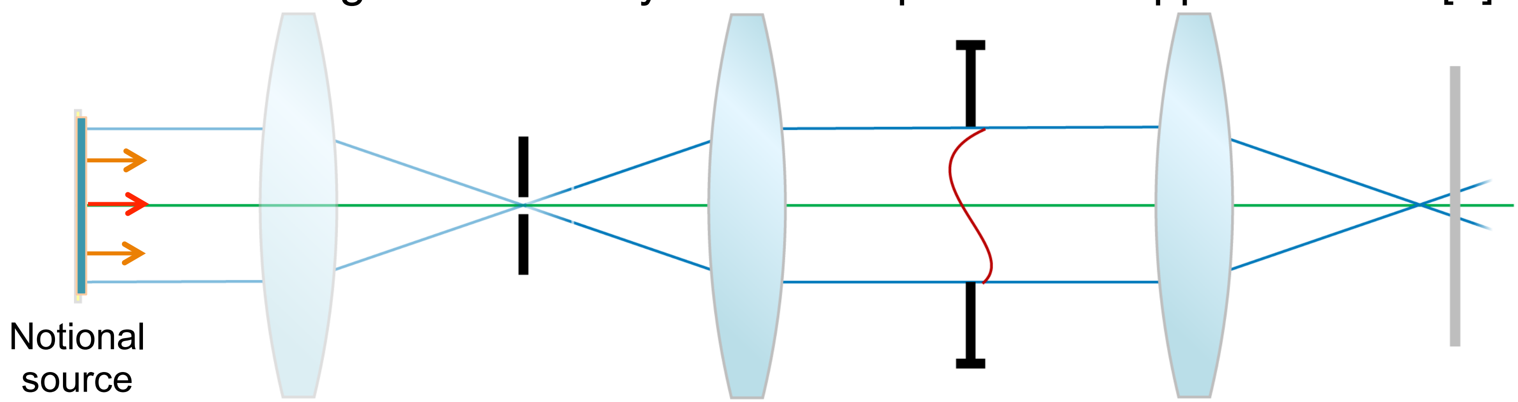

  - Point-wise approximation leads to computational efficiency
  - Includes special term for full incoherence so different than a classic coherent-mode decomposition [2]

- Results of joint spatial-coherence and phase retrieval:
  - One point model (red) improves accuracy of retrieved phases by an order of magnitude over ignoring partial coherence [1]
  - Multi-point model (blue) increases accuracy of model to arbitrary fidelity
  - Fast compared to calculating full 4D partially-coherent intensity integral

1. D. B. Moore, and J. R. Fienup, "Fast Linear Approximation for Phase Retrieval of Partially Coherently Illuminated Objects," (Optical Society of America2012), p. FTu2F.4.
2. L. Mandel, and E. Wolf, *Optical Coherence and Quantum Optics* (Cambridge, 1995).

Analytic Gradients for Prescription Retrieval

Analytic Gradients for Prescription Retrieval

- Prescription retrieval: What physical prescription parameters and misalignments explain measured PSFs?
  - Example: Compare PSFs from multiple NIRCam fields to infer alignment of secondary
  - Example: Estimate as-built prescription of the system from PSFs:

PSFs acquired at

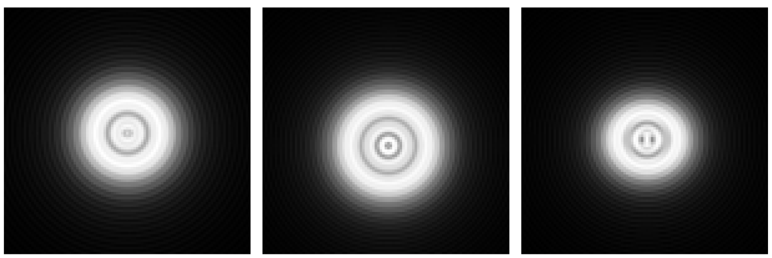

various field points

Prescription Retrieval

Surf.	Radius (mm)	Thick. (mm)	Material
Obj	-	350.262	Air
1	275.03	7.0	N-SF2
2	-120.4	7.0	N-BK7
3	-330.0	150.4	Air
Stop	-	150.9	Air
4	-330.0	7.0	N-BK7
5	-120.0	7.0	N-SF2
6	275.0	353.83	Air

- Requires computationally expensive raytrace of many fields/defocuses
  - Necessity usually forces linearization of mechanical and wavefront parameter connection with a Linear Optical Model (LOM) [1-2]

[1] J. M. Howard and K. Ha, "Optical modeling activities for the James Webb Space Telescope (JWST) project: II. Determining image motion and wavefront error over an extended field of view with a segmented optical system," Proc. SPIE **5487**, 850–858 (2004).

[2] D. C. Redding, N. Sigrist, J. Z. Lou, Y. Zhang, P. D. Atcheson, D. S. Acton, and W. L. Hayden, "Optical state estimation using wavefront data," Proc. SPIE **5523**, 212–224 (2004).

Analytic Gradients for Prescription Retrieval

- How can we do nonlinear prescription retrieval outside the limited validity region of LOM?
  - Finite-differences (FD) gradient of error metrics involve expensive full raytrace for every unknown
- Recent work [1] introduced the reverse mode of algorithmic differentiation (RMAD) [2] for phase retrieval gradients, we extended it to raytracing [3]
  - RMAD gradient cost is about 1.4 raytraces worth of time, rather than the number of unknowns worth of raytrace times for FD
  - Like special forms of differential raytracing, TOR in CodeV
- Example: Cassegrain telescope with primary surface described by 100 Zernikes and a secondary surface described by 19 Zernikes
  - 120 unknowns, RMAD yields speedup of ~50x over FD
- **RMAD makes nonlinear prescription retrieval problems that were previously too computationally expensive much faster**

[1] A. S. Jurling and J. R. Fienup, "Applications of algorithmic differentiation to phase retrieval algorithms," J. Opt. Soc. Am. A **31**, 1348–1359 (2014).
[2] A. Griewank, and A. Walther, *Evaluating Derivatives: Principles and Techniques of Algorithmic Differentiation* (SIAM, 2008).
[3] D. B. Moore and J. R. Fienup, "Efficient Prescription Retrieval from PSF Data," in *Frontiers in Optics 2015*, OSA Technical Digest (Optical Society of America, 2015), paper FTu5D.2.

Scott Paine Research – Expanding Capture Range for Segment Piston

- With polychromatic light, normal capture range for piston is ~1 wave
- In error metric space, local minima are all separated by ~1 wave per segment
- Perform grid search where integer amounts of piston are added to see if error metric improves
- Capture range increases to coherence length of polychromatic light with uniform spectrum
  - Further improvements with different spectral shapes

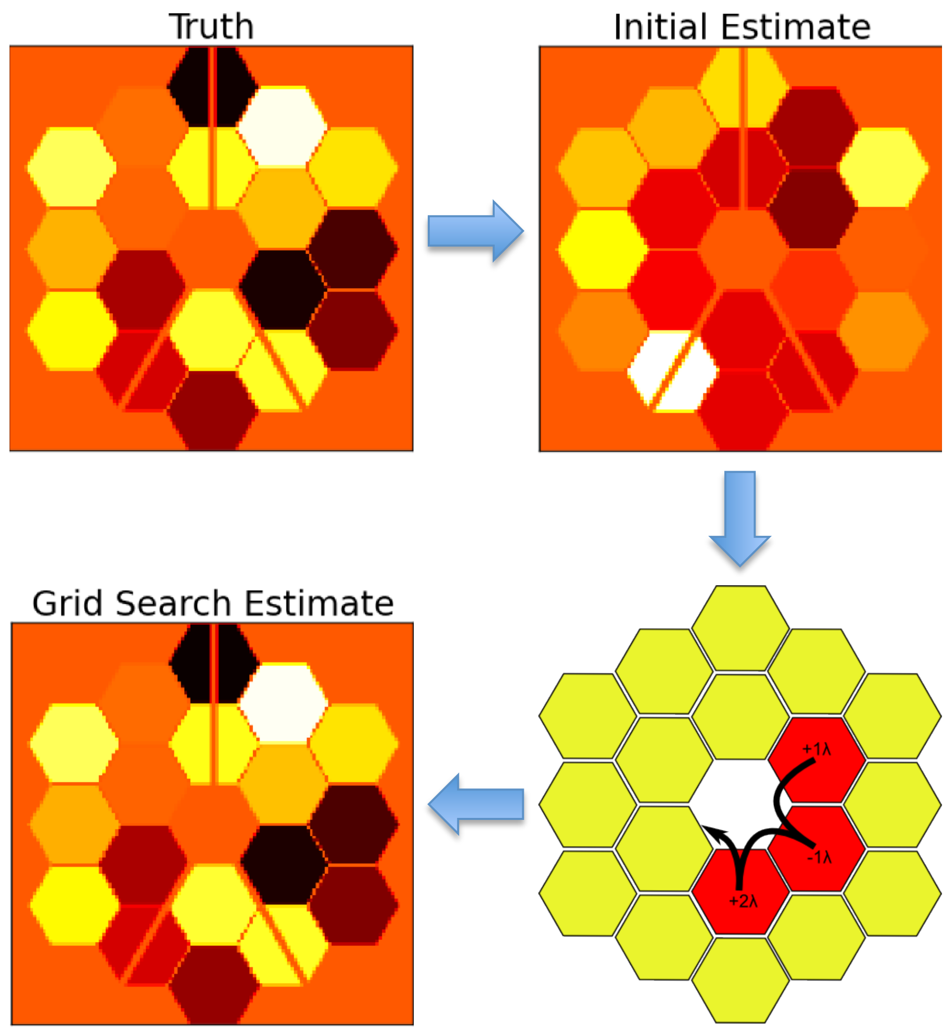

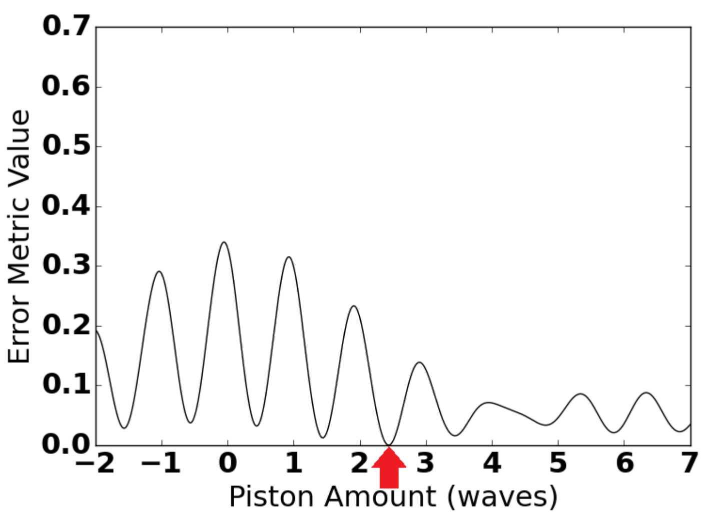

Scott Paine Research – WFIRST Grism Simulation and Low-Q Retrieval

GRISM simulation

- WFIRST Grism includes linear chromatic dispersion
- In order to appropriately model dispersion, need wavefront that is dependent on wavelength
- New wavefront model:

$$W(\lambda, u, v) =$$

$$\Delta\lambda \left[b_1 Z_1(u, v) + b_2 Z_2(u, v)\right] + \sum_n a_n Z_n(u, v)$$

Where Z is a Zernike polynomial, a and b are monochromatic and chromatic weighting parameters, and $\Delta\lambda$ is the difference between the wavelength λ and some reference wavelength λ_0

- Parameters can be easily inserted into existing models and expanded for higher order chromatic aberrations

Low-Q Phase Retrieval

- WFIRST Grism testing includes detector with Q < 1
- Gather diversity by performing sub-pixel dithering of source
- Jointly fit a number of dithered frames
- How many frames are necessary for a given Q?
- Currently running Monte Carlo
  - Different Q amounts
  - Different amounts of frames
  - Noise included
  - Examine RMS error in retrieved parameters

The Institute of OPTICS

Outline

- Image-based wavefront sensing for optical telescopes
  - Hubble Space Telescope
  - JWST
    - NIRCam/ISIM testing
    - On orbit
  - Other Future Systems (WFIRST)

- Other Wavefront Sensing
  - Freeform Optics
  - High-energy laser beams
  - Hermite-Gaussian and Laguerre-Gaussian beams

- Interferometric Imaging
  - Of geosynchronous satellites from the ground
  - NASA space-based interferometric imaging

Freeform Optics Metrology by Transverse Translation Diversity Phase Retrieval

James R. Fienup, Aaron M. Michalko
University of Rochester

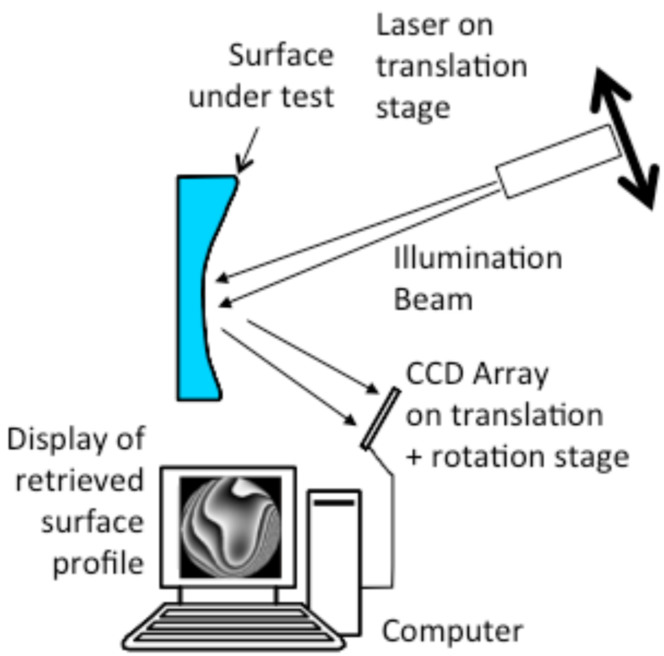

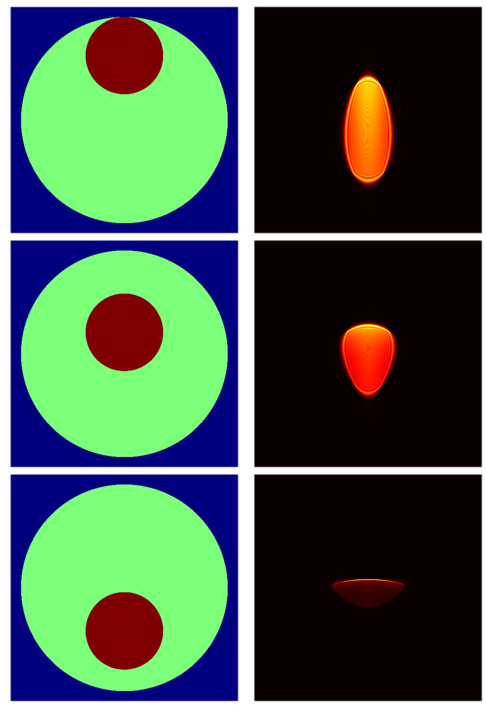

Funded by NSF I/UCRC Center for Freeform Optics (IIP-1338877 and IIP-1338898)

Background and Motivation

- **Freeform optics**
  - Rotationally asymmetric surfaces open up conventional design space
  - Increased optical performance with decreased size, weight, number of elements
  - Example: Three mirror unobscured LWIR imager[1]
    - Three φ-polynomial mirrors
    - F/1.9, 10 degree full field of view imager
  - However, metrology capabilities limited
  - Interest in new ways to perform accurate form metrology

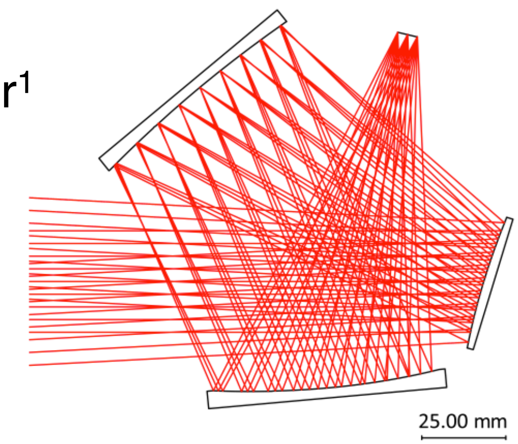

- **Motivation**: Metrology for optical manufacturing shop testing
  - For rotationally asymmetric surfaces with large spherical departures
  - **Form**, MSF, and possibly finish (roughness) measurements
  - Want interferometric accuracy without associated cost and complexity
  - Alternative to existing profilometry and interferometric approaches

1. Kyle Fuerschbach, Jannick P. Rolland, and Kevin P. Thompson, "A new family of optical systems employing ϕ-polynomial surfaces," Opt. Express 19, 21919-21928 (2011)

Approach

- **Method:** Phase retrieval with transverse translation diversity (TTD)
  - Form of ptychography, very robust
  - Scan illumination mask across part under test and gather intensity information in image plane
  - Perform joint reconstruction of wavefront in exit pupil using data from many subaperture positions
  - Reconstruct surface prescription based on wavefront reconstruction

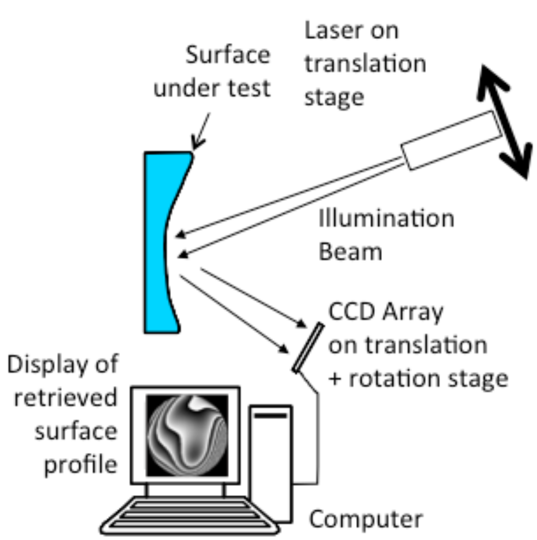

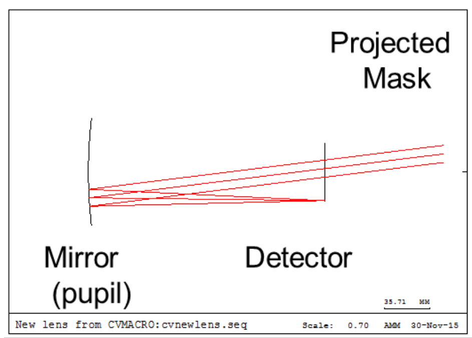

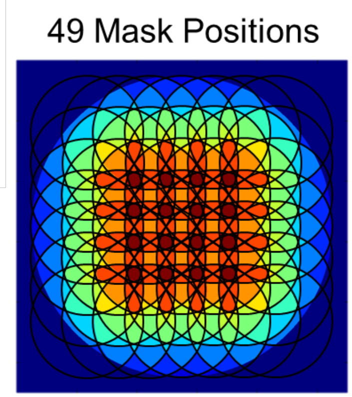

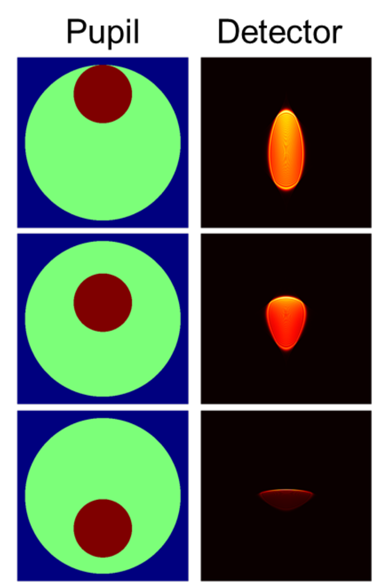

Simulation

- Realistic simulation based on existing freeform mirror
  - Simulated secondary mirror from LWIR imager
  - Off-axis test configuration modelled in CodeV
- Wavefront reconstruction performed using simulated data
  - Initial estimate (before optimization): 55 waves P-V departure from truth
  - **Final estimate: 0.0017 waves P-V departure**
  - Wavefront reconstruction shows good agreement with truth in preliminary simulations

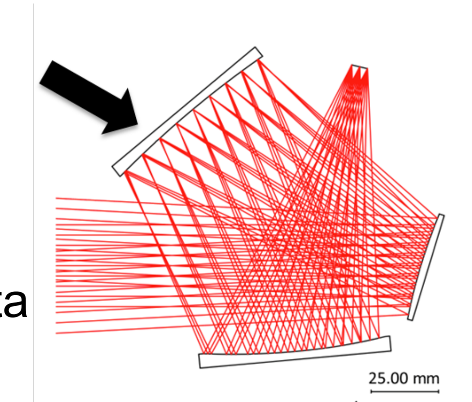

LWIR imager [1]

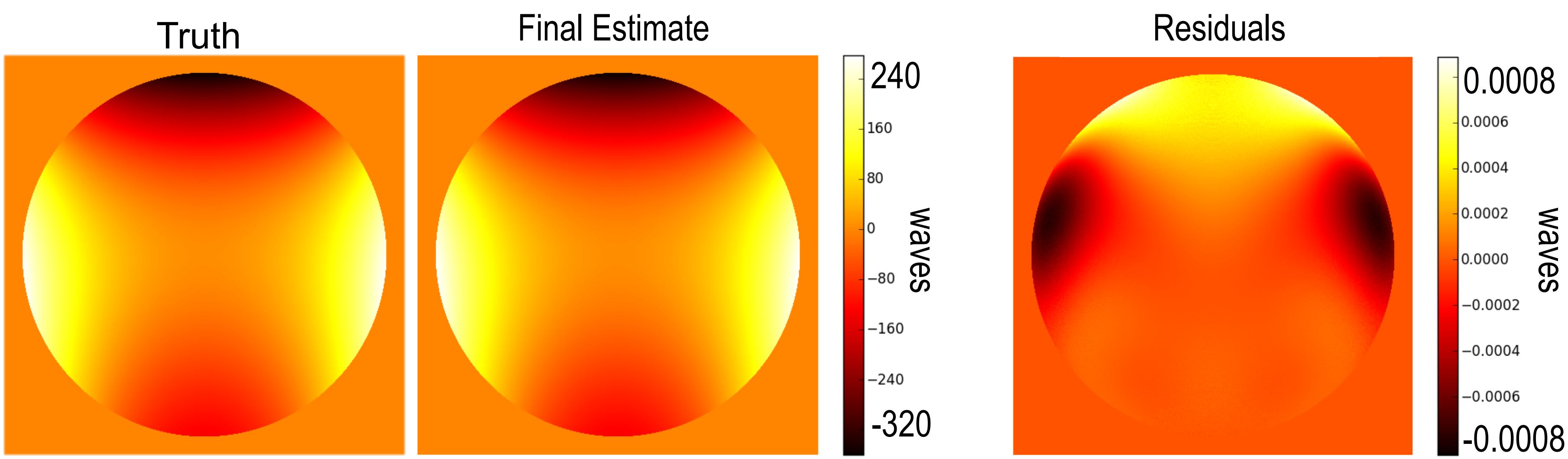

1. Kyle Fuerschbach, Jannick P. Rolland, and Kevin P. Thompson, "A new family of optical systems employing φ-polynomial surfaces," Opt. Express 19, 21919-21928 (2011)

Soft-Edged Aperture Simulation

- Subaperture: Gaussian amplitude (beam waist)
- 9 x 9 grid of subaperture positions
- Wavefront synthesized from 77 Zernike polynomials

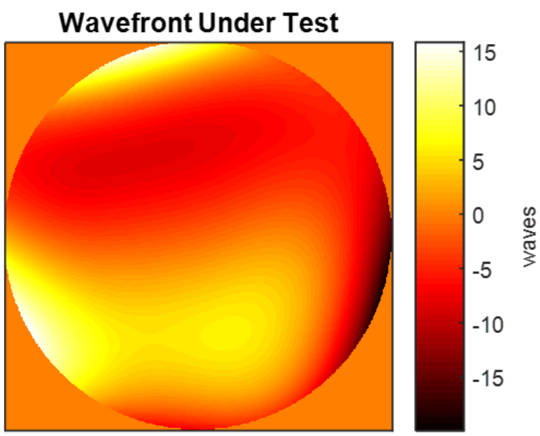

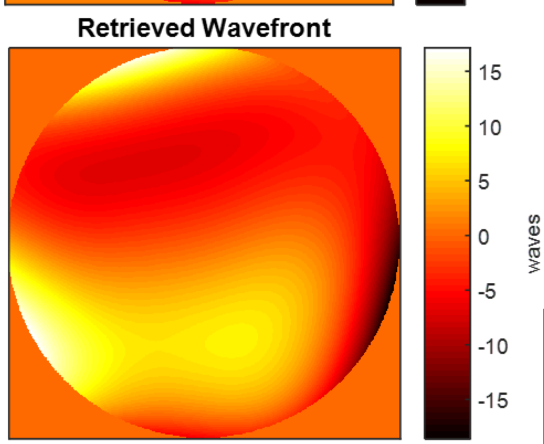

True Wavefront:
P-V = 36.4 waves
RMS = 4.74 waves
(PTT removed)

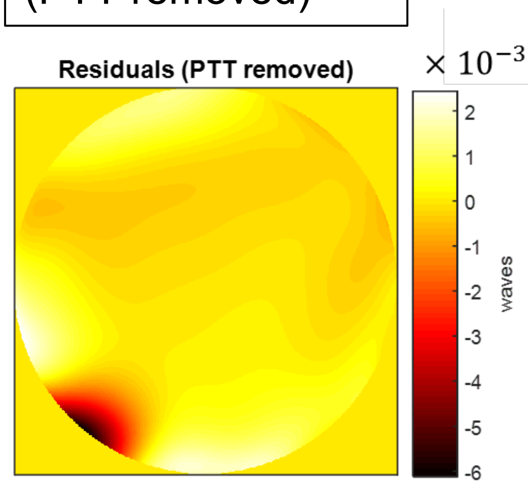

Residuals (waves):
0.0086 P-V, 0.00077
RMS (PTT removed)

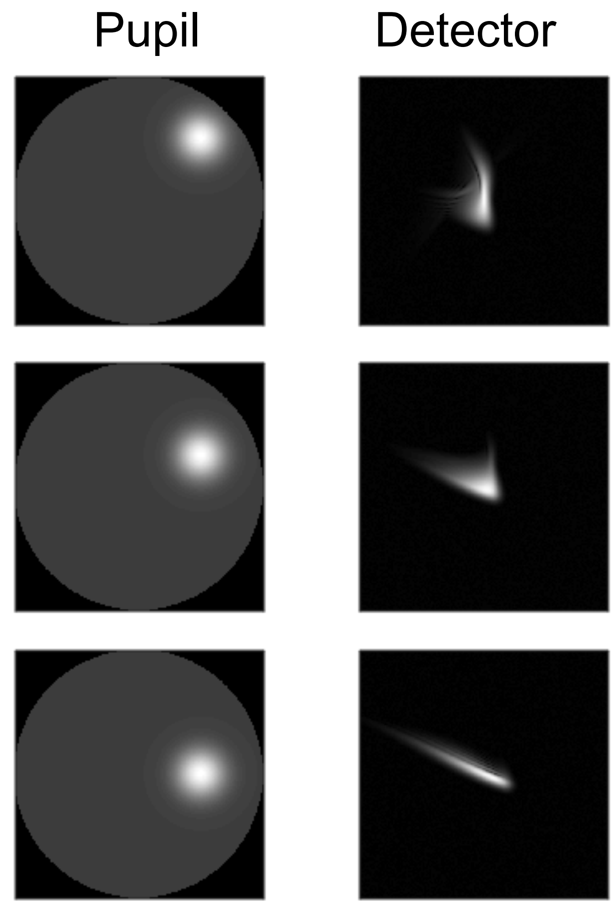

The Institute of OPTICS

Outline

- Image-based wavefront sensing for optical telescopes
  - Hubble Space Telescope
  - JWST
    - NIRCam/ISIM testing
    - On orbit
  - Other Future Systems (WFIRST)
- Other Wavefront Sensing
  - Freeform Optics
  - High-energy laser beams
  - Hermite-Gaussian and Laguerre-Gaussian beams
- Interferometric Imaging
  - Of geosynchronous satellites from the ground
  - NASA space-based interferometric imaging

Focal Spot Diagnostics for Omega-EP Peta-Watt Laser

Matt Bergkoetter

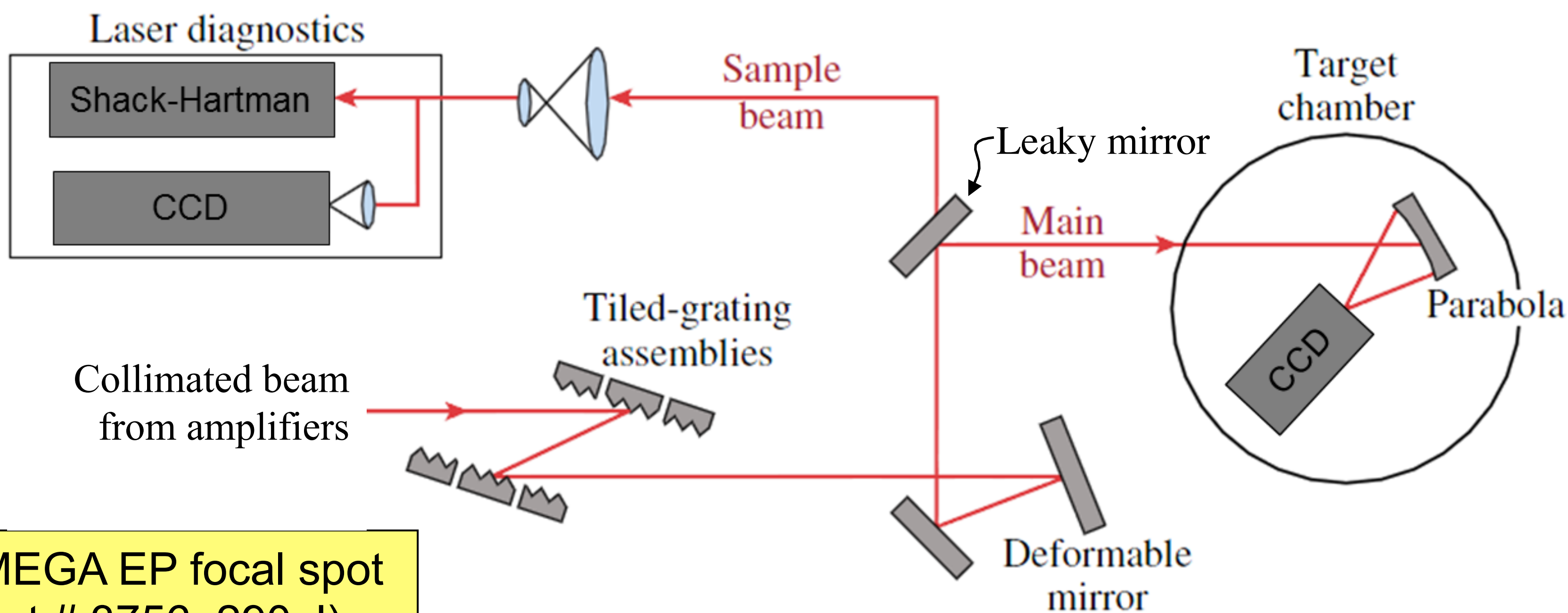

OMEGA EP focal spot
(shot # 3756, 290 J)

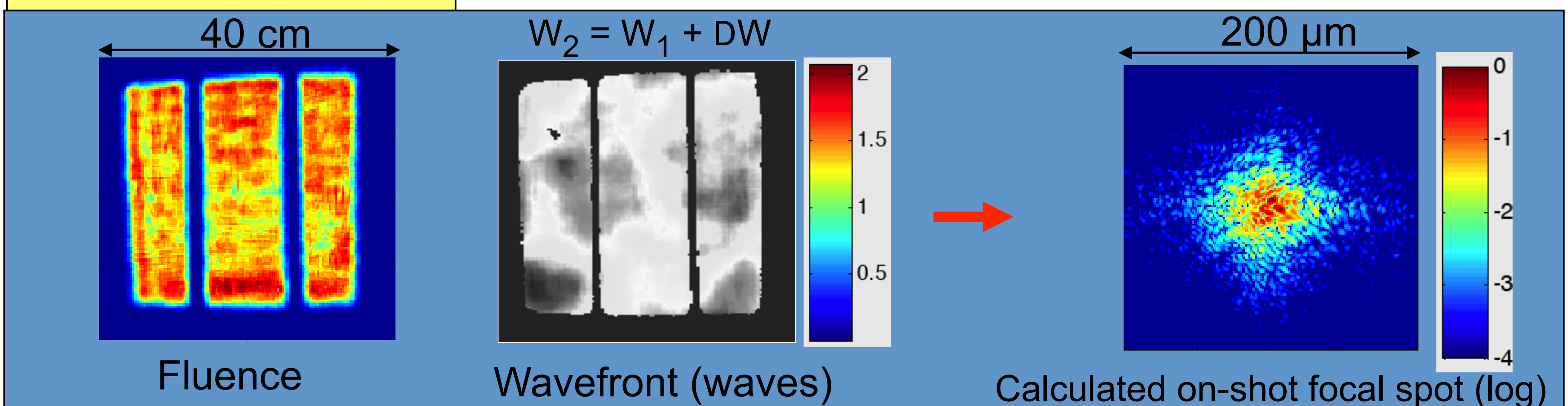

Focal Spot Diagnostics for Omega-EP Peta-Watt Laser

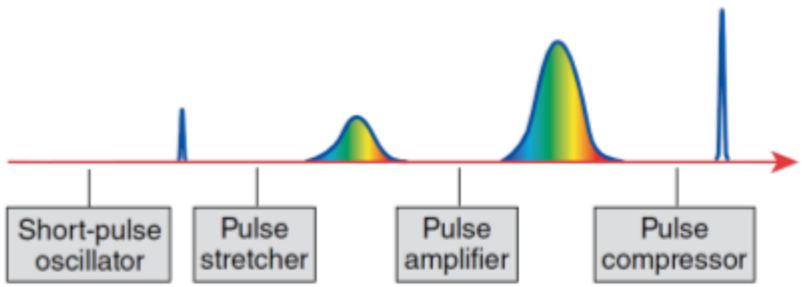

Chirped pulse amplification (CPA)

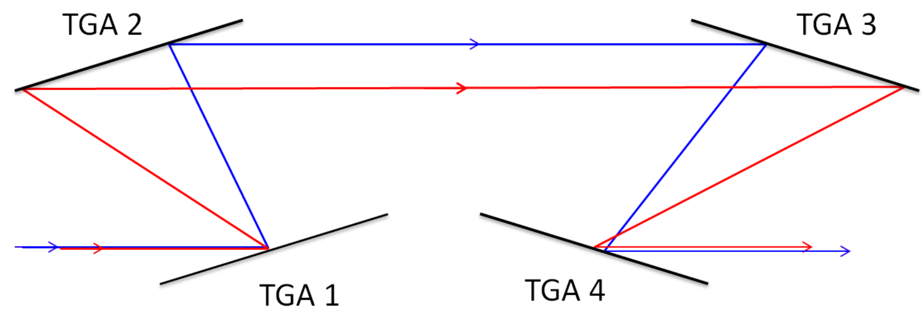

Pulse compressor

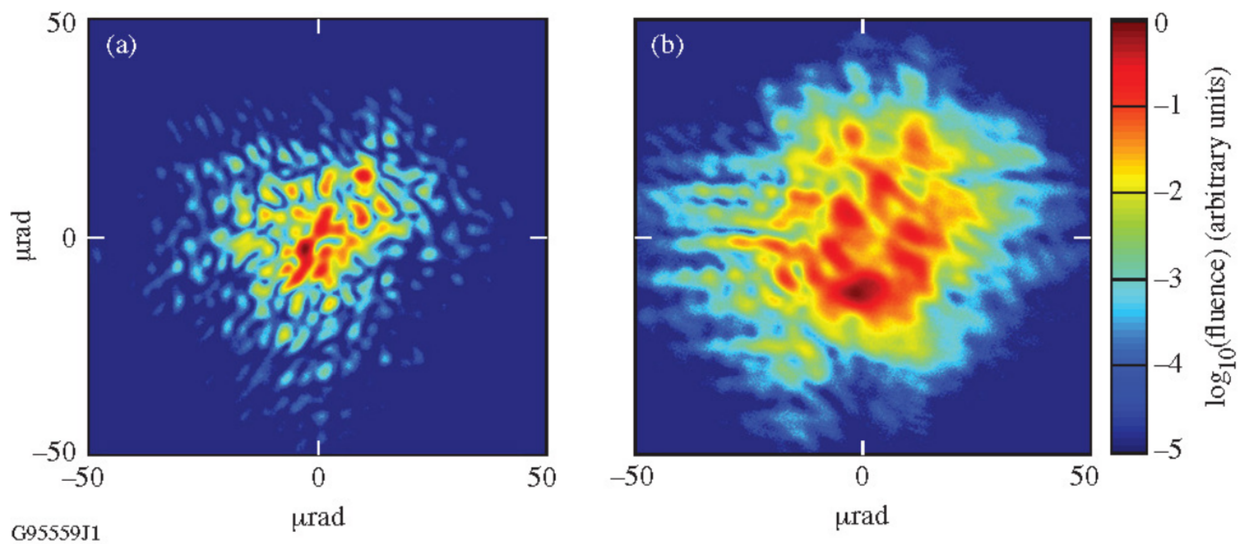

(left) PSF with narrowband laser source (right) PSF with 8nm source exhibits chromatic aberrations

Computational Model

Linear chromatic dispersion

$$W_\lambda = W_{\mathrm{mono}} + W_{\mathrm{disp}}$$

$$W_{\mathrm{mono}}(x,y) = \sum_n^N a_n Z_n(x,y)$$

$$W_{\mathrm{disp}}(x,y) = \sum_n^N (\lambda - \lambda_0) c_n Z_n(x,y)$$

$$W_\lambda(x,y) = \sum_n^N \left[a_n + (\lambda - \lambda_0) c_n \right] Z_n(x,y)$$

- Parameterized dispersion model enforces consistency between W_λ's
- Axial color and angular dispersion are both linear (to 1st order)

Arbitrarily-sampled DFTs

- Chirp Z-transform and Triple Matrix Product
- Array size independent of λ
- Similar or better performance for:
  - Well-sampled data (Q = q = 2)
  - Large Q
  - Broadband
  - Narrowband with chromatic aberrations

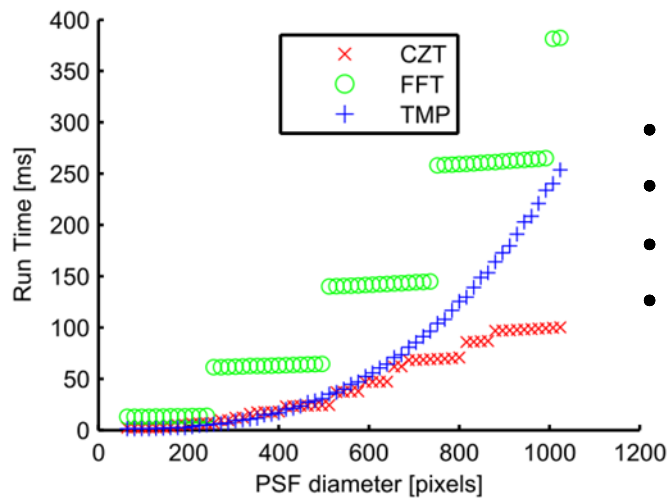

- BW = 8 nm
- 5 Wavelengths
- λ
- Q = q = 2

Outline

- Image-based wavefront sensing for optical telescopes
  - Hubble Space Telescope
  - JWST
    - NIRCam/ISIM testing
    - On orbit
  - Other Future Systems (WFIRST)
- Other Wavefront Sensing
  - Freeform Optics
  - High-energy laser beams
  - Hermite-Gaussian and Laguerre-Gaussian beams
- Interferometric Imaging
  - Of geosynchronous satellites from the ground
  - NASA space-based interferometric imaging

GENERALIZED OPTICAL INTERFEROMETRY

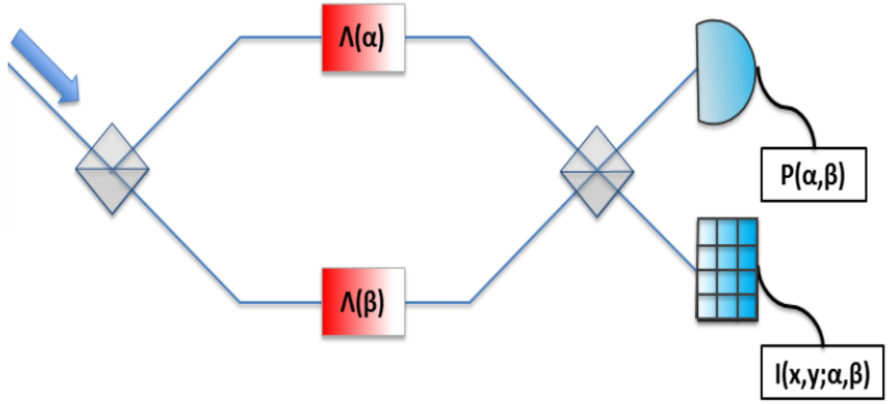

Generalized optical interferometry (GOI)

- M-Z interferometer has temporal delay replaced by generalized phase operators(GPO), $\Lambda(x, x'; \alpha)$,

$$\Lambda(x, x'; \alpha) = \sum_n e^{in\alpha} \psi_n(x) \psi_n^*(x')$$

  - $\psi_n(x)$ are the members of some orthonormal basis set.

- Generalized cylindrical lenses in each arm of the interferometer create GPOs that correspond to fractional-Fourier transforms
  - α corresponds to x-axis,

$$\Lambda(x, x'; \alpha) = \sum_{mn} e^{im\alpha} HG_{mn}(x, y) HG^*_{mn}(x', y)$$

  - β corresponds to y-axis,

$$\Lambda(y, y'; \beta) = \sum_{mn} e^{in\beta} HG_{mn}(x, y) HG^*_{mn}(x, y')$$

- $HG_{mn}(x, y)$ is the Hermite-Gaussian transverse mode of the mn-th order

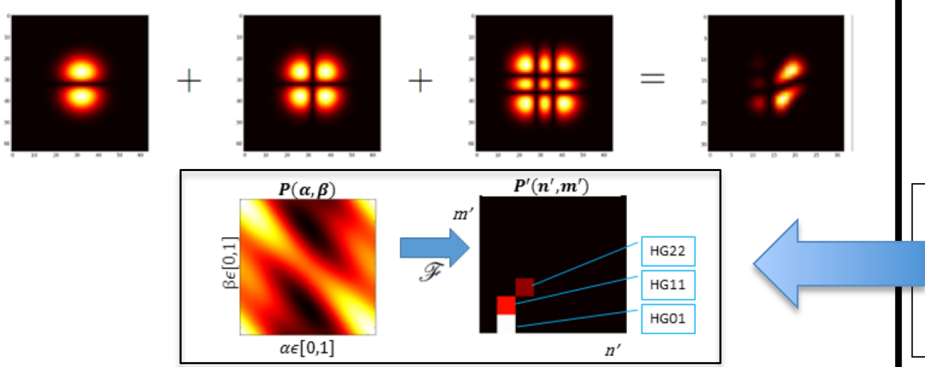

Figure: (Top)HG01, HG11,and HG22 are superposed. (Bottom)Respective $|c_{mn}|$ are recovered using GOI.

Modal Amplitude Determination:

- Superpose three modes
- Sweep interferometer through range of α and β, save array of $P(\alpha, \beta)$ values
- Fourier transform from $P(\alpha, \beta)$ array from α, β space to m, n space and remove bias term to find $|c_{mn}|^2$ values

$$\mathscr{F}_{\alpha\beta \to m'n'} \{P(\alpha, \beta)\} = \left(\sum_{mn} |c_{mn}|^2\right) \delta(m', n') + \sum_{mn} |c_{mn}|^2 \left[\delta\left(m' - \frac{m}{2}, n' + \frac{n}{2}\right) + \delta\left(m' + \frac{m}{2}, n' - \frac{n}{2}\right)\right].$$

OPTICS The Institute of

GOI PHASE RETRIEVAL

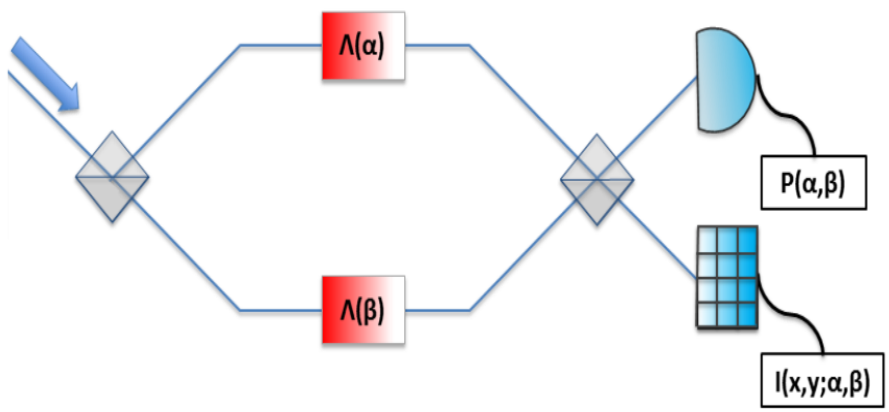

- For phase retrieval, we need to retain spatial information.

- For optimization, estimated intensity of a single detector pixel is

$$I_{EST}(x,y) = \left| \sum_{m,n} |c_{mn}| e^{i\phi_{mn}} \left[e^{i\pi m\alpha} + e^{i\pi n\beta} \right] U_{mn}^{HG}(x,y) \right|^2$$

- The error metric, E, is a sum of squared differences

$$\hat{\phi} = \underset{[\phi]}{\text{argmin}}\{E\} = \underset{[\phi]}{\text{argmin}} \left\{ \sum_{x,y} [I_{EST}(x,y) - I_{ACT}(x,y)]^2 \right\}$$

- Minimize using L-BFGS-B

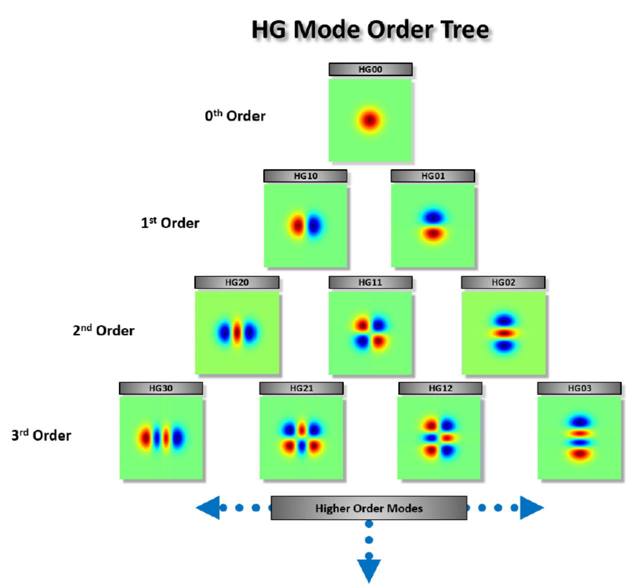

- α, β planes where $\left[e^{i\pi m\alpha} + e^{i\pi n\beta} \right] = 0$ “suppress" the HG_{mn} mode in the intensity distribution

- Phase retrieval in these planes only retrieves un-“suppressed" modes

  - Can use this to bootstrap retrieval

- Can use multiple α, β planes simultaneously to add diversity to retrieval

- Currently able to retrieve phase for up to 36 superposed modes

- Working on improving convergence rate and speed

Outline

- Image-based wavefront sensing for optical telescopes
  - Hubble Space Telescope
  - JWST
    - NIRCam/ISIM testing
    - On orbit
  - Other Future Systems (WFIRST)

- Other Wavefront Sensing
  - Freeform Optics
  - High-energy laser beams
  - Hermite-Gaussian and Laguerre-Gaussian beams

- Interferometric Imaging
  - Of geosynchronous satellites from the ground
  - NASA space-based interferometric imaging

Zack DeSantis

Imaging Interferometry for Ground-Based Imaging of Geo Satellites

DARPA Galileo Program

DARPA-BAA-12-08, Galileo

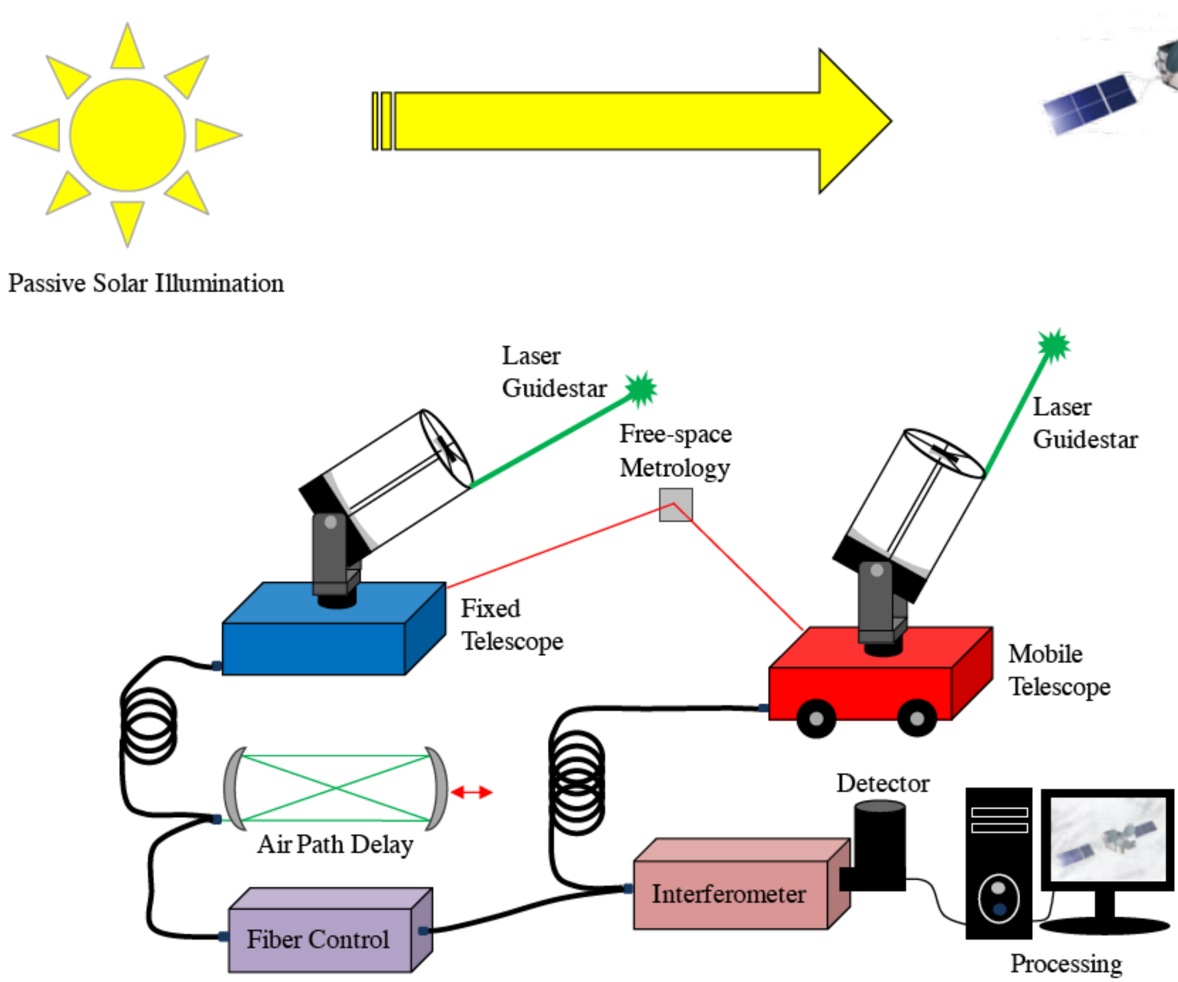

Figure 1: Schematic diagram of notional Galileo technical concept of operations. Fixed and mobile 1.5 meter class telescopes are equipped with adaptive optics (Rayleigh guidestar depicted). Telescopes are linked by a fiber backbone, allowing full 2D baseline flexibility. Air path delay provides coarse optical path length matching, while fiber control provides fine optical path length matching/locking and dispersion control.

Image Reconstruction from Interferometer Data

- Minimize objective function by nonlinear optimization
  - with respect to image pixel values
  - Data consistency metric
  - Nonnegativity constraint
  - Dynamic support constraint: “shrinkwrap”
  - Bootstrapping
    - Low freq. –> high freq.

Sparse, noisy Fourier data, large unknown phase errors, non-Cartesian grid

Sampled at half the Nyquist rate

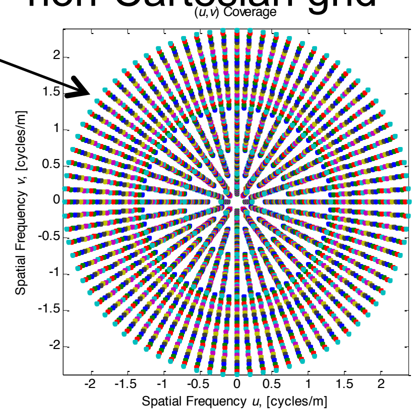

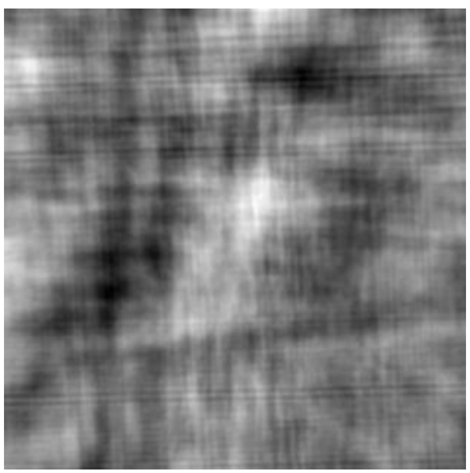

Initial Image

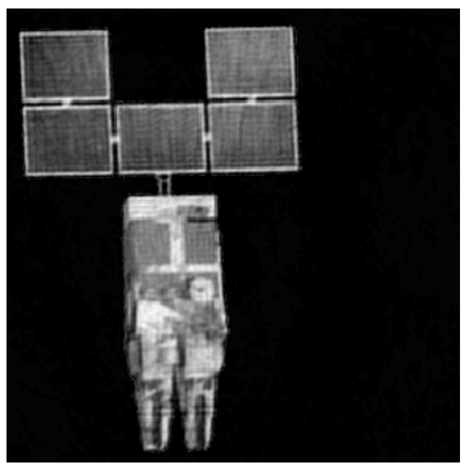

Reconstructed Image

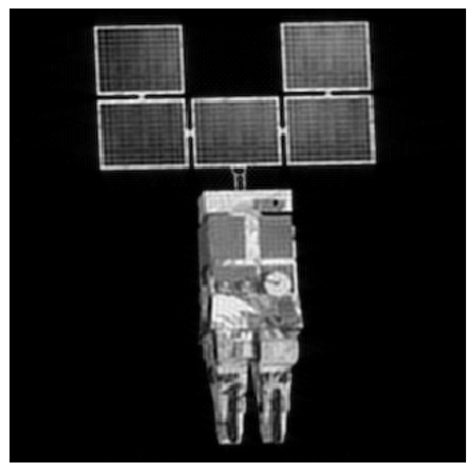

Ideal Image

Z.J. DeSantis and J.R. Fienup, “Image Reconstruction from Sparse Interferometric Data,” in Imaging and Applied Optics 2014, OSA Technical Digest (online) (Optical Society of America, 2014), paper STu2F.4

Outline

- Image-based wavefront sensing for optical telescopes
  - Hubble Space Telescope
  - JWST
    - NIRCam/ISIM testing
    - On orbit
  - Other Future Systems (WFIRST)

- Other Wavefront Sensing
  - Freeform Optics
  - High-energy laser beams
  - Hermite-Gaussian and Laguerre-Gaussian beams

- Interferometric Imaging
  - Of geosynchronous satellites from the ground
  - NASA space-based interferometric imaging

Spatio-Spectral Interferometry: Motivation

PROBLEM:

- Weight and cost limitations prevent arbitrarily large monolithic observatories
  - Science goals require resolutions that cannot be met by a single-aperture telescope, especially in FIR

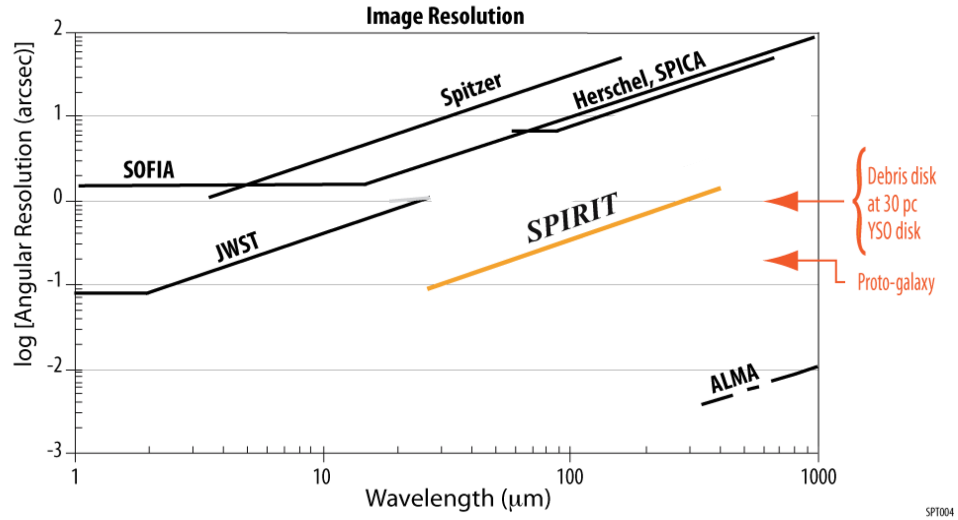

SOLUTION:

- Spatio-spectral (double-Fourier) interferometric imaging
  - Reduced size/weight compared to monolithic
  - Lengthier data collection and requires image synthesis algorithm

D. T. Leisawitz, et al., "The space infrared interferometric telescope (SPIRIT): A far-IR observatory for high-resolution imaging and spectroscopy," white paper submitted to the Astronomy and Astrophysics Decadal Survey of 2010

Spatio-Spectral Interferometric Imaging

- Combines Fourier transform imaging spectroscopy (FTIS) and aperture synthesis techniques
  - Extends to wide-FOV

J.-M. Mariotti and S. T. Ridgway, “Double Fourier spatio-spectral interferometry – combining high spectral and high spatial resolution in the near infrared,” Astron. Astrophys., vol. 195, p. 350-363, 1988.

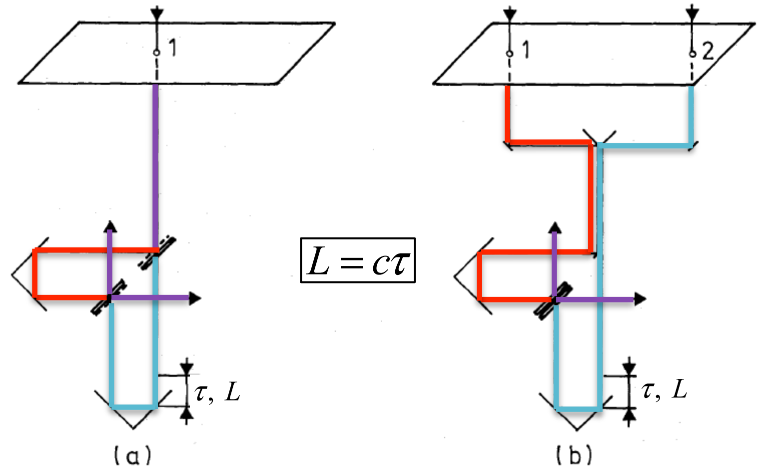

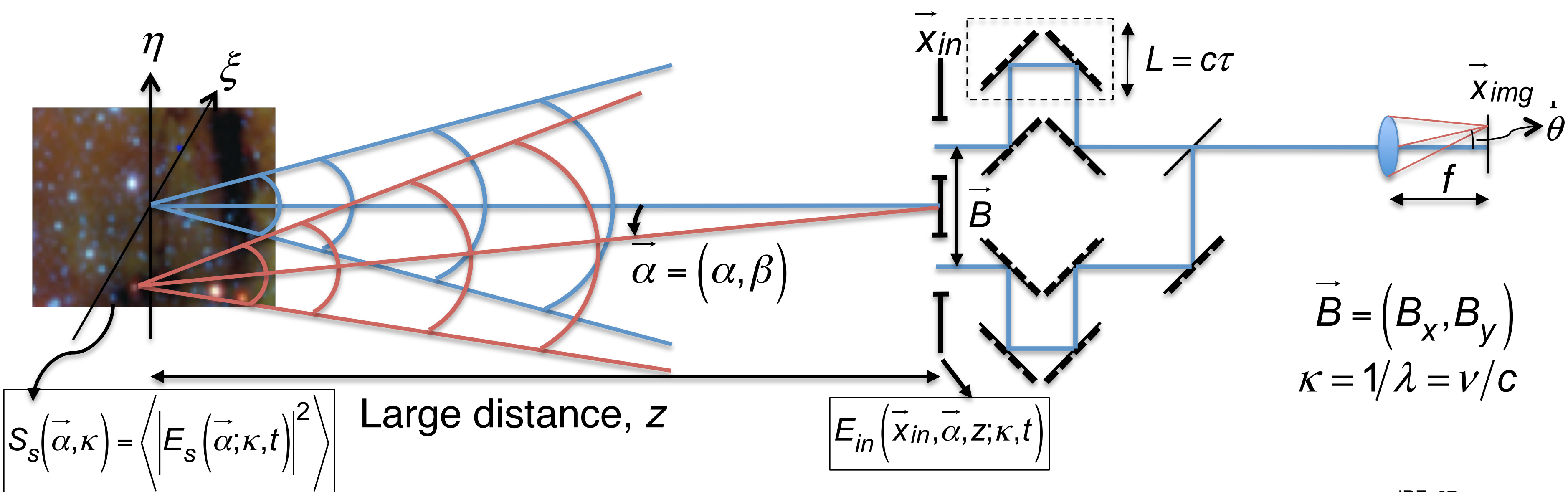

Spatio-Spectral Interferometric Imaging

- Interference fringe at each pixel (like FTIS)
  - Contains spatial and spectral information
- Spatial frequencies proportional to baseline and wavenumber $(1/\lambda)$
  - FTIS measures DC info
- Recover high resolution hyperspectral image

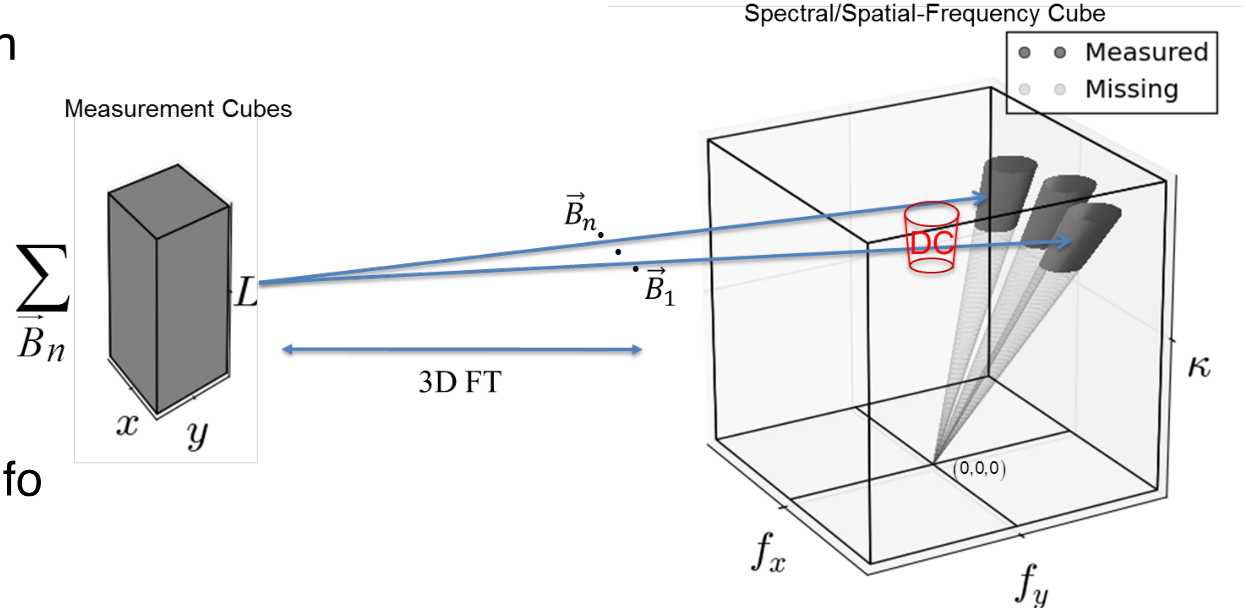

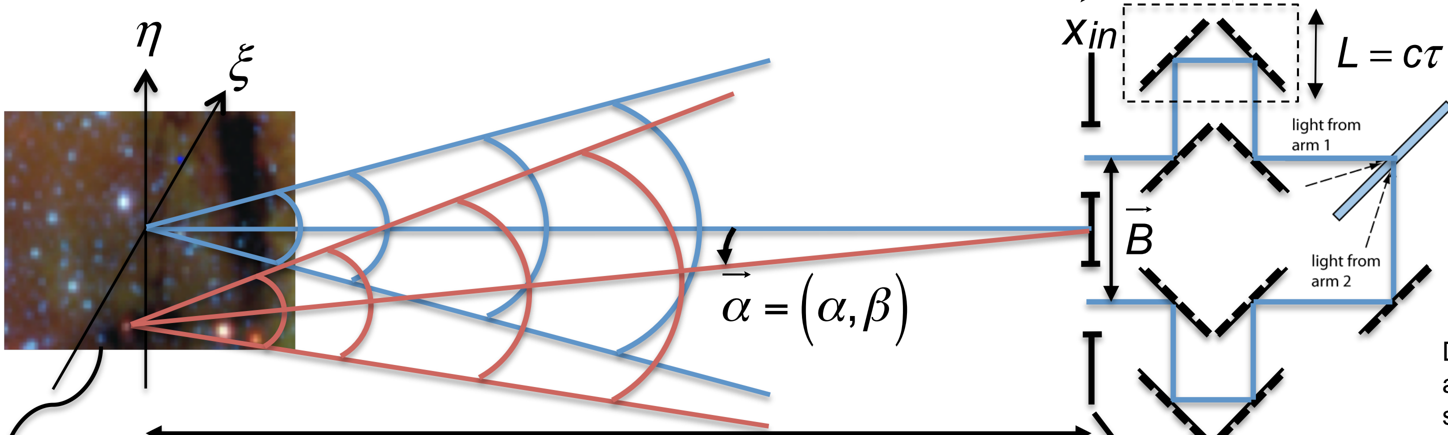

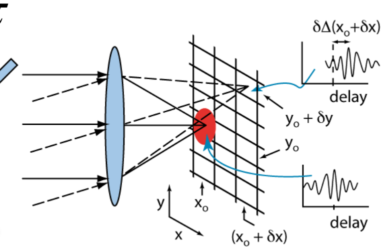

$$S_o(\vec{\alpha},\kappa) = \left\langle \left| E_s(\vec{\alpha};\kappa,t) \right|^2 \right\rangle w$$

Large distance, z

$$E_{in}(\vec{x}_{in},\vec{\alpha},z;\kappa,t)$$

D. T. Leisawitz, M. R. Bolcar, et al., "Developing wide-field spatio-spectral interferometry for far-infrared space applications," Proc. SPIE 8445, 84450A, 2012.

Spatio-Spectral Interferometric Imaging

- Interference fringe at each pixel (like FTIS)
  - Contains spatial and spectral information
- Spatial frequencies proportional to baseline and wavenumber ($1/\lambda$)
  - FTIS measures DC info
- Recover high resolution hyperspectral image

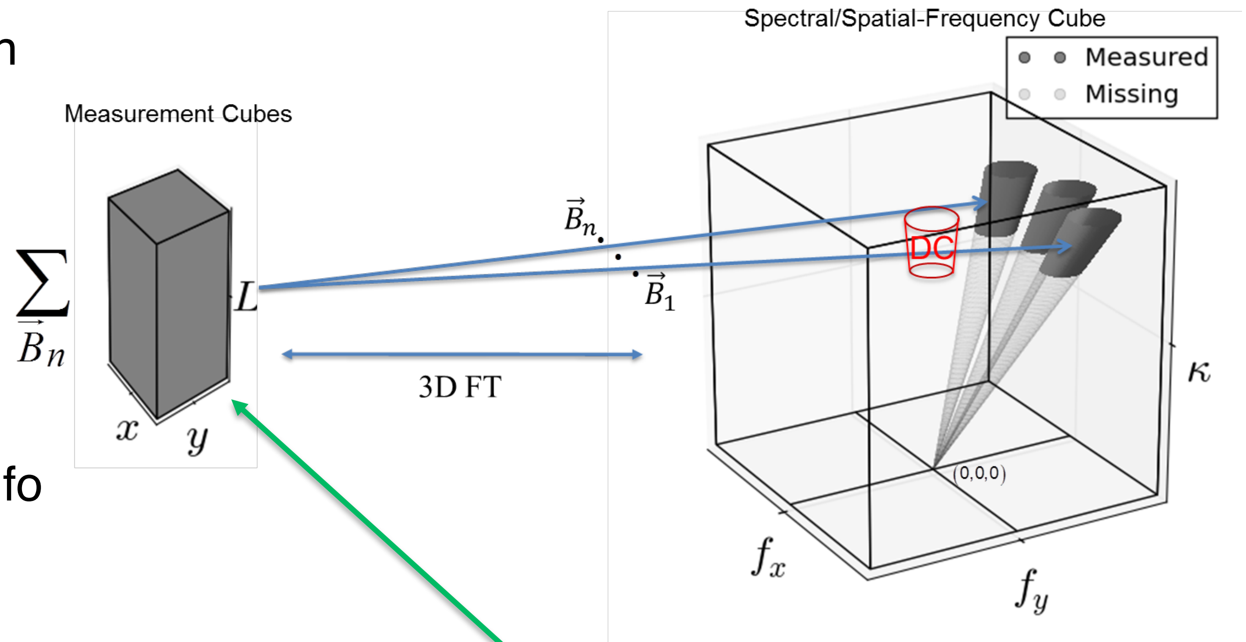

$$I_{im}\left(\vec{\theta},\vec{B},L\right) = \frac{\sigma}{2}\int_{0}^{\infty}\int_{-\infty}^{\infty}\sum_{n=1}^{2} p_{n,n}\left(\vec{\theta}-\vec{\alpha},\kappa\right)S_s\left(\vec{\alpha},\kappa\right)d^2\vec{\alpha}\,d\kappa$$

$$+\mathrm{Re}\left\{\sigma\int_{0}^{\infty}\int_{-\infty}^{\infty} p_{1,2}\left(\vec{\theta}-\vec{\alpha},\kappa\right)S_s\left(\vec{\alpha},\kappa\right)\exp\left\{i\left[2\pi\kappa\left(\vec{\alpha}\cdot\vec{B}-L\right)+\Delta\varphi\left(\kappa\right)\pm\frac{\pi}{2}\right]\right\}d^2\vec{\alpha}\,d\kappa\right\}$$

- Subtract off before image reconstruction
  - Panchromatic image of source
  - Fringe bias at each pixel, independent of $\vec{B}$ and L

Wide-field Imaging Interferometry Testbed (WIIT)

- Developed by NASA to probe viability of space-based interferometry
  - Experimental realization of wide-field double-Fourier interferometer
    - Photon-noise-limited and operates at visible wavelengths
  - Calibrated Hyperspectral Image Projector (CHIP)
    - Simulates hyperspectral scene to be measured

(a) CHIP
(b) Collimating mirror (parabolic)
(c) Baseline pickoff mirrors
(d) Optical delay stage
(e) Beam splitter
(f) Imaging system
(g) Detector

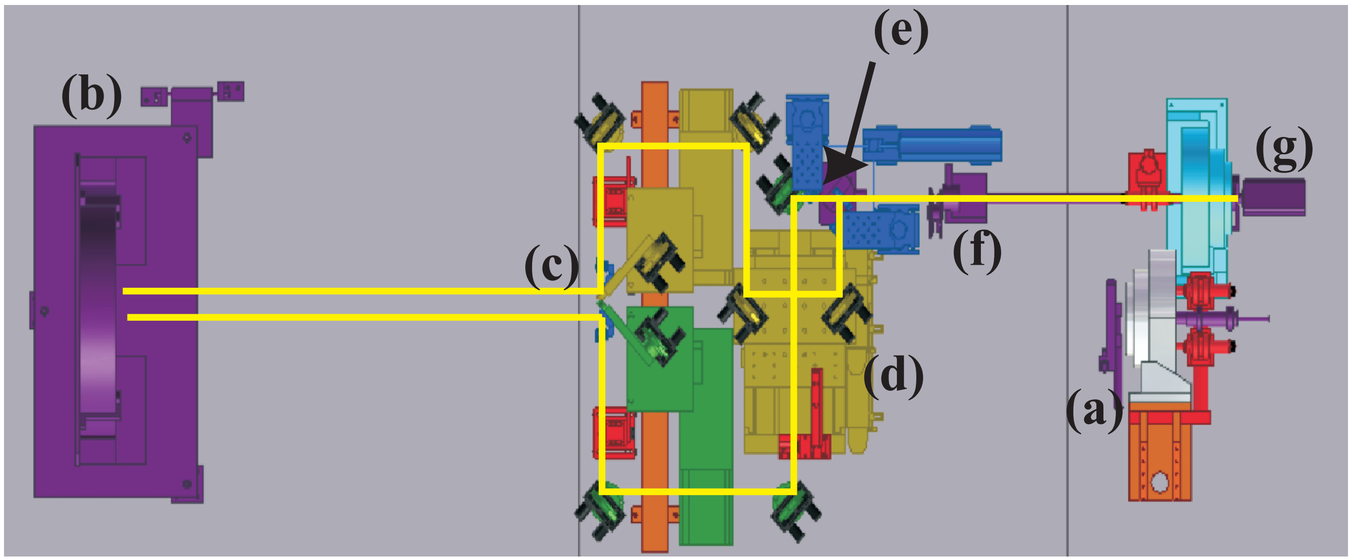

D. T. Leisawitz, M. R. Bolcar, et al., “Developing wide-field spatio-spectral interferometry for far-infrared space applications,” Proc. SPIE 8445, 84450A, 2012.

Hyperspectral Image Projector

- At any given time, produces spatially-spectrally separable scene
- Cycle through multiple spatially-spectrally separable images during camera's integration time to simulate hyperspectral image

$$f(x,y,\lambda) = \sum_{n=1}^{p} g_n(\lambda) h_n(x,y)$$

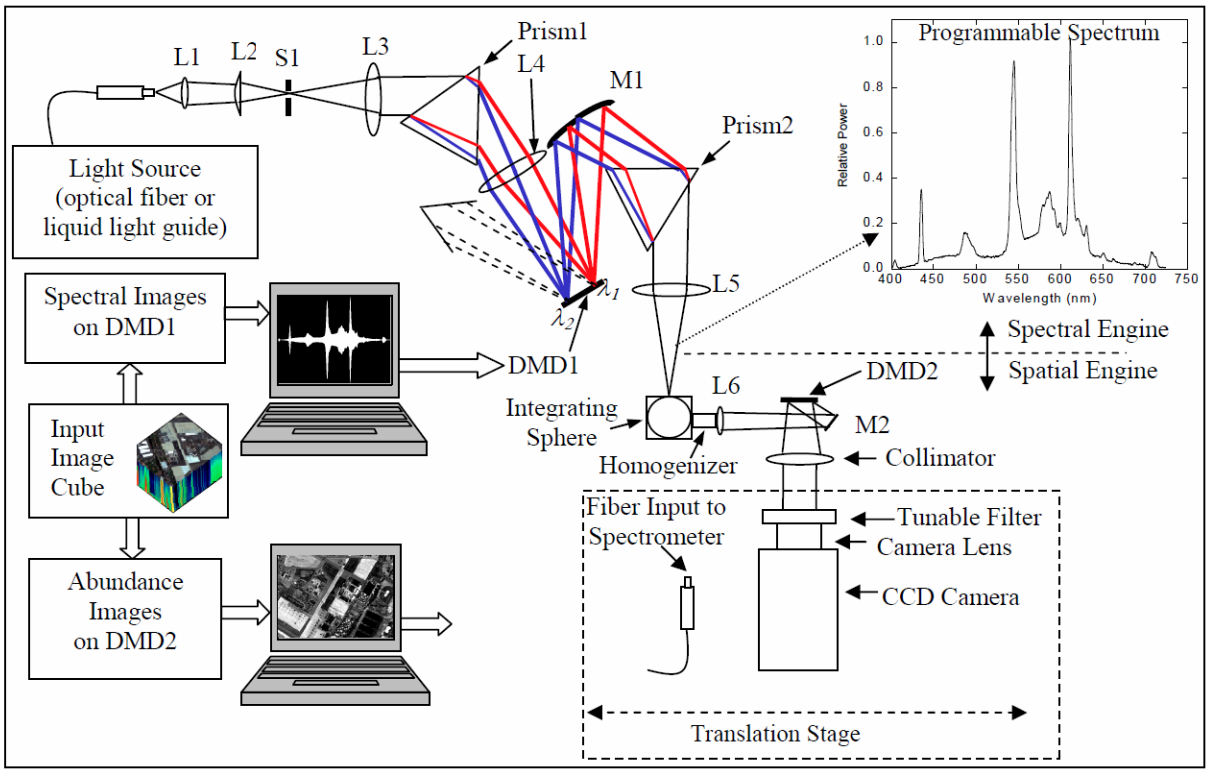

Rice, J. P., S. W. Brown, D. W. Allen, H. W. Yoon, M. Litorja, and J. C. Hwang, "Hyperspectral image projector applications," Proc. SPIE 8254, 82540R (2012).

Contributions and Future Work

- Derive measurement model and image synthesis algorithm in detail, using Fresnel propagations
  - Demonstrate generalized van Cittert-Zernike
- Develop phase referencing algorithm using known point sources in measured scene
  - Determine sub-pixel image registration parameters to desired resolution
  - Incorporates chirp z-transform rotation/translation/resampling
- Produce a model-based image reconstruction algorithm, incorporating various regularization techniques and nonlinear optimization
  - Recover missing spatial frequencies, especially at and around DC
- Facilitate experimental measurement of complicated/realistic astronomical test scenes using a modified version of Nonnegative Matrix Factorization
  - Integrate spectral influence functions as measured by spectrometer
  - Reduce effects of quantization

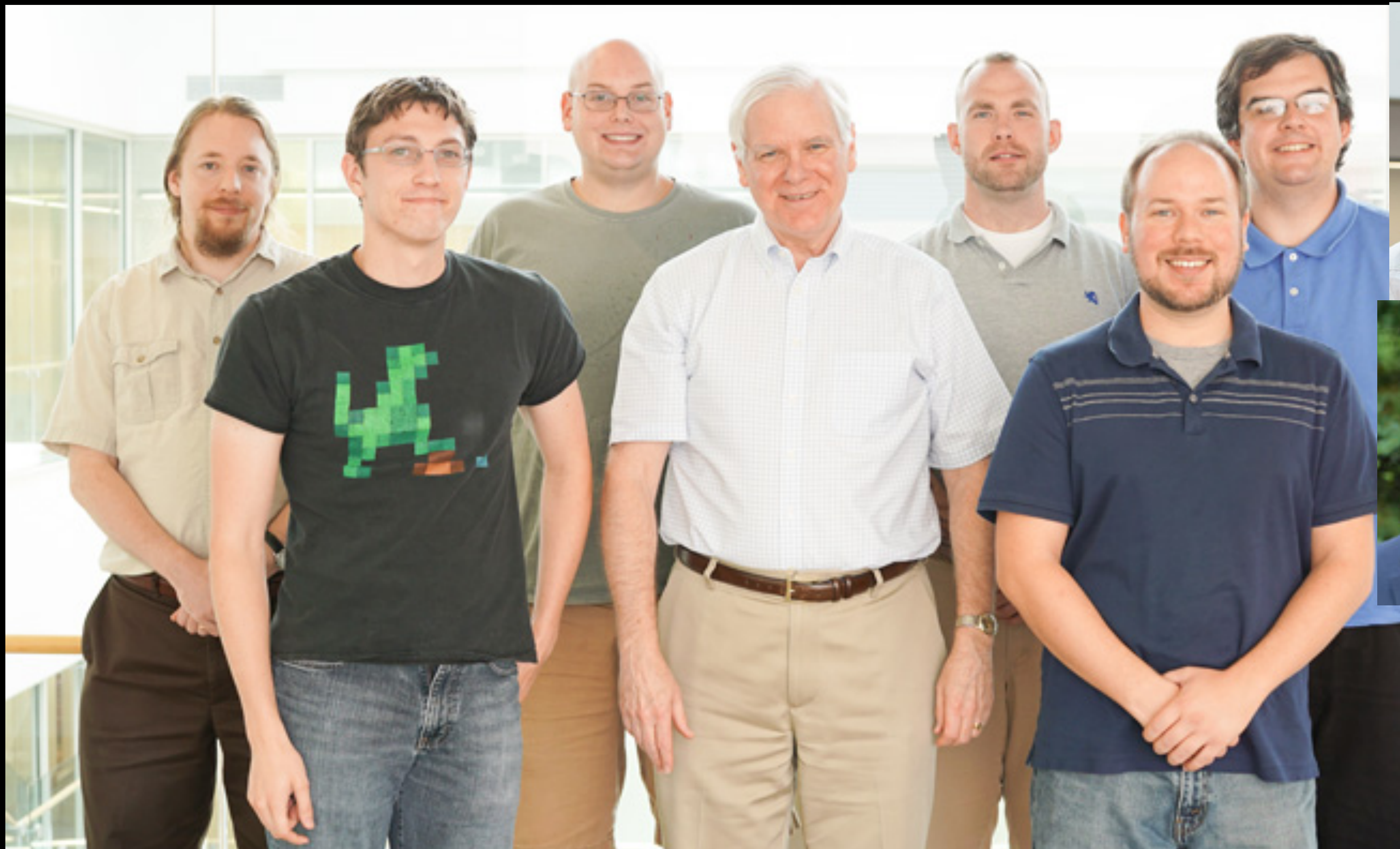

Phase Retrieval and Imaging Science Group

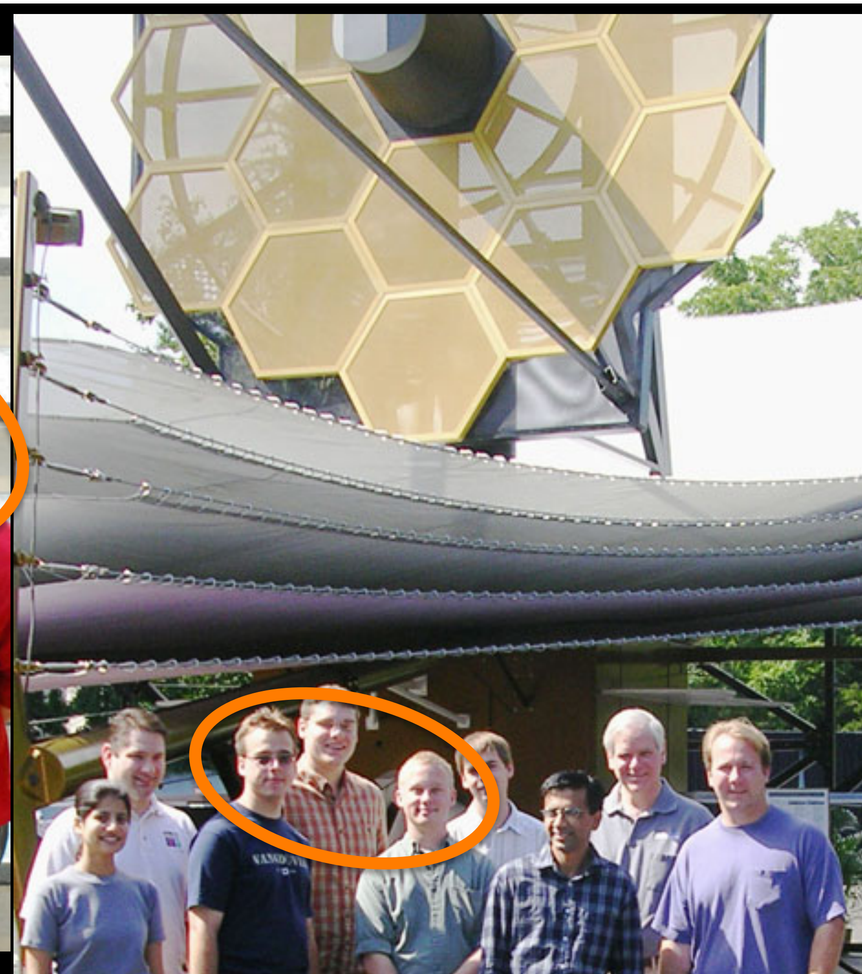

Phase Retrieval and Imaging Science Group